

During most of the time that the red beds of the Danley Ranch Tongue were being deposited north of Sand Canyon the marine limestone and shale of the Hueco Limestone were being deposited at the extreme southern end of the area. The general northward transgression of the sea during Hueco time was intermittently interrupted by minor regressions which are reflected by the many thin beds of the Danley Ranch Tongue that interfinger with the Hueco Limestone. These interfingering relations are particularly common near the areas of marked relief before deposition of the Abo and suggest that very slight movement continued into Hueco time. After the sea covered the highest Pennsylvanian hills near Sand Canyon during Hueco time, it transgressed much more rapidly with only minor periods of retreat, as indicated by the less abrupt interfingering in the northern part of the area. Thus, interfingering of the Danley Ranch Tongue with the lower part of the Hueco Limestone is of two types: (1) local complex interfingering as a result of local supply of sediments of the Abo from mendips which existed well into Hueco time, and (2) regional interfingering of the two formations as a result of the transgressive onlap of the sea during Hueco time. The advance of the sea ended late in Wolfcamp or early in Leonard about 15 miles north of the Sand Canyon area. The sea then retreated quite rapidly but with some fluctuation. Interfingering between the Hueco Limestone and the Lee Ranch Tongue just north of Culp Canyon reflects some of this fluctuation.

The total thickness of marine sediments left by the sea during Hueco time ranges from about 350 feet at the north end of the Sand Canyon area to about 600 feet at the south end. Red-bed sediments of the Lee Ranch Tongue were deposited to a thickness of about 100 feet over

the Sand Canyon area while deposition of the Hueco Limestone was continuing to the south. The close of late Abo time was marked by the beginning of evaporite and carbonate deposition alternating with deposition of red beds of the Yeso Formation.

REFERENCES CITED

- Darton, N. H., 1928, "Red beds" and associated formations in New Mexico: U. S. Geol. Survey Bull. 794, 356 p.
- Jones, T. S., 1953, Stratigraphy of the Permian basin of West Texas: West Texas Geol. Soc., 63 p.
- King, P. B., 1930, Geology of the Glass Mountains, Texas; Pt. 1, Descriptive geology: Univ. Texas Bull. 3038, 167 p.
- King, P. B., and Knight, J. B., 1945, Geology of Hueco Mountains, El Paso and Hudspeth counties, Texas: U. S. Geol. Survey Prelim. Map 36, Oil and Gas Inves. Ser.
- Lloyd, E. R., 1949, Pre-San Andres stratigraphy and oil-producing zones in southeastern New Mexico: N. Mex. Bur. Mines and Min. Res. Bull. 29, 79 p.
- Merrill, G. P., 1906, Rocks, rock-weathering and soils: N. Y. Macmillan Co., 400 p.
- Miller, A. K., and Parizek, E. J., 1948, A lower Permian ammonoid fauna from New Mexico: Jour. Paleontology, v. 22, p. 350-358
- Pray, L. C., 1949, Pre-Abo deformation in the Sacramento Mountains, New Mexico (Abstract): Geol. Soc. America Bull., v. 60, p. 1914-1915
- 1954, Outline of the stratigraphy and structure of the Sacramento Mountain escarpment: N. Mex. Geol. Soc. Guidebook 5th Field Conf. p. 92-107
- Thompson, M. L., 1954, American Wolfcampian fusulinids: Univ. Kansas Paleont. Contr., Protozoa, Art. 5, 226 p.
- U. S. GEOLOGICAL SURVEY, BOX 4083, STATION A, ALBUQUERQUE, N. MEX.
- MANUSCRIPT RECEIVED BY THE SECRETARY OF THE SOCIETY, APRIL 23, 1957
- PUBLICATION AUTHORIZED BY THE DIRECTOR U. S. GEOLOGICAL SURVEY

URANO-ORGANIC ORE AT TEMPLE MOUNTAIN, UTAH

By DANA R. KELLEY AND PAUL F. KERR

ABSTRACT

Urano-organic substances form essential constituents of the uranium ore at Temple Mountain, Utah. These occur in the vicinity of highly altered collapse structures associated with carbonaceous and petroliferous materials. Chemically, the ore is similar to low-rank coals. Geological conditions, the uranium distribution, texture, physical properties, and microscopic characteristics are indicative of a petroliferous origin. The ore is considered a uranium analogue corresponding to thucolite, the thorium and rare-earth radioactive mineral. The writers believe that induration resulted from polymerization and oxidation-devolatilization of hydrocarbons, caused by the interaction of ore solutions and organic materials at elevated temperatures. The limits of temperature postulated are a minimum of 100° C. and a maximum possibly as high as 350° C.

A characteristic group of metallic elements is present in the ore, as shown by the X-ray spectrograph. A rough zonal relation exists. Arsenic, cobalt, and selenium are concentrated near the collapse, whereas uranium, zinc, and vanadium appear more abundant in the mining area away from the collapse. Small particles of uraninite and sphalerite are disseminated throughout the ore, but the zonal relation is emphasized by the occurrence of native arsenic near the collapse and by the occurrence of montroseite, the primary vanadium oxide, in the mining area. The distribution of supergene oxidation minerals of vanadium and arsenic is further confirmation.

Ore textures suggest the emplacement of uranium-bearing organic material by the flocculation and subsequent accretion of hydrocarbons immiscible in aqueous ore solutions. Replacement of the sediments took place under the corrosive influence of the ore and pre-ore solutions. Contemporaneously, metallic elements were extracted from the solutions by the organic material. During emplacement and induration, dispersed particles of metallic minerals were formed. Banded nodules of the organic material and associated metallic minerals developed as the intensity, composition, and quantity of the solutions varied through time.

A change in the character of the ore solutions is indicated in the vicinity of the collapse by the presence of large replacement masses of dolomite and siderite above the ore horizon, abundant late hydrothermal jarosite in the Chinle, marcasite below the ore horizon, and the replacement of carbonate at depth. Slightly acidic conditions prevailed at depth, and neutral to slightly alkaline conditions prevailed above the ore horizon. Collapse features provided channels for the migration of organic materials and for the penetration of hydrothermal solutions.

The occurrence of native arsenic, 2M₁ mica clay, and large masses of dolomite, and the character of the urano-organic ore indicate heating in excess of the effects ordinarily attributed to ground water. The distribution and character of the alteration, the ore-mineral suite, and the presence of collapse structures suggest an epithermal hot-spring origin for the uranium mineralization. The features at Temple Mountain are significant in the delineation of centers of uranium mineralization elsewhere on the Colorado Plateau.

CONTENTS

| TEXT | | | Page |
|-------------------------------|-----|--|------|
| Introduction | 702 | Organic materials | 707 |
| Acknowledgments | 705 | General statement | 707 |
| Techniques of investigation | 705 | Relics of vegetation | 707 |
| General statement | 705 | Range in uranium content | 707 |
| Microhardness | 705 | Silicified logs | 708 |
| Differential thermal analysis | 705 | Coalified wood trash | 708 |
| X-ray spectrographic analysis | 706 | Organic material of petroliferous origin | 709 |
| X-ray diffraction | 706 | Range in uranium content | 709 |
| | | Fluid and semifluid tar | 709 |

| | Page | Figure | Page |
|---|------|---|------|
| Dry oil impregnating sandstone | 709 | 18. Some ore-bearing nodules | 741 |
| Asphalt | 710 | 19. Composite electron micrographs of urano-organic ore | 742 |
| Urano-organic materials | 713 | 20. Paragenesis of alteration and mineralization of the Moss Back Sandstone | 744 |
| Distribution | 713 | 21. Pre-ore alteration in upper and lower strata | 745 |
| Description | 715 | | |
| Origin of urano-organic constituents | 723 | | |
| Extraction of uranium from solution | 725 | | |
| Induration of the organic ore | 726 | | |
| Metallic element suite | 727 | | |
| Metallic minerals of the ore | 732 | | |
| General statement | 732 | | |
| Arsenic minerals | 733 | | |
| Iron minerals | 734 | | |
| Lead minerals | 735 | | |
| Uranium minerals | 735 | | |
| Vanadium minerals | 736 | | |
| Zinc minerals | 736 | | |
| Distribution of metallic minerals | 737 | | |
| Ore aggregates | 738 | | |
| General statement | 738 | | |
| Included metallic minerals | 742 | | |
| Other ore textures | 743 | | |
| Mineral sequence | 744 | | |
| Alteration associated with mineralization | 744 | | |
| Hypogene alteration | 744 | | |
| Supergene alteration | 748 | | |
| Conclusion | 751 | | |
| References cited | 753 | | |

ILLUSTRATIONS

| Figure | Page | Table | Page |
|--|------|--|------|
| 1. Sketch map showing the location of Temple Mountain | 703 | 1. Microhardness of some organic materials | 711 |
| 2. Columnar section of formations in the vicinity of Temple Mountain | 704 | 2. Loss of weight on heating of hydrocarbons | 720 |
| 3. X-ray spectrograph calibration curve for uranium | 707 | 3. Analysis of Temple Mountain asphalt and urano-organic ore | 722 |
| 4. Differential thermal analysis of Temple Mountain "asphalt" | 712 | 4. Ash and moisture-free elemental analysis of some organic materials | 723 |
| 5. Schematic cross-section through Temple Mountain mining district | 713 | 5. Comparison of physical properties of some organic materials | 725 |
| 6. Distribution of urano-organic ore, Temple Mountain mining district | 714 | 6. Percentage loss of weight in time from heating semifluid tar | 727 |
| 7. Hardness of Temple Mountain urano-organic ore | 715 | 7. Metallic elements in the ash of petroliferous materials | 727 |
| 8. Comparison of hardness and equivalent per cent U ₃ O ₈ of urano-organic materials | 716 | 8. Metallic trace elements | 728 |
| 9. Differential thermal analysis, indurated hydrocarbons | 717 | 9. X-ray spectrographic distribution with relation to the collapse area | 729 |
| 10. Differential thermal analysis, low-rank coals and urano-organic ore | 718 | 10. X-ray diffraction of some organic materials from Temple Mountain | 730 |
| 11. Range of reaction maxima of differential thermal analyses of representative organic materials | 719 | 11. X-ray diffraction of native arsenic | 732 |
| 12. Urano-organic ore-impregnated log | 719 | 12. X-ray measurements for heavy-mineral mixture | 733 |
| 13. Loss of weight and hardness upon heating Temple Mountain hydrocarbons | 721 | 13. Partial X-ray-diffraction measurements of iron sulfides | 734 |
| 14. Urano-organic ore along bedding and fracture | 738 | 14. X-ray-diffraction measurements of two varieties of urano-organic materials | 735 |
| 15. Urano-organic ore pod along lithologic contact | 738 | 15. X-ray-diffraction measurements of montroseite | 735 |
| 16. Urano-organic ore along fracture | 739 | 16. X-ray-diffraction measurements of sphalerite | 736 |
| 17. Diagrammatic development of masses of urano-organic material | 740 | 17. Heavy metallic minerals separated from selected ore zones | 737 |
| | | 18. Metallic-element distribution in argillic alteration associated with urano-organic materials | 746 |
| | | 19. Minerals of the Temple Mountain uranium area | 747 |
| | | 20. X-ray diffraction of jarosite from the Camp Bird mines | 748 |
| | | 21. X-ray diffraction of jarosite, Temple Mountain | 749 |
| | | 22. X-ray-diffraction measurements of faintly translucent material associated with organic materials | 750 |

INTRODUCTION

Temple Mountain first became an important mining area during the epoch of radium exploration, about 1920. The search for uranium

revived mining operations in recent years. The mining district has lately been one of the major uranium producers on the Colorado Plateau.

The ore is a urano-organic material. Such

INTRODUCTION

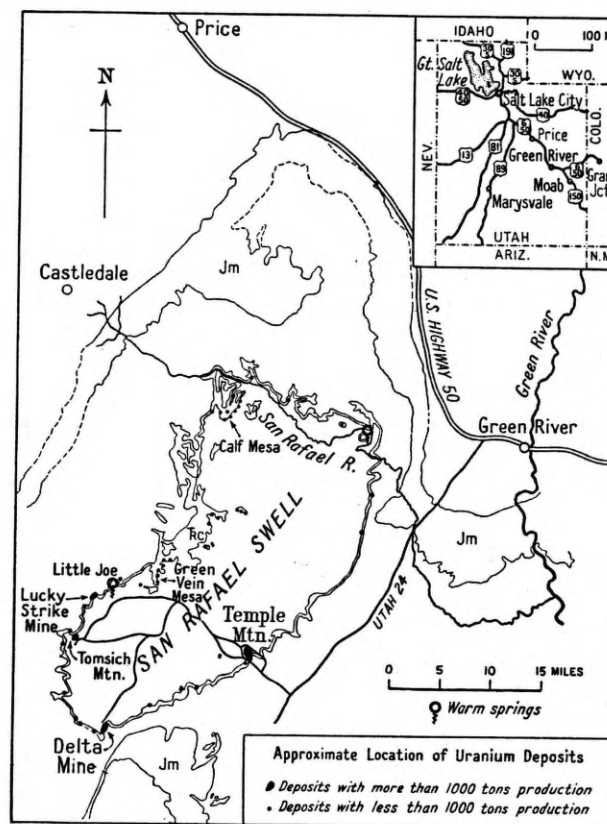


FIGURE 1.—SKETCH MAP SHOWING THE LOCATION OF TEMPLE MOUNTAIN
Warm springs occur in the vicinity of producing uranium mines.

deposits occur in a number of places on the San Rafael Swell, at Elk Ridge in eastern Utah, in New Mexico, at Placerville, Colorado, and probably elsewhere. At Temple Mountain, most of the ores are concentrated in the Moss Back Member of the Chinle Formation and are distributed throughout an area of about a square mile. Isolated ore patches in several horizons establish a vertical spread of approximately 1500 feet from the Triassic Wingate to the Permian Kaibab. The zone of widespread vertical distribution of ore is accompanied by alteration and lies close to the Temple Mountain collapse (Kerr, Kelley, Bodine, and Keys, 1955; Kerr, Bodine, Kelley, and Keys, 1957) where great blocks of down-dropped strata lie partly buried in consolidated debris.

A study of the Temple Mountain mining

district began in 1954. A preliminary report on the mechanism of emplacement of the ore (Kelley and Kerr, 1956) is herein revised and expanded. A brief discussion of phases involved in the mechanism of ore emplacement has been published (Kerr and Kelley, 1956).

Temple Mountain lies along the southeastern side of the San Rafael Swell in Emery County, Utah, 44 miles southwest of Green River (Fig. 1). A description of Temple Mountain and the San Rafael Swell in general is furnished in the report on the collapse features cited above (Kerr, Bodine, Kelley, and Keys, 1957). A columnar section (Fig. 2), cross section (Fig. 5), and a diagram showing the distribution of the ore in the mining district (Fig. 6) indicate the geologic setting.

Two major types of organic material are as-

sociated with the organic ore: plant detritus and petroliferous residue.

Plant debris and fossilized logs are found in the Moss Back Sandstone and sparsely through

Tar seeps occur in many places, and porous sandstones from the Coconino through Wingate formations are locally oil-stained. Oil staining extends through Moss Back strata for several

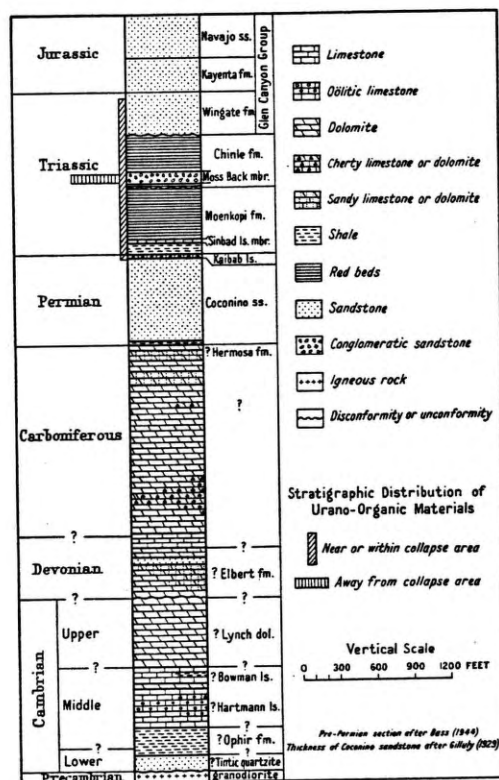


FIGURE 2.—COLUMNAR SECTION OF FORMATIONS IN THE VICINITY OF TEMPLE MOUNTAIN

the rest of the Chinle. At the Delta mine, near the southeastern corner of the swell, logs and carbonaceous trash have been replaced by pitchblende. No urano-organic ore or petroliferous material have been reported from this locality. Calf Mesa, at the north end of the swell, contains deposits of urano-organic materials. As at Temple Mountain, the coalified plant fragments associated with the ore are essentially unmineralized. Elsewhere on the swell, particularly along the western side, urano-organic ore is associated with both nonuranium- and uranium-bearing plant remains.

miles east of Temple Mountain. Similar staining also occurs in a number of localities elsewhere in the swell in Coconino, Moenkopi, and Chinle siltstones and sandstones. An asphaltic material similar physically to asphaltite is present in minor amounts in much of the Temple Mountain collapse. Locally, mixtures of petroliferous materials and coalified wood may be recognized.

Since the strata exposed at the surface do not generate oil the source of the petroleum lies either at depth or to one side of the swell in older Paleozoic rocks. The existence of petro-

liferous sands in the general region has long been known. Prommel and Crum (1927) recognized petroliferous strata in the vicinity of the Colorado and Green rivers; Gilluly (1929), Baker (1946), and Wengard and Strickland (1954) confirmed the presence of oil in the vicinity of the San Rafael Swell, particularly to the south, east, and north. Oil and gas showings have been reported from the subsurface of the Pennsylvanian Hermosa-Paradox sequence of sediments to the Glen Canyon Group of Triassic-Jurassic age.

ACKNOWLEDGMENTS

The writers wish to express their gratitude to Dr. H. D. Glass of the Illinois Geological Survey and Dr. H. S. Yoder of the Geophysical Laboratory for discussions that have aided this study. Appreciation is expressed to Miss P. K. Hamilton of the Department of Geology, Columbia University, for useful suggestions and assistance, and to Mr. Samuel Kamhi for electron photomicrography of the ores.

This study has been made possible through the assistance of the Division of Research and the Division of Raw Materials of the U. S. Atomic Energy Commission. The co-operation of Dr. Daniel R. Miller, Mr. Robert D. Nininger, Mr. Ernest Gordon, Mr. Hiram Wood, and their associates is greatly appreciated.

TECHNIQUES OF INVESTIGATION

General Statement

Study of the uranium-bearing organic ore included a survey of physical properties and the interpretation of the mechanism of emplacement. The principal methods used have been X-ray diffraction, X-ray spectrographic analysis, microscopic examination of polished surfaces and thin sections, fragment immersion, microhardness determination, and differential thermal analysis.

The greatest handicap in the study of natural organic materials at Temple Mountain may be attributed to the finely mixed nature of the materials. Various contaminant mineral grains in the insoluble urano-organic ore range from a millimeter in diameter to submicroscopic dimensions and are irregularly distributed in size and area. Destructive techniques for obtaining pure organic material were avoided, since the resulting organic substance might be so altered that the determination of the original physical properties would be irrelevant. The

best samples of material separated for physical testing contained about 10 to 15 per cent microscopically visible contaminants. Although the presence of fine-grained matter decreases the reproducibility and accuracy of experiments, the results of studies show that variations are restricted, and valid and significant interpretations are possible.

Various techniques have been used to isolate and identify the small contaminant mineral particles. Single minerals and mineral mixtures were separated from the ore by hand picking, elutriation, settling in tetrabromethane, and by the use of the Frantz Isodynamic Separator. The resulting small quantities of material were subjected to X-ray-diffraction study, X-ray spectrographic analysis, microscopic examination, and qualitative chemical tests.

Descriptive data on color and streak are based on Ridgway Color Standards (1912). Qualitative estimates of relative solubilities of organic material refer to powder immersed in carbon tetrachloride for 10 minutes at room temperature. Specific-gravity determinations were made, with a Roller-Smith Precision Berman Balance, on fragments weighing between 5 and 17 milligrams. All fragments were visibly free from contaminants under low magnification.

Microhardness

A Tukon Microhardness Tester, Model MO, manufactured by the Wilson Mechanical Instrument Division of the American Chain and Cable Company, was used to determine microhardness (Kopp, 1955, M.A. Thesis, Columbia Univ.). The Knoop Indenter was used, and hardnesses are recorded in Knoop numbers. Indentations were made in areas visibly free from contamination under microscopic observation. All materials were tested more than four times. Distinguishable ranges of hardness were obtained for various types of organic substances.

Differential Thermal Analysis

Differential thermal analyses were undertaken with the multiple apparatus described by Kerr and Kulp (1948). The rate of temperature increase was $12\frac{1}{2}^{\circ}$ per minute to 1020° C. All materials were ground to approximately 0.07 mm, and similar packing and quantities were used.

Glass (1954) summarized attempts at differential thermal analyses of coals. By using conventional equipment with a nickel sample cover, he has been able to differentiate ranks.

Variability reflects plasticity and to some degree the amount of weathering, particularly in low-rank coals. Differential thermal analyses of naturally occurring carbonaceous material are not reproducible with the precision obtained in many cases with inorganic substances. Differential thermal analyses of organic materials in air, without covering, have little significance, because of dominant oxidation (exothermic).

In order to reproduce experimental conditions used by Glass (1954), runs were made varying the weight and fit of the sample cover.

Results obtained with a heavy cover are used in this report and are considered generally comparable to the study of coals by Glass. Forms of the curves for the same sample are reproducible, and similar samples are, in general, alike. However, variation occurs in the maximum temperatures of endothermic dehydration, endothermic devolatilization, and exothermic oxidation reactions. Reproducibility of high-temperature reactions has not been consistent; hence comparisons of curves of the different organic substances studied may be made only for the lower-temperature reactions. The variations are believed to be the result of:

- (1) Contaminant reactions differentially produced by slight variations in the rate of oxidation, because of differences in total amount and packing of the material
- (2) Minor reactions characteristic of the organic material but differentially masked
- (3) Varying volatile partial pressures caused by differing rates of volatile escape between samples in the covered multiple sample head

About 45 thermal analyses have been made of coals and indurated hydrocarbons; the significant examples are included.

X-ray Spectrographic Analysis

The theory and method of using internal standards for semiquantitative determinations of elements have been outlined by Stevenson (1954) for columbian ores.

X-ray spectrographic analysis of the organic materials was used, not only to determine associated metallic elements, but also for the semiquantitative determination of uranium equivalent to U_3O_8 . A North American Philips X-ray Spectrograph was used. Samples were run in air, and the fluorescent spectra were diffracted by a lithium fluoride crystal. To guard against the unpredictable effect of variable amounts of

contaminant elements, an internal standard was used. Bismuth was selected, since it has not been detected in the organic materials at Temple Mountain, because the wave lengths of the emission lines are relatively close to those of uranium, and the other elements present should have little effect on the standard-calibration reference lines. Standards were prepared, using approximately 4 per cent bismuth, pure silica as a diluent, and a range from 0.1 to 10.0 per cent U_3O_8 . The resulting calibration curve was used for the semiquantitative determination of per cent U_3O_8 in the organic materials tested (Fig. 3). Small quantities of organic materials were mixed with the internal standard to total 2 grams. Mixing was accomplished by grinding. Identically sized sample holders were used, and grinding and packing were essentially uniform.

The approximate content of elements other than uranium could be estimated by comparison with the uranium standards and 1, 5, and 10 per cent standards of Cr, Fe, and Zn. Accuracy by comparison yields an order of magnitude of .x, x., and xx. per cent.

All runs were made under identical conditions, so that the minimum lower limit of element detection was kept constant. Total mechanical error is estimated at 6.5 per cent of the U_3O_8 determination. Under the established experimental conditions, the minimum lower limit of uranium detection was equivalent to 0.3 per cent U_3O_8 .

X-ray Diffraction

X-ray-diffractometer, powder-camera, and X-ray-microcamera techniques were used to identify minerals associated with the organic materials. Young (1954), in a preliminary investigation of solid hydrocarbons, described one- and two-ring powder patterns. X-ray patterns of the organic materials at Temple Mountain have not revealed significant ring characteristics. X-ray-diffraction patterns show that the major graphite spacing (002) is present as a warp in coals as low in rank as high-volatile bituminous (Siever, 1952). The presence of prographite spacings in the organic materials at Temple Mountain has not been demonstrated. Other less definitive X-ray-diffraction spacings noted for various natural organic substances (Dietrich, 1956) are either absent or masked by contaminant mineral particles. Most of the lines from patterns of organic materials may be attributed to included contaminant grains, although the possibility exists that some un-

assigned lines may be due to one or more organic or metal-organic substances crystalline enough to give a pattern.

Standard tests were used in thin section and polished surface analyses (Larsen, 1921; Short,

Relics of Vegetation

Range in uranium content.—The uranium content of fossil plant debris in general is limited to trace amounts (Gott, Wyant, and

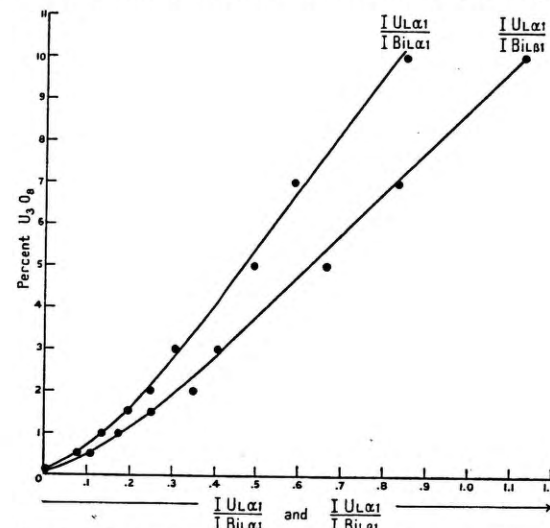


FIGURE 3.—X-RAY SPECTROGRAPH CALIBRATION CURVE FOR URANIUM
Bismuth is the internal standard

1940), and a few autoradiographs were made of polished surfaces of ore samples.

ORGANIC MATERIALS

General Statement

Several forms of organic material have been reported at Temple Mountain (Kerr, Bodine, Kelley, and Keys, 1957). These show a range in color, luster, hardness, microscopic appearance, radioactivity, chemical content, association, and field occurrence. The field occurrences recognized are:

- Relics of vegetation
- Silicified logs
- Trash: vitrain, fusain, and clarain and durain
- Organic material of petroliferous origin
- Fluid and semifluid tar
- Dry oil impregnating sandstones
- Asphaltic material
- Urano-organic materials

Beroni, 1952). Almost no uranium has been reported in the major coal fields of the Appalachian and Mid-Continent regions of the United States. Apparently, only in the Rocky Mountain region do certain large deposits of coal carry uranium (Vine, 1955). However, up to 10 per cent uranium occurs locally in lignitic units in the Dakotas.

Many of the uranium mines and prospects on the Colorado Plateau show an association of uranium with relict organic materials. Plant debris and logs may be replaced by pitchblende; some excellent replacements are found in the Delta mine at the southern end of the San Rafael Swell. Although replacements by the pitchblende may occur, the plant material in many cases retains microscopically the appropriate wood structure (Miller, 1955a).

Preliminary experiments show that coals and comparable substances can remove uranium from solution under laboratory conditions. The extraction of uranium by peats, lignites, and sub-bituminous coals may amount to between

98 and 99.9 per cent of the uranium present in solution (Moore, 1954). Uranium found in sub-bituminous coals and lignites is apparently associated with the humic components of coal, probably as a urano-organic compound (Breger, Deul, and Rubinstein, 1955; Breger, Deul, and Meyrowitz, 1955). Miller (1955b) believes that the formation of pitchblende associated with plant remains resulted from the reaction of ore solutions containing uranium (as a complex uranyl carbonate or uranyl hydroxide ion) with organic sulfur or pyritic sulfur genetically associated with the plant remains. Pitchblende also could be precipitated from reduction of uranium in solution by the organic materials. In the laboratory, uraninite has been precipitated between 25° C. and 260° C. Crystallite study by Croft (1954) suggests that coarser crystals result at the higher temperatures.

Although uranium ore is concentrated in wood replacements in the Colorado Plateau, plant detritus in the Temple Mountain uranium district yields little if any ore. Plant remains, both removed from and intimately associated with the urano-organic ore, yield no uranium above the lower limits of X-ray spectrographic detection (plus 0.3 per cent U_3O_8). In general, the usual types of plant remains characteristic of basal Chinle sandstones of the Plateau region appear to be present at Temple Mountain. These types include silicified logs and coalified wood trash. The Temple Mountain coalified fragments appear to be low-rank bituminous coal or lignite. Plant detritus is abundant in the Moss Back Sandstone but may also occur in upper Chinle and the lower Monitor Butte members.

Silicified logs.—Fossil logs are in many cases silicified, but a few have a ½- to 1½-inch rim of vitrain. Pyrite replaces the rim in many

cases, and desiccation cracks in the outer portion of the logs are also filled with organic materials, detrital grains, pyrite, or secondary hydrous iron minerals. Cell texture is in many cases clearly outlined by the silica replacement. Association and content suggest that the organic rim may be in part impregnated with petroliferous material.

Coalified wood trash.—Coalified wood fragments constituting trash zones, in most places are restricted to bedding planes, have microscopic and physical properties characteristic of organic materials of the coal rock types vitrain, fusain, and possibly minor clarain and durain (Hacquebard, 1950; Marshall, 1955). In a few places pyrite is associated with the trash zones.

VITRAIN: The woody parts of original vegetation, composed predominantly of anthraxylon, represent the vitrain. The organic rims of silicified logs are made up mainly of this material. Trash fragments are commonly vitreous and black. In thin section, the material is weakly translucent, either deep red or reddish brown (Pl. 2, fig. 1; Pl. 3, fig. 2). Cell structure is uncommon. On polished surfaces, the material is gray and smooth (Pl. 2, fig. 2). X-ray spectrographic analyses reveal x. per cent Fe and traces of Zn, As, and V (0.x to x. per cent). Microhardness ranges between 26.0 and 32.1 Knoop (Moh's 2), typical of coals (Table 1).

FUSAIN: Commonly, the trash zones contain fusain that is dull and brown to brownish black. It is predominantly opaque in thin section and variably gray on polished surface. On polished surfaces, cell structure is common (Pl. 2, fig. 3). X-ray spectrographic analyses reveal x. per cent Fe, with a few traces of Zn and As (0.x per cent). The microhardness is

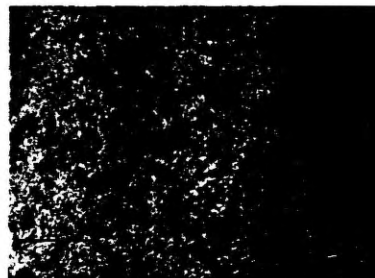


FIGURE 1

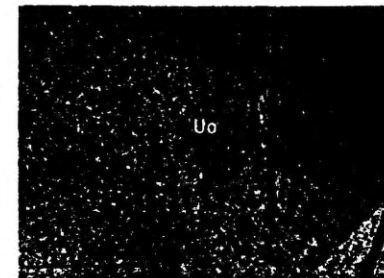


FIGURE 2



FIGURE 3

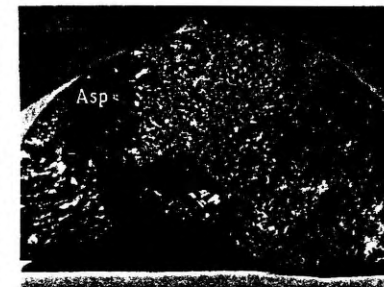


FIGURE 4

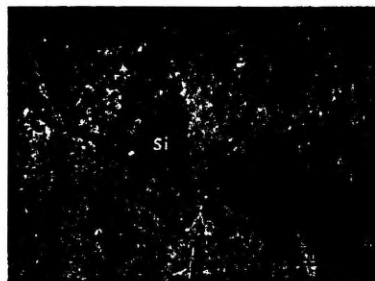


FIGURE 5



FIGURE 6

PLATE 1.—TEXTURES OBSERVED IN HAND SPECIMENS

FIGURE 1. Tar-soaked sandstone. A Moss Back core fragment from the collapse area. Semifluid tar (black mass) and scattered spots are shown in the bordering unsaturated sandstone.

FIGURE 2. Ore-impregnated sandstone. Rounded, partially spherical masses of urano-organic ore (Uo) in the Moss Back Sandstone are surrounded by a zone of pyrite replaced sandstone (Py). Calyx area. (The vertical mark is a hardness indentation.)

FIGURE 3. Ore-impregnated sandstone penetrated by nonuranium-bearing asphalt. Asphaltic material (black) lies at the bottom of the view. It follows bedding in the Moss Back Sandstone in a specimen from Flat Top Mesa.

FIGURE 4. Nonuranium-bearing asphaltic material in mineralized sandstone. Asphalt (Asp)-filled fracture in low-grade urano-organic ore (Uo)-impregnated sandstone. Core fragment from the collapse area equivalent to upper Coconino or Kaibab.

FIGURE 5. Silicification along fracture. Sandstone along one side of a fracture is completely silicified (Si) and contains coatings of realgar and orpiment (Or). The other side of the fracture is composed of argillized sandstone (ss). Core fragment is from the breccia zone in the collapse area.

FIGURE 6. Marcasite in the collapse area. Bands of marcasite parallel and subparallel to bedding in silty mudstone. Core fragment is from the breccia zone in the collapse area.

TEXTURES OBSERVED IN HAND SPECIMENS

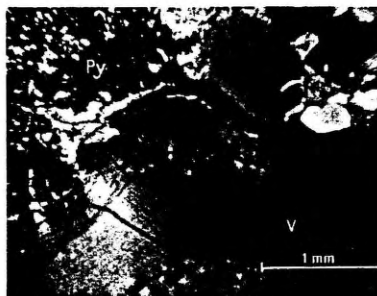


FIGURE 1

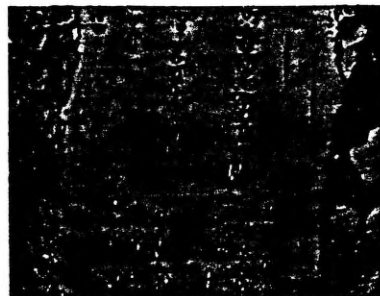


FIGURE 2

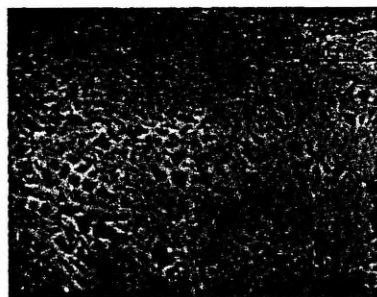


FIGURE 3



FIGURE 4

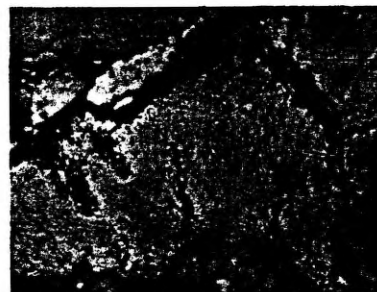


FIGURE 5

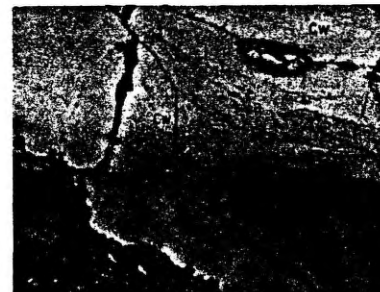


FIGURE 6

PHOTOMICROGRAPHS: SOME TEXTURES IN NONURANIUM-BEARING ORGANIC MATERIALS

approximately 24 Knoop (Moh's 2), typical for coals (Table 1).

CLARAIN AND DURAIN: Although most of the coalified wood fragments contain fusain or vitrain, some of the associated carbonaceous matter reveals in thin section small patches of granular or amorphous opaque material (opaque attritus or micrinite) and, rarely, translucent attritus. Sufficient amounts of these materials are not present to identify the constituents. The terms clarain and durain are tentatively applied to these attrital materials.

The larger fossil plant remains are generally silicified, whereas the smaller fragments are still organic. Possibly the species of fossil wood, as well as the type of woody material, influences its receptivity to replacement by mineralizing solutions. Most of the remains show compression, implying either soft vegetation or the existence of a considerable thickness of sediments on top of the Moss Back before silicification and pyritization.

Organic Material of Petroliferous Origin

Range in uranium content.—Organic material of petroliferous origin is found along fault and fracture planes, along bedding planes, on contacts between lithologic units, and impregnating permeable strata.

Crude oil, in general, contains uranium in concentrations of less than 0.02 ppm (Erickson, Myers, and Horr, 1954). Indurated hydrocarbons, however, generally contain slightly more uranium; the amount varies considerably with the type of material and locality. Three types of nonradioactive petroliferous materials are recognized at Temple Mountain: fluid or

semifluid tar, dry oil impregnating sandstones, and asphalt.

Fluid and semifluid tar.—Black to dark-brown viscous tar is common. It has been found in the Moss Back ore horizon (Marshbank Incline and Calyx Hole mines no.'s 3, 6, and 9, for example), in the Sinbad Member of the Moenkopi at the northern edge of collapse no. 4, in upper Chinle-lower Wingate dolomite near the collapse, in the Temple Mountain collapse (Pl. 1, fig. 1), in drill holes lower in the structure east of Temple Mountain, and along South Temple Mountain Wash. The tar forms seeps and viscous impregnations along bedding planes, fractures, and faults. In places it seeps over ore and plant debris. It is soluble in most organic solvents. It is present interstitially as thin coatings on the detrital grains and has no corrosive or replacement effect on the host rock.

Semiquantitative spectrographic analyses of the ash of two samples of "viscous asphalt" by Erickson, Myers, and Horr (1954) indicate that the uranium content is below 50 ppm (0.005 per cent) and that traces of the metallic elements common to petroliferous materials are present (Table 7). X-ray spectrographic analyses reveal .x per cent Fe and in a few samples traces of As and Ni (0.x per cent). An X-ray spectrographic analysis of the ash of one sample at approximately 1000° C. indicated only iron, since the arsenic was probably volatilized during calcination.

Dry oil impregnating sandstones.—Sediments impregnated with dry oil are conspicuous in the area. Bleaching, within and bordering the Temple Mountain collapse, may be attributed in part to the reduction of iron by petroleum.

PLATE 2.—PHOTOMICROGRAPHS: SOME TEXTURES IN NONURANIUM-BEARING ORGANIC MATERIALS

FIGURE 1. Vitrain, distorted with wavy extinction. Translucent fragment of vitrain (V) surrounded by pyrite (Py). From the Moss Back Sandstone in the calyx area. Thin section, crossed nicols.

FIGURE 2. Pyrite particles in vitrain follow partly destroyed cell structure. Pyrite is aligned along scattered cells in a fragment of vitrain. From the Moss Back Sandstone of the calyx area. Microhardness indentations (K) are shown. Polished surface.

FIGURE 3. Coalified wood fragment impregnated with asphalt. Distorted cell walls of fusain (?) are white. Asphaltic cell filling is dark gray. From the Moss Back Sandstone bordering the collapse area. Polished surface.

FIGURE 4. Distortion of coalified wood material by asphalt. White cell wall materials have been broken, distorted, and partially displaced by dark-gray asphalt (a). From the Moss Back Sandstone bordering the collapse area. Polished surface.

FIGURE 5. An intimate mixture of coalified wood and asphalt. The texture of the white cell walls of a coalified fragment is barely discernible. Dark-gray asphalt (a) appears as scattered patches and follows small fractures in the fossil wood. From the Moss Back Sandstone bordering the collapse area. Polished surface.

FIGURE 6. Mixed coalified wood and asphalt. Cell texture is absent. Asphalt (a) occurs surrounding and as streaks within, coalified wood (Cw). Canada balsam cement appears darker gray (Cb). From the Moss Back Sandstone bordering the collapse area. Polished surface.

Moenkopi sandstones and siltstones are locally oil-impregnated, particularly adjacent to fractures, faults, and collapse structures. The Moss Back and Wingate sandstones are commonly saturated. Some Chinle sandstones and siltstones are locally bleached adjacent to faults. Most of the section of Moss Back northeast of Temple Mountain is impregnated. The Coconino Formation is petroliferous northeast of collapse no. 4, along Straight Wash to the northeast, and where encountered in drill holes in the Temple Mountain collapse area. Throughout the swell, many other localities are similarly impregnated.

Though Temple Mountain is an outlier, and the Wingate cap is not connected with Wingate strata to the east, possibly the distribution of the dry oil before erosion assumed the form of a cone, with the apex in the Wingate or even higher on Temple Mountain, and with a slope decreasing away from this center. However, distribution of the oil depended largely on the permeability of strata.

Spectrographic analyses of the ash of four samples of hydrocarbons extracted from "petroliferous rocks" by Erickson, Myers, and Horr (1954) show traces of metallic elements in the ash corresponding to viscous asphalts (Table 7). Uranium content ranges between 0.2 ppm and 67 ppm (less than 0.006 per cent).

The impregnated fresh rock is light brown, and the oil forms a thin coating on detrital grains, without corrosive effect. The organic material represents a stage in the normal oxidation of petroleum.

Dry oil, because of its uniform nature and wide distribution, is independent of the uranium mineralization. It both predates and postdates the ore. In places, oil-impregnated sediments are cut by fractures filled with ore and indurated hydrocarbons. Petroleum impregnation after ores were deposited is shown by the low concentration of uranium in dry oil, the lack of replacement of the host rock, and the lack of induration even where associated with the ore.

Asphalt.—A hardened, brittle, black, lustrous nonuranium-bearing petroliferous material, asphalt,¹ occurs in fractures in dolomitized, sideritized, and goethite-bearing masses on and near Temple Mountain (Pl. 3, fig. 1). It fills small fractures in core fragments in ore at a depth of 777 feet in hole V-5 (Pl. 1, fig. 4). It is present as coatings on calcite-filled fractures in

¹ In physical properties, the material is similar to asphaltite, but chemically it corresponds to an asphalt or mineral wax.

upper Chinle strata along the south edge of South Temple Mountain.

The asphalt appears to form within and near the collapse areas. It fills vugs and fractures in the Sinbad northwest of collapse no. 4 and is present along bedding planes and fractures in ore-impregnated Moss Back Sandstone at the north end of Flat Top Mesa (Pl. 1, fig. 3), and locally in the calyx area.

DESCRIPTION: The physical characteristics of the asphalt (Table 5), are somewhat variable. In general, the hardness values agree with those of asphaltites and asphaltic pyrobitumens (Table 1). The material is softer and more elastic than coals and ore. Microhardness indentations in asphalts are more poorly developed than in coalified wood and ore.

Erickson, Myers, and Horr (1954) recorded spectrographic analyses of the ash of two samples of asphalt from the San Rafael Swell. Metallic elements in the ash are essentially the same as those found in the ash of viscous asphalts and hydrocarbons extracted from petroliferous rocks in the swell (Table 7). X-ray spectrographic analysis of the asphalt reveals 0.2 to 0.3 per cent Fe and a few traces of As, Cr, and Ni (0.2 per cent), similar to X-ray spectrographic analyses of semifluid tars (Table 8). However, the ash of an asphalt yielded only iron. As in the semifluid tars, the arsenic appears to have volatilized during ashing.

If one allows for the ordinary variations to which differential thermal analyses of organic materials are subject, particularly at higher temperatures, the asphalt at Temple Mountain appears to correspond to uintaite—a variety of gilsonite from eastern Utah (Fig. 4). Major endothermic dehydration occurs between 160° C. and 185° C. A secondary water loss apparently occurs between 195° C. and 245° C. Exothermic oxidation reactions occur as two peaks separated by the major endothermic devolatilization reaction between 430° C. and 445° C. The first oxidation peak is broad, between 350° C. and 400° C., and the secondary peak occurs between 540° C. and 550° C. Following the oxidation reactions, a small subsidiary endothermic devolatilization peak occurs between 600° C. and 620° C. The higher-temperature reactions are variable. The exothermic reaction in the vicinity of 865° C. and 880° C. may represent a structural change similar to the condensation of hexagonal carbon planes following volatile loss, as proposed by Glass (1954) for coals. The presence of secondary water loss and the temperature ranges of

oxidation, as well as volatilization reactions, distinguish the curves of the asphalts from the general variable patterns of other asphaltites, asphaltic pyrobitumens, urano-organic materials, and low-rank coals (Figs. 9, 10, 11).

has reached a stage between asphalt and asphaltite.

ASSOCIATIONS: Mineral fragments plucked from surrounding rocks by the asphalt yield X-ray-diffraction lines (Table 10, lower Wingate

TABLE 1.—MICROHARDNESS OF SOME ORGANIC MATERIALS

| Material | Range in hardness (Knoop) | Average hardness (Knoop) | Equivalent Moh's hardness |
|---|---------------------------|--------------------------|---------------------------|
| Indurated hydrocarbons* | 1.9-15.9 | 9.5 | -1 to 1.5 |
| Asphaltites* | 6.8-15.9 | 12.6 | 1 to 1.5 |
| Grahamite | 15.3-15.9 | 15.6 | ... |
| Gilsonite (var. uintaite) | 6.8-11.8 | 9.5 | ... |
| Asphaltic pyrobitumens* | 1.9-10.3 | 6.5 | -1 to 1 |
| Wurtzilite | 1.9-3.9 | 2.9 | ... |
| Albertite | 9.5-10.3 | 10.0 | ... |
| "Asphaltum" | 8.6-10.4 | 9.4 | ... |
| Temple Mountain asphalts | 3.1-15.0 | 8.4 | 1 to 1.5 |
| Some coals* | 22.3-62.3 | 43.0 | 2 to 2.5 |
| Lignite | 34.3-60.5 | 46.7 | ... |
| Bituminous | 22.3-29.0 | 25.0 | ... |
| Anthracite | 53.8-62.3 | 57.4 | ... |
| Temple Mountain coalified fragments | 24.2-32.6 | 28.5 | 2 |
| Thucholite | 52.0-89.7 | 65.5 | 2 to 3 |
| Elk Ridge, Utah urano-organic materials | 37.2-62.3 | 54.2 | 2 to 2.5 |
| San Rafael Swell urano-organic materials* | 31.1-129.4 | 67.7 | 2 to 3 |
| Temple Mountain | 31.1-129.4 | 71.9 | ... |
| Elsewhere | 55.3-76.4 | 63.5 | ... |
| Uraninite*† | 412.0-624.6 | 505.7 | 5.5 to 7 |
| Elk Ridge, Utah | 465.4-624.6 | 532.8 | ... |
| Happy Jack Mine, Utah | 412.0-562.0 | 478.6 | ... |

* Recorded range and average hardness include all types listed under this category.

† Palache *et al.* (1944) gives Moh's hardness of 5.5 for uraninite.

The physical characteristics of this material are those of asphaltites, particularly uintaite. However, chemically, the asphaltic material at Temple Mountain differs from asphaltites in having a lower percentage of fixed carbon and more oxygen (Tables 3, 4). In concentration of fixed carbon, it corresponds closely to mineral wax, such as ozokerite, which occurs as vein or fissure fillings in Utah (Abraham, 1920). The greater concentration of oxygen in the Temple Mountain material, compared with any of the indurated hydrocarbons, suggests oxidation subsequent to deposition. Iron sulfates are in many places associated with the material in fractures.

The writers consider that the Temple Mountain asphaltic material represents a product of induration and oxidation of a petroleum that

asphalt). In order of decreasing relative abundance, these are quartz, illite, dolomite, a little pyrite, and one or more additional substances, depending on the sample. Asphalt from fractures in dolomitic Wingate contains primarily quartz and dolomite, whereas asphalt from clay-bearing sediments, to a great extent, contains quartz and illite.

A sequence in deposition appears in asphalt-filled fractures where hematite and goethite cement lower Wingate Sandstone (Pl. 3, fig. 1). From the outside of the fracture inward the relationships are:

- (1) A thin outer zone of massive goethite
- (2) An intermediate zone of thin discontinuous stringers—dominantly magnetite, with minor intermixed calcite
- (3) Massive asphalt which fills the center of the fracture

These relationships indicate that initially goethite and hematite replaced the lower Wingate Sandstone, fracturing and secondary deposition of goethite followed, and petroleum impregnation occurred along fractures. Finally,

believed to be impregnated with asphaltic material.

Near the collapse, at the Camp Bird mines, polished surfaces of sandstone surrounding ore show two types of organic substances, neither

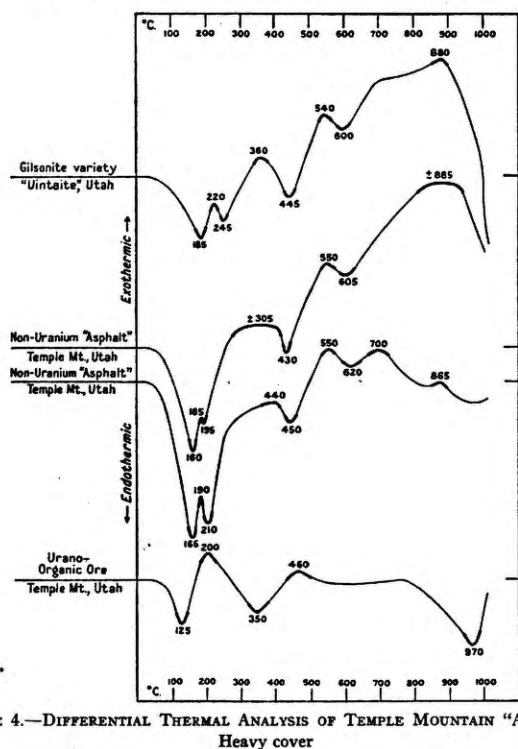


FIGURE 4.—DIFFERENTIAL THERMAL ANALYSIS OF TEMPLE MOUNTAIN "ASPHALT" Heavy cover

the petroleum became indurated, shrinkage occurred, and magnesite and calcite were deposited in contraction cracks along the edge and through the asphalt. The goethite is not corroded by the asphalt and little corroded by the carbonate.

In places asphalt has directly filled fractures in the dolomite masses and in ore-impregnated sandstones. Asphalts fill fractures that cut carbonate, clay, iron-altered sediments, and ore, indicating introduction subsequent to the major period of alteration and mineralization (Pl. 1, figs. 3, 4).

COALIFIED WOOD IMPREGNATED WITH ASPHALT: A few fragments of coalified wood are

of which contains uranium. The first is light gray, relatively free from foreign particles, and exhibits woody cell-wall texture. The second is darker gray, turbid with foreign particles, and forms as mobile impregnations having no woody texture.

A sequence of intimate textural relations shown with the microscope indicates that coalified wood distorted by compression along bedding planes was infiltrated by a hydrocarbon. The cells were first filled with the hydrocarbon (Pl. 2, fig. 3). Distortion of the cell walls and moderate destruction of the woody texture followed (Pl. 2, fig. 5). Finally, the two materials, although still retaining their identity,

became so intimately mixed that the original cell structure was obliterated (Pl. 2, fig. 6). In a few cases, nodular forms of organic material represent distorted cell structure (Pl. 2, fig. 4). The microhardness of these mixtures (24–29 Knoop, Moh's 2) is similar to coalified wood fragments (24–33 Knoop, Moh's 2), harder than indurated hydrocarbons (2–16 Knoop, Moh's 1).

The mobilization of cell-wall components of the fossil plant debris is apparently localized near the original site of the wood and is restricted to destruction of woody texture. The microscopic relationships indicate an accompanying introduction of a hydrocarbon.

Urano-Organic Materials

Distribution.—Uranium-bearing organic materials constitute the uranium ore in the Temple Mountain mining district. Near or within the collapse, these materials occur at scattered intervals in strata where surface pits, adits, and drill cores show a vertical range of approximately 1300 feet from Coconino through Wingate (Fig. 5). The ore is most abundant in the Moss Back but occurs in Wingate, Chinle, upper Moenkopi, and Kaibab or Coconino units.

In the major mining area away from the collapse, the ore is found in the Moss Back Sandstone, where deposits are small and most are discontinuous; their abundance and proximity make the district productive. Small ore bodies are characterized by predominantly lithologically controlled streaks of high-grade ore, with encircling halos of disseminated low-grade ore. Adjacent halos join in a few places and make a low-grade ore connection between the high-grade cores. However, many more halos are separated by barren to weakly mineralized sandstone. In a few places ore-impregnating sandstones cut across sedimentary structures and form ore rolls. Two levels of ore-impregnated Moss Back are represented at Calyx Hole mine no. 8, the South workings, and part of the Camp Bird workings. The lower level is close to the base of the Moss Back; the upper level is 25–30 feet above, toward the top of the sandstone. The greatest production of ore has been from the lower horizon.

Ore bodies in the calyx mining area, about half a mile southeast of the collapse, form a belt approximately a mile long and up to half a mile wide, trending northeast (Fig. 6). Near the collapse, deposits decrease in size and number.

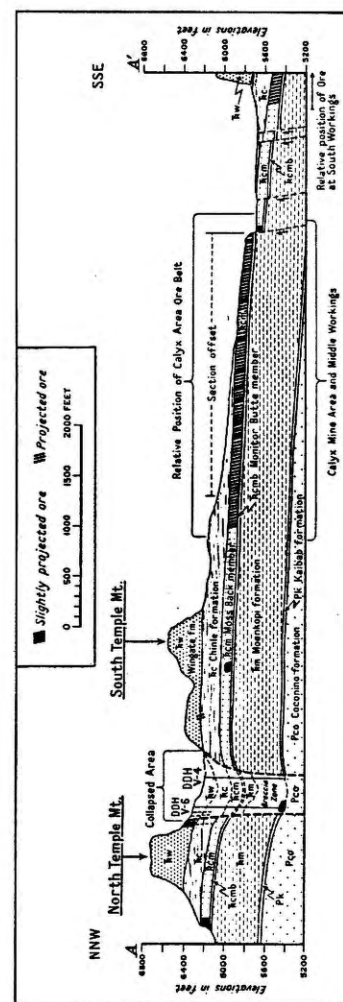


FIGURE 5.—SCHEMATIC CROSS-SECTION THROUGH TEMPLE MOUNTAIN MINING DISTRICT See figure 6 for location of A-A' and for identification of symbols.

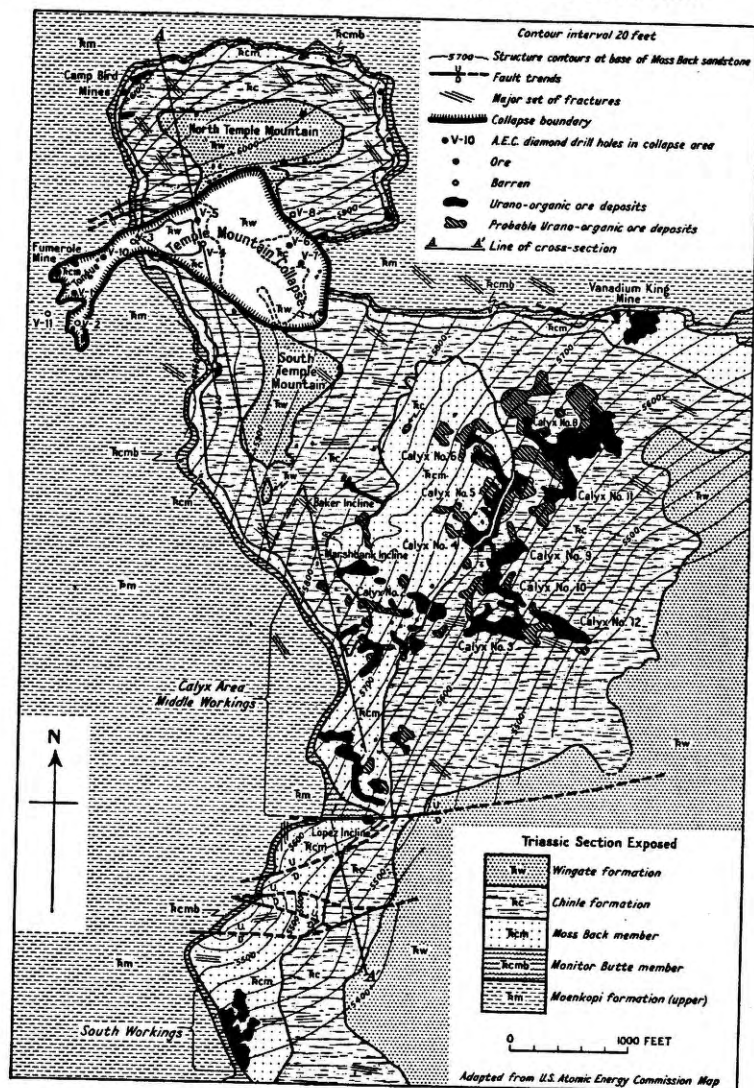


FIGURE 6.—DISTRIBUTION OF URANO-ORGANIC ORE, TEMPLE MOUNTAIN MINING DISTRICT

A thick cover of Wingate to the southeast necessitates deeper exploratory drilling. However, drilling has developed ore in places in the Moss Back where canyons cut into the Wingate.

Thus the width of the ore belt is probably greater than shown in Figure 6.

Erosion removed the sediments above the Moenkopi, north and west of Temple Moun-

tain. Thus, the mining area represents a remnant of a Moss Back belt of ore which before erosion probably encircled the collapse. The alignment of the belt that remains with regional

the local direction of flow and perhaps the sites of concentrations. The terrain nearest the source may also have been more porous from the effects of deformation and early alteration. The

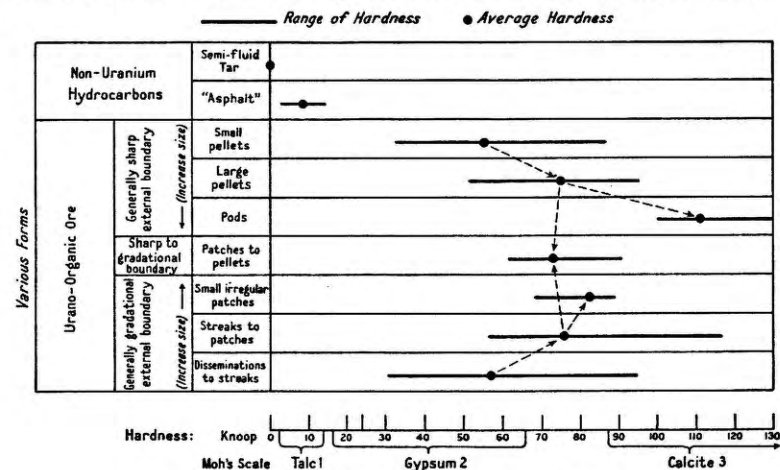


FIGURE 7.—HARDNESS OF TEMPLE MOUNTAIN URANO-ORGANIC ORE

structure led Keys and White (1956) to suggest a broad contour-level ore control.

The calyx area is inclined at 4° - 6° , but the regional dip increases southeast of the ore belt. Local patterns suggest a rough east to southeast elongation and alignment of individual ore bodies. This trend roughly corresponds to the strike direction of major faults, including the direction of elongation of the collapse, and to the direction of sedimentation in the Moss Back, as indicated by cross-bedding, ripple marks, and channel structures. The influence of sedimentary trends would be expected, in view of the strong lithologic control of ore distribution.

The presence of the ore in some fractures and faults and the widespread vertical distribution near and within the collapse indicate a vertical influx of ore fluids along the collapse conduit, as well as along fractures and faults. Lateral migration proceeded outward from these local centers, mainly into the permeable Moss Back. To a lesser extent, emplacement occurred in the overlying Wingate and possibly some strata below. Channels of least resistance, earlier used by the fluid organic material, were followed by the mineralizing and rock-altering solutions. Sedimentary structures and textures influenced

site of concentration of the organic material, either in a zonal band around the source or as a belt down-dip from the source, was determined by a combination of several factors. These included an increase in viscosity of the organic material, relative impermeability of the sediments outward from the broken source area, the volume, pressure, and distribution of ore fluids, temperature, and regional anticlinal structure.

Description.—The physical characteristics of the urano-organic ore are outlined in Table 5. The comparative insolubility of the ore has been noted. In determining uranium extractability, O'Brien (1953) lists 12 solvents, 9 organic and 3 inorganic. He states (p. 4), "The only effective solvents seem to be basic substances with the possible exception of xylene." In insolubility, the ore is similar to coals, asphaltic pyrobitumens (Abraham, 1920), and thucholite.

The urano-organic materials are harder, on the average, than coals (Table 1). They are also considerably harder than Temple Mountain asphalt and the indurated hydrocarbons (asphaltes and asphaltic pyrobitumens). A slight increase in hardness appears with increased size of the ore mass (Fig. 7). Where both hardness and uranium content were determined, it

appears that hardness increases slightly with an increase in uranium content (Fig. 8). Among such specimens, the hardness fails to increase with an increase in metallic elements other than uranium.

120° C. and 160° C. Exothermic oxidation is generally represented by two peaks, separated by a variable intense endothermic devolatilization reaction between 320° C. and 400° C. The first and major oxidation peak occurs between

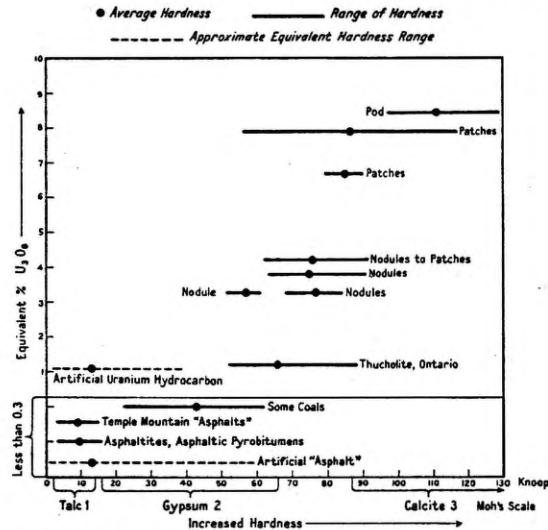


FIGURE 8.—COMPARISON OF HARDNESS AND EQUIVALENT PER CENT U_2O_3 OF URANO-ORGANIC MATERIALS

Differential thermal-analysis curves of organic materials range to such an extent that differentiation of indurated hydrocarbons (with the possible exception of uintaite) from low-rank coals is uncertain. The general forms of curves of indurated hydrocarbons (Fig. 9) and low-rank coals (Fig. 10) have been compared with urano-organic ore. A summary of low-temperature reactions for a number of curves is given at bottom of this page.

In general, oxidation and devolatilization reactions occur at a slightly lower temperature in indurated hydrocarbons than in lignites, but the difference is small, considering the temperature ranges.

The ore reveals the reactions shown in Figure 9. Endothermic dehydration occurs between

| Material | Dehydration, endothermic | Oxidation, exothermic | Devolatilization, endothermic |
|------------------------|--------------------------|-----------------------|-------------------------------|
| Lignites | 120°–170° C. | 240°–440° C. | 445°–515° C. |
| Asphaltic pyrobitumens | 120°–160° C. | 210°–265° C. | 420°–440° C. |
| Asphaltites | 140°–170° C. | 235°–265° C. | 385°–410° C. |
| Urano-organic ore | 120°–160° C. | 200°–280° C. | 320°–400° C. |

200° C. and 280° C., and the secondary peak between 440° C. and 490° C. A few small endothermic peaks in the vicinity of 560° C. probably represent the inversion of quartz present as a contaminant. In some cases the devolatilization peak is small and poorly developed, so that oxidation appears nearly continuous between 200° C. and 500° C. The presence of either a poorly developed endothermic reaction or the presence of two oxidation peaks constitutes a difference between the ore and indurated hydrocarbons and low-rank coals. Most samples of ore reveal a variable intense endothermic reaction between 970° C. and 1010° C., which may represent the evolution of hydrogen. Corresponding reactions oc-

curing at this temperature in other materials are not reproducible.

Uraninite occurs as minute particles in the ore. Differential thermal analyses of uraninite in air give variable results, and the effect due to

small, variably translucent patches along the edges of ore masses and, rarely, within the mass (Fig. 18; Pl. 5, fig. 1). The translucence results from (1) smearing and extra thinning of the organic material near the edge of a slide or be-

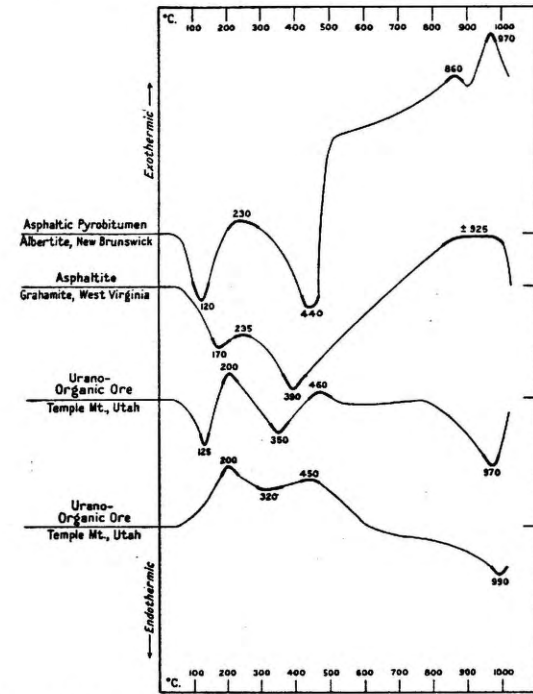


FIGURE 9.—DIFFERENTIAL THERMAL ANALYSIS, INDURATED HYDROCARBONS
Heavy cover

small amounts of uraninite in the organic material has not been determined.

Figure 11 is a diagram summarizing the reaction temperature ranges of several organic materials. Ultimately, it may be possible to demonstrate a sequence in the reactions of the indurated hydrocarbons, such as has been demonstrated for the ranks of coal, but at present it does not appear feasible to establish on the basis of differential thermal analysis alone whether a particular organic ore sample is more closely allied to low-rank coals or to petroliferous materials.

In thin section, the urano-organic materials are nearly always opaque, except for a few

tween the organic material and harder minerals, during preparation of the thin section, (2) rare impregnation by nonradioactive asphalt, which may be variably translucent, and (3) intimate mixtures of ore and associated minerals. In polished surfaces, a rarely observed light-gray, clear ore is associated with the common darker-gray, turbid ore (Pl. 5, figs. 3–5). No difference appears between the two materials in microhardness, U_2O_3 content and radioactivity distribution, solubility, and other physical properties. The turbidity in the darker ore is caused by minute contaminant mineral particles and is the cause for the slight difference in appearance on polished surfaces.

COALIFIED WOOD IMPREGNATED WITH ORGANIC ORE: On the basis of physical characteristics radioactive plant remains appear to be mixtures of unmineralized fossil wood and urano-organic ore. An example of this may be observed at

silica-filled wood cells and parallel to the log structure.

On polished surfaces, the translucent material is generally light gray and shows scattered collapsed wood cells. The microhardness (19.3 to

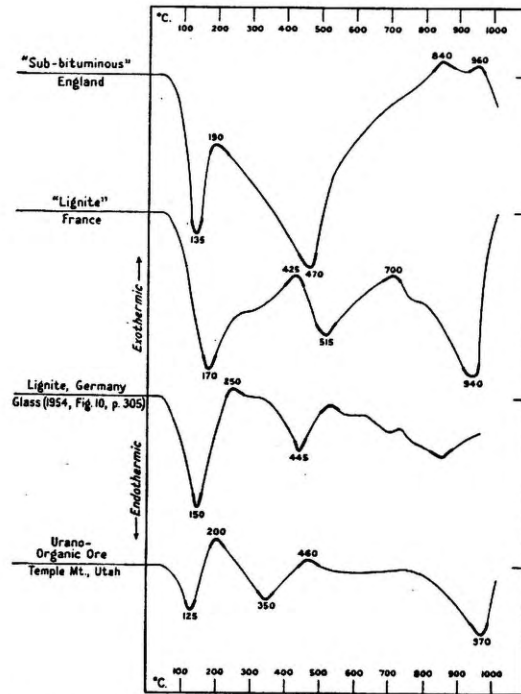


FIGURE 10.—DIFFERENTIAL THERMAL ANALYSIS, LOW-RANK COALS AND URANO-ORGANIC ORE
Heavy cover

North Mesa No. 9 mine, where a black, organic-appearing silicified log is highly radioactive (Fig. 12). Dull and vitreous black organic materials and pyrite form streaks and patches in fractures and also outline woody texture in streaks parallel to the log structure. Small amounts of nonradioactive asphalt coat some of the fractures. X-ray spectrographic analysis shows that the radioactive organic material contains 6.9 per cent U_2O_5 .

In thin section, the organic material is seen to consist of two textureless substances, one red brown translucent and the other opaque. These may occur either as separated masses or gradationally mixed. Either may be found in fracture fillings and also in streaks outlining

36.3 Knoop, Moh's 2) is similar to coal. The sharpness of the indentation is also similar to coal. Microscopically and physically, this material appears identical to vitrain elsewhere on Temple Mountain. X-ray spectrographic analysis of the vitrain, however, yields less than 0.5 per cent U_2O_5 and traces of Fe, As, and V.

The opaque material is generally light gray, clear to turbid, and exhibits no woody texture on polished surfaces. The microhardness (88.4 to 107.8 Knoop, Moh's 2½ to 3) is similar to that of the urano-organic ore containing up to 12.1 per cent U_2O_5 and impregnating the sandstone along bedding adjacent to the log (63.0 to 111.4 Knoop, Moh's 2½ to 3). The hardness indentations are less well developed than for

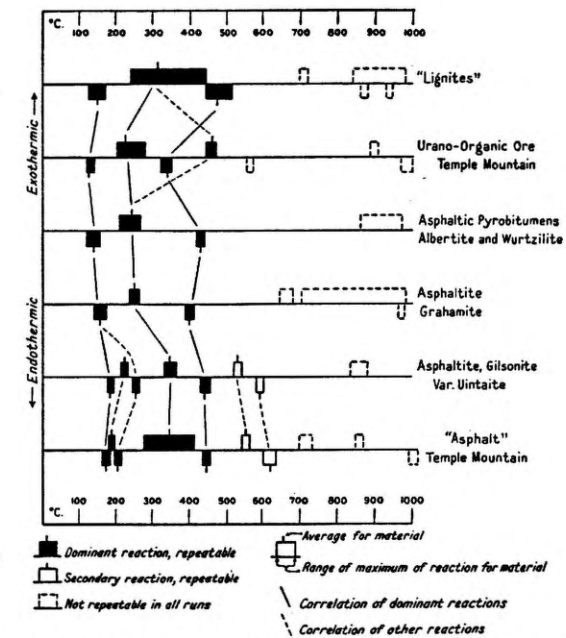


FIGURE 11.—RANGE OF REACTION MAXIMA OF DIFFERENTIAL THERMAL ANALYSES OF REPRESENTATIVE ORGANIC MATERIALS

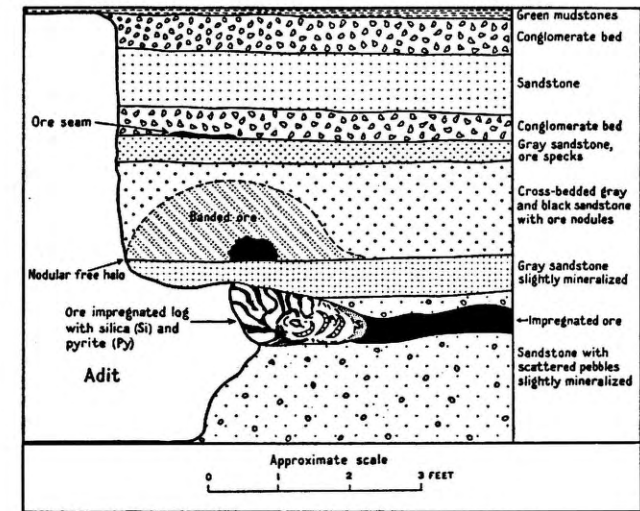


FIGURE 12.—URANO-ORGANIC ORE-IMPREGNATED LOG

TABLE 2.—LOSS OF WEIGHT ON HEATING OF HYDROCARBONS
(In per cent)

Original weight recalculated = loss of weight recalculated as 100 per cent at 1000° C.

| Temperature °C. | Tar | | Asphalt | | Urano-organic ore | |
|-----------------|----------------|--|------------------------|--|-------------------|--|
| | Loss of weight | Loss of weight recalculated | Loss of weight | Loss of weight recalculated | Loss of weight | Loss of weight recalculated |
| 200 | 1.27 | 1.31 increased viscosity | 3.51 | 2.50 black, granular | 2.25 | 3.83 no visible change |
| 400 | 94.98 | 97.60 gray-black flakes, masses, fibers | 94.50 | 96.66 mottled brown orange, granular | 39.01 | 66.42 grayish, no change in form |
| 600 | 97.29 | 99.97 brown yellow, granular | 97.22 | 99.44 red orange, granular | 58.39 | 99.41 yellow brown, no change in form |
| 800 | 97.29 | 99.97 brown yellow, granular | 97.62 | 99.72 mottled orange, brown, granular | 58.62 | 99.80 orange brown, granular |
| 1000 | 97.32 | 100 brown yellow, granular | 900° 97.76 as above | 100 | 58.73 | 100 purple brown, granular |
| Original weight | 7.4150 g | | 0.1472 g | | 1.5376 g | |

| Temperature interval °C. | Loss of weight (recalculated) | | |
|--------------------------|-------------------------------|-----------------------|--------------------|
| | Tar loss | Asphalt loss | Urano-organic loss |
| 25-200 | 1.31 | 2.50 | 3.83 |
| 200-400 | 96.29 | 94.16 | 62.59 |
| 400-600 | 2.37 | 2.78 | 32.99 |
| 600-800 | 0.00 | 0.28 | 0.39 |
| 800-1000 | 0.03 | 800°-900° C.: 0.23 | 0.20 |
| Total | 100.00 | 99.95 | 100.00 |

coals, a feature typical of urano-organic materials. Sufficient material for X-ray spectrographic analysis has not been satisfactorily separated, but microscopically and physically this material corresponds to urano-organic ore.

The microscopic relationships indicate that urano-organic material impregnated the log along fractures, filling voids in coalified and silicified woody material, as well as replacing included sedimentary and alteration minerals. The vitrain intimately mixed with the ore is neither mobilized nor mineralized above 0.5 per

cent U_3O_8 . Subsequently, a nonuranium-bearing hydrocarbon impregnated the log along the same paths and formed, upon induration, the asphalt fracture coatings.

A few vermicular remnants of organic material, similar to the cell-wall substance described under asphalt-impregnated coalified wood, are included in some of the ore masses near the collapse (Pl. 5, fig. 4). Woody texture is not observable, and there is no difference in microhardness, trace metallic-element content, and distribution of radioactivity, as revealed by

nuclear-track plates, between the remnants and the surrounding ore. The existence of these remnants as mobilized coalified wood-cell wall material was not established. However, coalified

fore weighing. The per cent loss of weight was calculated directly and also recalculated to 100 per cent at 900° C. or 1000° C., assuming that the remaining material at that temperature

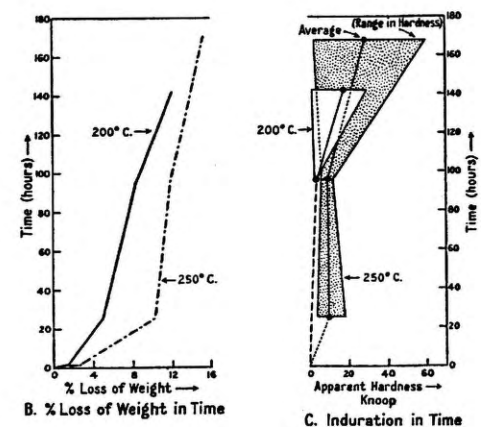
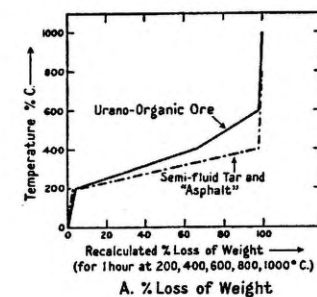


FIGURE 13.—LOSS OF WEIGHT AND HARDNESS UPON HEATING TEMPLE MOUNTAIN HYDROCARBONS

wood intimately mixed with urano-organic ore elsewhere neither contains vermicular remnants nor shows any evidence of mobilization.

CHEMICAL NATURE OF THE URANO-ORGANIC MATERIALS: The loss of volatile constituents in a high-temperature oven differs significantly for organic ore, tar, or asphalt (Table 2; Fig. 13, A). Powdered samples of semifluid tar, asphalt, and ore were each heated to arbitrary intervals of 200°, 400°, 800°, and 1000° C. (The sample of asphalt was heated to only 900° C.) To insure temperature equilibrium, though not loss of volatile equilibrium, the samples were allowed to remain at each temperature for 1 hour be-

represented nonvolatile constituents in the range studied.

The tar (96.29 per cent) and the asphalt (94.16 per cent) suffered major loss in the 200°-400° C. range. The ore loss (62.59 per cent) in the same range was substantially less. Volatile constituents amounting to 32.99 per cent in the ore required a 400°-600° C. temperature range for removal. The greater resistance of the ore to heat suggests a more highly polymerized material.

The pine-splint test for porphyrins in the organic ore and the petroliferous material at Temple Mountain is negative, but negative

TABLE 3.—ANALYSIS OF TEMPLE MOUNTAIN ASPHALT AND URANO-ORGANIC ORE
(In per cent)

Analyst: W. C. Bowden, Ledoux & Company, Teaneck, New Jersey, May 22, 1956.

| | Asphalt* | Urano-organic ore† | |
|---|----------|--------------------------------|--------|
| Volatile matter | | | |
| Total carbon | 75.30 | | 34.90 |
| Fixed carbon | 1.04 | | 34.20 |
| Hydrogen | 8.82 | | 2.80 |
| Oxygen | 6.02 | | 7.41 |
| Sulfur | 4.54 | | 4.48 |
| Nitrogen | 0.84 | | 0.18 |
| Arsenic | 0.06 | | 0.03 |
| Halogens | -0.01 | | -0.01 |
| Water at 105° C. | 0.59 | | 2.10 |
| Total | 96.17 | | 51.90 |
| Nonvolatile matter spectrographic examination | 0.70 | Chemical determination | 45.26 |
| Aluminum | 1-10 | Alumina | 4.15 |
| Calcium | 1-10 | Chromium | Trace |
| Copper | 0.1-1 | Fe ₂ O ₃ | 1.66 |
| Iron | 0.1-1 | Magnesia | Trace |
| Lead | -0.1 | Silica | 63.86 |
| Magnesium | 1-10 | TiO ₂ | 0.15 |
| Manganese | 0.1-1 | U ₂ O ₃ | 8.30 |
| Nickel | 0.1-1 | V ₂ O ₅ | 19.33 |
| Silica | 10-100 | Zinc | Trace |
| Titanium | -0.1 | Unaccounted for | 2.55 |
| Vanadium | 0.1-1 | | |
| Total | 100.00 | | 100.00 |
| Unaccounted for | 3.13 | | 2.84 |
| Total | 100.00 | | 100.00 |

* Sample no. 735910. Nonuranium-bearing asphalt from fracture in dolomite replaced lower Wingate Sandstone. Collapse area.

† Sample no. 735909. Urano-organic ore pod from Moss Back Sandstone, Calyx Hole mine No. 8.

results do not necessarily establish the absence of porphyrins.

O'Brien (1953) considered that the ore at Temple Mountain has an unusually high acid content.

Analyses have been published of soluble asphalts, asphaltites, and relatively insoluble asphaltic pyrobitumens by Abraham (1920), Crawford (1949), and Hunt, Stewart, and Dickey (1954); thucholites by Ellsworth (1928), Spence (1930), Davidson and Bowie (1951), Barthauer, Rulfs, and Pearce (1953), and Bowie (1955); and the urano-organic materials at Temple Mountain by O'Brien (1953) and Breger and Deul (1955). Since many of the published analyses are incomplete, comparison

of the materials is difficult. In thucholites and urano-organic ores, ash content is considerably influenced by contaminant material.

One sample of nonuranium-bearing asphaltic material and one sample of urano-organic ore have been analyzed (Table 3). Although the ore sample was selected to be as free from impurities as possible by hand picking, contaminant mineral particles account for the high ash. The two materials differ chemically to a considerable degree, since the organic material containing uranium yields greater fixed carbon, water, oxygen, and less hydrogen than the asphaltic material.

Elemental analyses of some indurated hydrocarbons, thucholite, low-rank coals, and organic

ore, on an ash-free and moisture-free basis, are compared in Table 4. The ore contains more hydrogen than thucholite but less than the asphalts. Fixed carbon and oxygen in the ore exceed the asphalts. The sulfur content of ore

"...aqueous solutions carrying organic material extracted from low-rank coals in the region, along with uranium and vanadium, may have saturated the pores of the sandstone. Eventually the organic matter was devolatilized and converted to its present insoluble state, perhaps radiochemically"

TABLE 4.—ASH- AND MOISTURE-FREE ELEMENTAL ANALYSES OF SOME ORGANIC MATERIALS
(In per cent)

| Element | Indurated hydrocarbons* | | | Temple Mountain† | | Thucholite** | Coals†† | |
|--------------|-------------------------|----------------------|---------------------------------|------------------|------------------------|--------------|--------------------------|------------|
| | Asphalt "tabbylite" | Asphaltite gilsonite | Asphaltic pyrobitumen albertite | Asphalt | Urano-organic material | | Lignite | Bituminous |
| Total carbon | 84 | 88 | 85 | 79 | 70 | 79 | 60 | 84 |
| Fixed carbon | 9 | 15 | 38 | 1 | 69 | 78 | (up to approximately 78) | |
| Hydrogen | 11 | 9 | 11 | 9 | 6 | 2 | 6 | 5 |
| Oxygen | ? | 1 | 1 | 6 | 15 | 11 | 31 | 9 |
| Sulfur | 2 | 2 | 1 | 5 | 9 | 8 | 2 | <1 |
| Nitrogen | 3 | <1 | 2 | 1 | <1 | | 1 | 2 |
| Total | 100 | 100 | 100 | 100 | 100 | 100 | 100 | 100 |

Data recalculated from:

* Abraham (1920)

† Table 2

** Barthauer *et al.* (1953)

†† Ries (1949)

and thucholite are reasonably comparable. A similarity in volatile concentrations exists between the ore and low-rank coals.

Origin of urano-organic constituents.—The writers applied two interpretations in seeking the source of the organic material in the ore. One involves interaction of solutions with petroliferous material, the other organic extraction from coal.

Drill-hole records show that oil exists in almost all porous sediments of the San Rafael Swell. The organic ore at Temple Mountain is associated with semifluid tar, petroleum-impregnated sediments, and asphaltic material. Under such circumstances it is reasonable to consider petroliferous material as a possible source of organic substances.

Logs and other forms of plant detritus are abundant in the Moss Back Formation. On the basis of differential thermal curves and chemical analyses, Breger and Deul (1955) suggest that the ore represents an organic extract from coals of sub-bituminous and lignitic rank. They state (p. 19):

With regard to uranium-bearing "carbonaceous pellets," they indicate the following trends (p. 20):

"...1) ash rises with specific gravity; 2) carbon and hydrogen both decrease with specific gravity; and 3) the total of oxygen, nitrogen, and sulfur rises regularly with specific gravity. There does not appear to be any specific relationship between uranium and any of the other components or properties of the pellets"

Breger and Deul conclude that the compositions of the pellets show similarities with low-rank coals. A survey of their data leads them to interpret "a non-marine and, therefore, a non-petroliferous origin for the pellets" (p. 24).

Similarities in volatile concentrations are insufficient to support a coal-extract origin. A wide range exists in volatile compositions for the various ranks of coal. As shown in Table 4 the organic ore at Temple Mountain might be assumed to be similar to coal. However, other possibilities exist.

The chemical structure of the organic ore is unknown. Infrared and chromatographic analy-

ses are unobtainable because of the relative insolubility of the material. Coals and indurate hydrocarbons, containing as their essential components carbon, hydrogen, and oxygen, will have at least some structural similarities which are reflected in part by similarities in some of the physical and chemical characteristics.

The lack of division between oil and coal has been emphasized by Dietrich (1956, p. 663) who states:

"Further, it would appear that the data presented here may suggest that contentions of workers like Schopf (18) and Berl (2) that there is no real division between oil and coal, that all suggested divisions are arbitrary, and that all these materials may be derived from essentially the same material are correct. Certainly all high rank materials (the end products?) have quite similar properties"

In consideration of the problem of classifying naturally occurring organic materials Schopf (1956) states:

"The distinction . . . (of coals) . . . from asphaltic rocks must be based largely on origin. In many instances this distinction is clear, but in other instances the origin of the carbonaceous material is obscure." (p. 522) . . . "For purposes of definition the demonstrable plant origin of organic matter in coal serves as a most convenient basis for distinguishing coal from asphaltic and certain kinds of graphitic rocks." (p. 526).

It has not been possible to demonstrate a plant origin for the organic matter in the urano-organic ore. In addition, it does not appear that the organic ore represents a coal extract, for the following reasons:

- (1) Approximately 99 per cent of the carbon in the ore is fixed. Only in coals of rank greater than medium volatile bituminous will more than 90 per cent of the carbon be fixed. Asphaltic pyrobitumens contain up to 85 per cent fixed carbon (impsonite, Abraham, 1920).
- (2) The X-ray spectrographic trace elements Cr, Ni, and Mn, which do not have a zonal distribution in the ore, are characteristic of both petroliferous substances and, locally, coals.
- (3) Differential thermal analyses of indurated hydrocarbons, low-rank coals, and the ore are not sufficiently characteristic to base a conclusion on analytical data alone.
- (4) A similarity of the indurated ore to low-rank coals, even if demonstrated, does not necessarily mean that the organic material was a coal extract at the time of emplacement and before induration. A petroliferous material could have undergone a metamorphism involving devolatilization and polymerization

that would result in an organic compound similar chemically to low-rank coals.

- (5) It is doubtful that extraction of organic materials from relatively insoluble carbonaceous compounds, after millions of years involving at least some leaching by ground water, will suddenly occur under unusual conditions that leave no evidence.
- (6) The sediments in the San Rafael Swell show essentially no metamorphism away from the collapse, the hydrothermal solutions were only moderate in temperature, and were not particularly concentrated in elements or complexes.
- (7) The sediments below the Chinle are essentially devoid of plant remains. Those of the Chinle, specifically the Moss Back within the ore deposits, are similar in all visible respects to plant remains outside of the mineralized area, which suggests no such unusual removal.
- (8) Coals in the Mancos shale and other overlying strata surrounding the San Rafael Swell represent typical low-rank coals.
- (9) The present remains of carbonaceous materials in the Chinle indicate that not enough organic material existed to form the large quantities of ore, particularly if there was some loss of volume on induration.
- (10) It is doubtful that a coal extract derived from the Chinle or above could be transported downward while the hydrothermal solutions were rising from depth to form ore in the Kaibab or equivalent.

The organic material could have originated by fractionation of a kerogen under the influence of heat and pressure, perhaps catalyzed by certain minerals and associated petroleum, as proposed by Crawford (1949) for gilsonite. However, this origin for the gilsonite in northeastern Utah, even though it is associated with the Green River shales, is not universally accepted. Some believe the gilsonite represents inspissation of petroleum (Murray, 1950). Hunt, Stewart, and Dickey (1954) demonstrated that the various indurated hydrocarbons of the Uinta Basin resulted from variations in the environment at the site of deposition.

The name thucholite was applied by Ellsworth (1928) to a primary hydrocarbon mineral from Parry Sound, Ontario; it is characterized by high percentages of uranium, thorium, and rare earths. The name has been extended subsequently to such uranium-bearing hydrocarbons as described by Barthauer, Rulfs, and Pearce (1953) from the Benser Mine, Ontario; Davidson and Bowie (1951) for several foreign localities; Joubin (1954) for the Blind River area, Canada; Robinson (1950) for the Goldfields

District, Saskatchewan; Kerr, Rasor, and Hamilton (1951) for Placerville, Colorado.

It is uncertain whether the ores at Temple Mountain and elsewhere are chemically similar to each other, or a thucholite type. There are

carbon is a prerequisite for the formation of thucholite. At Elk Ridge, Utah, polished surfaces from two localities show veinlets of urano-organic ore bordered by pitchblende (Kerr, Kelley, Bodine, and Keys, 1955). Field evidence

TABLE 5.—COMPARISON OF PHYSICAL PROPERTIES OF SOME ORGANIC MATERIALS

| Property | Temple Mountain asphalt | Urano-organic ore | Thucholite | Asphaltic pyrobitumen |
|------------------------------------|--|---|-----------------------------|-----------------------|
| Form | Massive to partially spherical fragments | Massive to pisolitic | Massive | Massive |
| Fracture | Uneven to subconchoidal | Uneven to subconchoidal | Subconchoidal to conchoidal | Hackly to conchoidal |
| Color | Black | Black | Black | Black |
| Luster | Vitreous | Subvitreous to vitreous | Subvitreous to vitreous | Vitreous |
| Streak | Fuscous | Fuscous, chaetura to fuscous black and chaetura black | Chaetura black | Brown to black |
| Specific gravity | 1.11-1.13 | 1.28-1.72 | 1.67-1.82 | 1.00-1.09 |
| Solubility in carbon tetrachloride | Soluble | Insoluble | Insoluble | Very slightly soluble |
| Hardness: | | | | |
| Range in Knoop's | 3-15 | 31.1-129.4 | 52.0-89.7 | 1.9-10.3 |
| Average in Knoop's | 8.15 | 71.9 | 65.5 | 6.5 |
| Moh's | -1 | 2-3 | 2-3 | -1 |

similarities in volatile concentrations (Table 4) and physical properties (Table 5) between the ore and thucholite. At least, thucholite and the ore represent a group of materials harder and denser than the insoluble petroliferous substances, asphaltic pyrobitumens. The increase in fixed carbon in the uranium-bearing organic material may be indicative of greater polymerization or devolatilization, which would account for the increase in hardness and specific gravity. This is also analogous to an increase in ranks of coal resulting from metamorphism.

Laboratory data are neither conclusive nor exclusive, but field evidence supports a petroliferous source for the organic constituents of urano-organic ore.

Extraction of uranium from solution.—Widespread, essentially nonuranium-bearing, low-rank coalified wood fragments are scattered through the ore horizon. These indicate the absence of radioactive minerals before the introduction of the organic ore. Davidson and Bowie (1955) and Spence (1930) believe that a radioactive source to react with the hydro-

suggests that the organic material in the Westwater Canyon Member of the Salt Wash near Grants, New Mexico, was accumulated before the introduction of uranium solutions along small faults and fractures.

A small amount of uranium in carbonized plant remains may result from the absorption of post-ore supergene-leached uranium. Previous chemical changes shown in silicified and pyritized logs and plant trash may make organic remains unresponsive to absorption.

Moore (1954) has shown that low-rank coals extract between 98 and 99.9 per cent of the uranium from uranyl sulfate solutions and 21 per cent from oil shale. The coalified fragments at Temple Mountain are low rank, but the extraction by coals relative to oils is not known.

The writers made an experiment to ascertain whether a uranium-saturated tar, when heated, might physically simulate the indurated urano-organic ore at Temple Mountain. A weight of 40.3 grams of natural semifluid tar from Temple Mountain was refluxed at 104° C. for 18 hours with 250 ml of 0.1844 molar acid uranyl sulfate

solution. After thorough washing and draining, the tar was heated for 96 hours at 250° C. Change in pH, concentration of the solution, and loss of weight were not determined in this experiment; its primary purpose was to determine whether the resulting asphaltic material contained uranium and became indurated. X-ray spectrographic analysis of the powdered asphalt yielded 1.05 per cent equivalent U₂O₈ and .x per cent Ni. The microhardness was between 2.5 and 26.0 Knoop (Moh's 1), and the indentation was more reliable than for heated nonuranium-bearing tar. Most of the "asphalt" dissolved in carbon tetrachloride at room temperature in a few minutes, but a small residue was insoluble after it was left in solution for a week. Differential thermal analysis revealed a similarity to the Temple Mountain asphalt. No crystalline compounds were revealed by X-ray diffraction. Some of the powdered material was leached for 20 hours in both concentrated nitric acid and ammonium hydroxide. X-ray spectrographic analysis of the leached material revealed 0.60 per cent equivalent U₂O₈. The leached material was only slightly soluble in carbon tetrachloride at room temperature. Apparently at an elevated temperature the Temple Mountain tar will extract uranium from a uranyl sulfate solution, and washing and leaching by strong acids and bases will not remove all the uranium absorbed or chemically combined with the organic material.

The development of the San Rafael Swell, which furnished the impetus for the petroleum migration, is considered to have taken place in post-Mancos time, probably post-Cretaceous, early Tertiary (Gilluly, 1929). Thus the folding probably occurred about 80 million years ago, the age of the "asphaltic type" ore at Camp Bird No. 13 Mine (Stieff, Stern, and Milkey, 1953), and probably during the period of the initial introduction of the petroleum. Only the early premineralization petroleum in contact with the ore solutions became urano-organic ore. Most of the nonuranium-bearing petroliferous materials at Temple Mountain were introduced after mineralization. The low uranium content of these materials in a few places may be attributed to absorption of post-ore supergene-leached uranium.

Induration of the organic ore.—Induration of the urano-organic materials accompanying emplacement of the uranium could have been accomplished by: (1) polymerization, (2) oxidation-devolatilization, or (3) a combination of the two. Davidson and Bowie (1951) and others proposed radioactive polymerization for the

induration of thucholite. However, this would not account for accompanying argillic alteration, carbonate replacement, and associated metallic mineralization.

In a summary of the problem of sulfate reduction in deep subsurface waters, Ginter (1934) outlined two methods of reduction of sulfate in solution, with attendant oxidation of hydrocarbon or carbonaceous material. The first is the reduction of sulfate to sulfide by the hydrocarbons, which in turn are oxidized to carbonate. In the absence of oxygen, this reaction would probably occur only at high temperatures. The second assumes that anaerobic micro-organisms cause sulfate reduction and oxidize hydrocarbons. Although sulfate-reducing anaerobes have been found in deep subsurface waters, the significance of the biochemical reactions has not been established.

Induration of petroleum may occur through long exposure to oxidizing conditions. Much of the nonuranium-bearing petroliferous material abundant on the San Rafael Swell was indurated in this way. However, it is much less indurated than the ore.

Hydrothermal conditions prevailed during the formation of thucholite, as indicated by Ellsworth (1928). Davidson and Bowie (1951) considered that thucholite belongs to a late hydrothermal stage. Kerr, Rasor, and Hamilton (1951) conclude that the urano-organic mineralization at Placerville, Colorado is hydrothermal. Abraham (1920) and others consider the formation of asphaltites and asphaltic pyrobitumens as the gradual conversion of petroleum under the influence of time, heat, and pressure.

Oil, air-blown in the vicinity of 145° C., will become indurated (Dr. G. Skaperdoes, Kellogg Corporation, personal communication). The semifluid tar at Temple Mountain will become indurated in time upon heating in an oxidizing atmosphere at temperatures of 200° C. and 250° C. In the experiments, the tar was heated in an oven at the given temperatures for consecutive arbitrary intervals (Table 6; Fig. 13, B). Temperatures were controlled to within 1° C. The greatest per cent loss of weight per hour at both temperatures occurred within the first hour and subsequently decreased with increased time of heating. Equilibrium was not established in 142 hours at 200° C. or 168 hours at 250° C. The per cent loss of weight was greater at any time at 250° C. than at 200° C. Physical changes occurred in the tar through time at both temperatures. It first became more viscous and then became indurated. Induration occurred earlier at 250° C. than at 200° C. The

TABLE 6.—PERCENTAGE LOSS OF WEIGHT IN TIME FROM HEATING SEMIFLUID TAR
Hardness is apparent. Comparison is relative. All indentations partially closed over after testing loss of weight in per cent.

| Time (hours) Accumulative | At 200°C. | | | | At 250°C. | | | |
|------------------------------|-------------------|-------------|------------------------------|---------|-------------------|-------------|------------------------------|---------|
| | Loss of weight | | Apparent hardness (Knoop) | | Loss of weight | | Apparent hardness (Knoop) | |
| | Accu- mulative | Per hour | Range | Average | Accu- mulative | Per hour | Range | Average |
| 1 | 1.27 | 1.27 | viscous | | 2.43 | 2.43 | viscous | |
| 25 | 5.24 | 0.21 | very viscous | | 10.26 | 0.41 | 4.2-18.6 | 11.2 |
| 96 | 8.66 | 0.09 | 2.4-4.4 | 3.4 | 11.74 | 0.12 | 7.8-13.3 | 10.4 |
| 142 | 12.01 | 0.08 | 1.5-29.6 | 10.7 | ... | ... | ... | ... |
| 168 | ... | ... | ... | ... | 12.77 | 0.08 | 2.6-59.0 | 20.4 |

TABLE 7.—METALLIC ELEMENTS IN THE ASH OF PETROLIFEROUS MATERIALS, SAN RAFAEL SWELL
After Erickson, Myers, and Horr (1954)

| Material | Per cent ash | U* PPM | Partial metallic composition of ash | | | | | | | |
|------------------------|--------------|------------|-------------------------------------|------|----------|----------|--------|-------|--------|------|
| | | | Fe | As | V | Cr | Zn | Ni | Cu | Pb |
| Viscous asphalt | 1.23-2.92 | 0.2-50 | .x-x. | | .x | .x | .0x | .x | .0x | .00x |
| Petroliferous rocks | 0.79-4.86 | 0.2-67 | .x. | | .x | .0x-.x | .0x-.x | .0x-x | .0x-.x | .0x |
| Asphalt | 2.32-13.61 | 30.0-1,137 | .x-x. | .x | .x | .00x-.x | .0x | .0x | .x | .0x |
| Uraniferous asphaltite | 17.0-62.0 | n.d. | x-x. | x | .0x-.00x | .0x-.00x | | .0x-x | x. | .x |

*Recalculated from: Per cent ash × per cent U in ash
10,000

Viscous asphalt: Two samples from the Moss Back at Temple Mountain and Flat Top Mesa.

Petroliferous rocks: Four samples from Temple Mountain and Flat Top Mesa. Two samples from the Moenkopi of Temple Mountain with a uranium content between 0.2 - 0.5 ppm. One sample from the Wingate at Temple Mountain; one sample from a slump block at collapse no. 1, Flat Top Mesa, with uranium content between 32 - 67 ppm.

Asphalt: Two samples from the Sinbad Limestone Member of the Moenkopi and the Moss Back Sandstone at Temple Mountain.

Uraniferous asphaltite: Two samples from Emery County, Utah.

indurated "asphalt" fractured conchoidally. In general appearance, the "asphalt" resembled the nonuranium asphalt material that naturally occurs at Temple Mountain. Microhardness tests of the artificial "asphalts" are not comparable to naturally occurring organic materials because of partial closure of the indentation after testing. However, they are relative, and comparison of hardness of the artificial materials may be made. There appears to be an increase in relative hardness with increased time of heating at both temperatures (Table 6; Fig. 13, C). The relative hardness was greater for any specific time at 250° C. than at 200° C. The minimum temperature of induration has not been established, since the hardening is related in part to time.

The induration of the urano-organic material

probably occurred under the influence of heat and the action of solutions rather than by radioactive polymerization. Whether the hardening resulted from oxidation-devolatilization, polymerization, or both processes together is unknown.

Metallic-element suite.—Erickson, Myers, and Horr (1954, p. 2213) report emission spectrographic analyses for the ash of two "uraniferous asphaltites" from the swell (Table 7), as characterized by high U, As, Cu, and Mo, and relatively low V. Among the metallic elements listed, there is a slight but noticeable increase of Fe, As, Cu, and Pb and a decrease in V in the ash of the ore compared with the ash of viscous asphalts, oil extracted from petroliferous rocks, and asphaltites.

X-ray spectrographic analyses of 12 samples

TABLE 8.—METALLIC TRACE ELEMENTS

Blank spaces and 0 indicate element not detected. Lower limit is approximately 0.1–0.3 per cent
A. Comparison of X-Ray Spectrographic Indications of Metallic Elements in Some Organic Substances

| Substance (and number of samples) | Per cent U ₃ O ₈ | Per cent Semiquantitative | | | | | | | | | | |
|--|---|---------------------------|--|------|------|------|------|------|------|------|------|--|
| | | Fe | Zn | As | V | Cr | Ni | Mn | Co | Se | Cu | |
| Temple Mountain Semifluid tar (1) "Asphalt" (4) | | .x | | — .x | | | — .x | | | | | |
| Urano-organic (12) Coalified plants (5) (in ore zones) | 1.8–15.0 | .x–x. | .x–x. | 0–x. | 0–x. | 0–x. | 0–x. | 0–x. | 0–x. | 0–x. | | |
| Thucholite (1) | 1.2 | x. | (Plus thorium, manganese, and rare earths) | | | | | | | | | |
| Indurated hydrocarbons Asphaltites (3) Asphaltic pyrobitumens (3) | | .x–x. | | | | | 0–x. | | | | 0–x. | |
| Some coals (4) (lignite to anthracite) | | .x–x. | 0–x. | | | 0–x. | 0–x. | | 0–x. | | 0–x. | |
| Ash (Temple Mountain) Semifluid tar (1) "Asphalt" (1) Urano-organic (1) | 15.5 | x. x. x. | .x | x. | x. | | .x | | | | | |

B. Analysis of X-Ray Spectrographic Indications of Metallic Elements in Temple Mountain Urano-Organic Ore

| Element | Per cent of samples having metallic element in: | |
|--|---|-------------|
| | .x per cent or less | x. per cent |
| Present in all samples | | |
| Fe | 33 | 67 |
| Zn | 75 | 25 |
| Present in over 90 per cent | | |
| As | 45 | 55 |
| V | 91 | 9 |
| Cr | 100 | ... |
| Present between 25–90 per cent | | |
| Ni | 100 | ... |
| Occasionally present (less than 25 per cent) | | |
| Mn | 67 | 33 |
| Co | 100 | ... |
| Se | 33 | 67 |

728

from 9 ore localities show a range in concentration of Fe, Zn, As, V, and Cr (Table 8). Nickel was found in half of the samples, and Mn, Co, and Se were noted in a few. Uranium concentration in the specimens selected ranged between 1.8 and 15.0 per cent equivalent U₃O₈.

TABLE 9.—X-RAY SPECTROGRAPHIC DISTRIBUTION WITH RELATION TO THE COLLAPSE AREA

| Element | Average concentration of elements (per cent) | | |
|-------------------------------|--|--------------------|---------------|
| | Calyx area | Bordering collapse | Collapse area |
| As* | 2.0 | 3.7 | 5.0 |
| U ₃ O ₈ | 5.4 | 3.5 | 3.0 |
| V* | 2.0 | 0.5 | 0.5 |
| Zn* | 2.8 | 0.5 | 0.5 |

* Average concentration: considering for each sample .x per cent = 0.5 per cent and x. per cent = 5.0 per cent. Uranium is recorded as average per cent equivalent U₃O₈.

The ash of one specimen revealed the same suite, with the exception of chromium. There was some loss on ashing. However, 97.5 per cent equivalent U₃O₈ in nonashed material was present in the ash.

Emission spectrographic analyses of the ash (Erickson, Myers, and Horr, 1954) and X-ray spectrographic analyses of the nonashed ore differ somewhat, because of differences in the technique and sensitivity of the two methods, as well as either loss or concentration of elements upon ashing. Copper has not been detected with the X-ray spectrograph, but contamination by the equipment may mask small amounts of this element. Copper minerals are rarely present in the mining district. Molybdenum may be present in amounts less than approximately 0.2 per cent, the lower sensitivity of the experimental method used. Vanadium is characteristic of the metallic-element suite, but most of the vanadium is probably volatilized on ashing.

ZONAL DISTRIBUTION OF ELEMENTS: Variations in concentration of some of the metallic elements appear to reflect a zonal distribution with relation to the collapse area. Cobalt, selenium, and high-arsenic concentrations are found near or within the collapse and possibly locally along some faults. Cobalt has been detected from two of the nine localities tested. One of these is at the eastern edge of the collapse, and the other is in a fault zone in the

calyx area (Lopez Incline). Selenium has been detected from the locality at the eastern edge of the collapse. Both of these elements may be present in the ore in concentrations below the sensitivity of the experimental method, as indicated by the presence of cobalt bloom in several mines and the widespread occurrence of the selenium indicator plant *Astragalus*. Cannon and Stillman (1952, in Keys and White, 1956) report high selenium content of the organic ores. Arsenic is present in more than 90 per cent of the samples. Ore from the calyx area yields concentrations generally of the order of .x per cent. A few yield x. per cent. Samples of ore from the collapse and surrounding area yield concentrations generally on the order of x. per cent; a few show .x per cent (Table 9).

In contrast, the average amounts of uranium, vanadium, and zinc seem to increase away from the collapse (Table 9). It had previously been reported that vanadium is more concentrated in the collapse (Keys, 1955; Keys and White, 1956). The concentrations of Fe, Cr, Ni, and Mn are irregularly distributed.

SOURCE OF METALLIC ELEMENTS: Erickson, Myers and Horr (1954) report trace-element analyses, as well as chemical determinations of uranium and other metals in petroliferous materials from many localities. Analytical data are given for 78 samples described as crude oil, petroliferous rock, asphalt, and asphaltite. The ash from asphalt and oil extracted from petroliferous rocks contains a nearly constant suite of metals: U, Co, Cr, Cu, Mn, Mo, Ni, Pb, V, and Zn. Ash from petroleum shows that V and Ni are the most abundant metallic elements, although Ag, W, As, Sn, and Au may be present. Crude oils from various localities are characterized by an abundance of particular elements. These metals are thought to be concentrated in the asphaltic fraction of petroleum.

The collapse and, to a lesser extent, faults represent the major channels for hydrothermal solutions, as indicated by the spatial distribution of alteration in the area (Kerr, Bodine, Kelley, and Keys, 1957) and argillite alteration in the ore horizon (Kelley and Kerr, 1957). Elements showing a zonal distribution with relation to the collapse are As, Co, Se, U, V, and Zn. Of these elements, only As and Se are not characteristic of the metallic suite of the ash of most petroliferous materials. Thus, with the exception of As and Se, the above metallic elements could have been derived from the organic materials present in the district by some mechanism of concentration. Erickson, Myers, and Horr (1954, p. 2216–2217) state:

be representative of the minute included metallic minerals formed by the action of the original material on hydrothermal solutions carrying these elements.

The irregular distribution of low concentra-

tionally microscopic and submicroscopic uraninite is present in all the ore. Such lines are also present in thucholite from Besner Mine, Ontario, in which zinc was not detected by the X-ray spectrograph.

TABLE 11.—X-RAY DIFFRACTION OF NATIVE ARSENIC
X-ray diffractometer, Cu/Ni

| Collapse border Camp Bird Mine No. 7 | | | | Collapse Fumarole Claim? | | Echizen Province Japan | |
|--------------------------------------|-----|----------------------|-----|--------------------------|------|------------------------|------|
| Nodule | | Disseminated in ore* | | Band in nodule† | | | |
| d(Å) | I | d(Å) | I | d(Å) | I | d(Å) | I |
| 3.504 | 74 | 4.247q | 15 | | | | |
| 3.330q | 6 | 3.504 | 22 | 3.516 | 13.4 | 3.516 | 18 |
| | | 3.336q | 85 | 3.336q | 11.2 | | |
| 3.108 | 7 | 3.097 | 19 | 3.108 | 6.4 | 3.198c | 10.0 |
| 3.066c | 4 | | | | | 3.108 | 3.6 |
| 2.769 | 100 | 2.761r | 100 | 2.776 | 100 | 3.066c | 1.2 |
| | | | | | | 2.776 | 100 |
| 2.045 | 53 | 2.043r | 42 | 2.047 | 19.6 | 2.540c | 3.5 |
| | | | | | | 2.047 | 26.3 |
| 1.875 | 44 | 1.871r | 39 | 1.876 | 22.5 | 1.959c | 1.6 |
| 1.763 | 18 | 1.763 | 14 | 1.766 | 7.8 | 1.878 | 24.5 |
| 1.653 | 8 | 1.653 | 12 | 1.769 | 9.3 | 1.769 | 9.3 |
| 1.550 | 21 | 1.549r | 17 | 1.656 | 5.3 | 1.656 | 5.5 |
| | | | | 1.552 | 8.5 | 1.553 | 11.1 |

c = contaminant impurities unidentified, q = quartz, r = realgar.

* Separated from ore by tetrabromethane settling and Frantz Isodynamic Separator. Partical size 60-120 mesh. Associated realgar lines are removed.

† From Kerr and Lapham (1954).

tions of Ni and Mn, which are not represented by primary minerals and are elements characteristic of organic materials, may indicate a source from the organic materials. Although the irregular distribution of low concentrations of Cr in the ore may also indicate an organic source for this element, the localized distribution of chromium mica clay (Kerr and Hamilton, 1958) in faults and near or within the collapse also may reflect transportation by late hydrothermal solutions. The widespread distribution of moderate concentrations of iron and the various generations of pyrite are indicative of a multiple source for that element.

METALLIC MINERALS OF THE ORE

General Statement

Two types of mineral assemblages occur in the ore. The first consists of host-rock particles,

uraninite, and montroseite, with secondary alteration products, realgar, orpiment, and jarosite. The two most abundant contaminants are quartz and pyrite.

X-ray powder-camera patterns of the ore are generally indistinct. However, X-ray diffractometer patterns of the urano-organic material yield lines corresponding to uraninite or sphalerite or both (Table 10). Pyrite is usually present. The spacings and intensities are such that many of the pyrite lines can be separated from those of uraninite-sphalerite. Sphalerite and uraninite concentrations of less than 1 or 2 per cent are not detected by the X-ray diffractometer technique used; however, the stronger X-ray reflections that could correspond to either of the two minerals are present everywhere in the ore. Uranium was present in more than 1.8 per cent equivalent U_2O_5 in samples, but zinc concentrations ranged from .X to X. per cent. Probably at least some

present also in the heavy minerals separated from organic material in drill cores taken at depth in the collapse area. Alteration of the arsenic resulted in coatings of realgar and orpiment. Partial X-ray-diffraction patterns of native arsenic are shown in Table 11.

TABLE 12.—X-RAY MEASUREMENTS FOR HEAVY-MINERAL MIXTURE
Camp Bird Mines

Separated from ore by tetrabromethane and Frantz Isodynamic Separator. X-ray diffractometer, Cu/Ni. Black grains which yield on X-ray spectrographic analysis xx. per cent Fe and As, x. per cent Zn and V, and 0.x per cent U, Ni, Mn, and Cr. vb = very broad line.

| d(Å) | I | Possibilities |
|-----------------|-----|---|
| 8.42 | 4 | Unknown |
| Very weak lines | | |
| 3.34 | 9vb | Quartz |
| 3.12 | 8 | Pyrite, sphalerite |
| 2.94 | 3 | Loellingite |
| 2.88 | 2 | Loellingite |
| 2.76 | 5 | Native arsenic |
| 2.70 | 7 | Pyrite |
| 2.60 | 3 | Loellingite |
| 2.34 | 10 | Loellingite, pyrite |
| Very weak lines | | |
| 2.04 | 1 | Native arsenic, loellingite |
| Very weak lines | | |
| 1.88 | 2 | Native arsenic, loellingite, sphalerite, pyrite |
| 1.81 | 1 | Unknown |
| 1.65 | 1 | Unknown |
| 1.62 | 3 | Pyrite, sphalerite, loellingite |
| 1.59 | 2 | Loellingite |

The identified metallic minerals may be discussed on the basis of the significant metallic elements.

Arsenic Minerals

Kerr and Lapham (1954) originally identified native arsenic in a band from a nodule taken from the collapse (Fig. 18, G). Native arsenic is relatively abundant in the ore zone at the Camp Bird mines north of the western collapse area. The arsenic not only forms as clusters of microscopic crystals (Pl. 3, figs. 3, 4) but as nearly solid nodules with dimensions up to 1 cm (Fig. 18, H, I) and as thin stringers and irregular patches. Minor native arsenic is

present also in the heavy minerals separated from organic material in drill cores taken at depth in the collapse area. Alteration of the arsenic resulted in coatings of realgar and orpiment. Partial X-ray-diffraction patterns of native arsenic are shown in Table 11.

Native arsenic has been found at a number of localities in the United States (Palache, Berman, and Frondel, 1944). Periodic deposition of the metal is common. Examples would be the reniform masses in Arizona (Warren, 1903) and concentric layered deposits near Montreal, Canada (Evans, 1903). Both of these occurrences are considered the result of "fumarole action." In general, native arsenic is believed to be deposited from hydrothermal solutions.

Sedimentary rocks range in average arsenic content from 1 to 2 ppm for limestones and sandstones and up to 10 ppm for shales (Onishi and Sandell, 1955). Arsenic increases with organic content; some organic shales contain as much as 59 ppm. Some pyrite contains up to 450 ppm. The distribution of arsenic in sedimentary rocks is believed to reflect arsenic carried up from depth by thermal springs and volcanic exhalations, probably in the form of a chloride or oxide (Onishi and Sandell, 1955). Spectrographic analyses of the ash of various petroliferous materials yield arsenic contents ranging between .x and x. per cent on the average (Erickson, Myers, and Horr, 1954). The possibility exists that the arsenic at Temple Mountain may have been derived from the organic materials. However, the zonal distribution of the element in the ore and the restriction of occurrences of native arsenic near the collapse favor hydrothermal solutions.

The abundance of pyrite and the presence of other sulfides associated with the ore suggest the system Fe-As-S. The presence of an iron arsenic mineral is suggested by X-ray-diffraction measurements of metallic mixtures separated from high-arsenic-bearing ore. One such pattern is shown in Table 12. X-ray spectrographic analysis of this heavy black-mineral aggregate yielded iron and arsenic concentrations on the order of xx. per cent. Sulfur is present qualitatively. Native arsenic and pyrite are present in the ore from which this material was separated. A number of the X-ray spacings suggest loellingite-leucopyrite. Similarly, arsenopyrite has not been conclusively identified, although suggestive X-ray patterns have been obtained. X-ray spectrographic analyses of pyrite from ore zones yield arsenic on the order of .x per cent. Possibly the arsenic

is in solid solution. The assemblage pyrite-arsenic-arsenopyrite suggests temperatures between 320° C., the melting point of realgar, and 675° C., the melting point of arsenopyrite at 1

TABLE 13.—PARTIAL X-RAY-DIFFRACTION MEASUREMENTS OF IRON SULFIDES

| Pyrite* | | Marcasite† | |
|-----------------------|----------------------|-----------------------|----------------------|
| Range in spacing d(Å) | Range in intensity I | Range in spacing d(Å) | Range in intensity I |
| 3.11-3.12 | 26-34 | 3.42-3.48 | 50 |
| 2.70 | 100 | 2.69-2.71 | 100 |
| 2.42 | 59-78 | 2.41-2.43 | 30-40 |
| 2.20-2.21 | 41-45 | 2.31-2.33 | 30-40 |
| 1.91 | 38-47 | 1.91-1.92 | 30-40 |
| 1.80-1.84** | 3-6 | 1.76-1.77 | 90 |
| 1.63 | 70-99 | 1.72-1.73 | 10 |
| 1.56 | 6-12 | 1.70 | 10-20 |
| 1.50 | 10-18 | 1.67-1.68 | 10 |
| 1.44-1.45 | 16-22 | 1.59-1.60 | 20-30 |
| 1.24 | 6-12 | (very faint lines) | |
| 1.20-1.21 | 6-12 | 1.43-1.44 | 10-30 |
| 1.18†† | 6-12 | 1.37-1.38 | 5-10 |
| | | 1.23 | 10 |
| | | 1.17 | 20 |

* X-ray diffractometer, Cu/Ni

† X-ray powder film, Cu/Ni

** Contaminant present in all patterns

†† hkl (421) used for estimate of unit cell dimensions. Actual measurements for four pyrites were 1.179, 1.180, 1.181, and 1.182 Å.

atmosphere pressure. In nature, however, increased pressure from the load of overlying sediments and the effects of water on the system would lower this temperature range somewhat.

The native arsenic at Temple Mountain is believed to have been derived from the ore solutions under elevated temperatures, inferred from other occurrences of the metal and the probable conditions of deposition in the presence of iron and sulfur.

Iron Minerals

Pyrite, the most abundant metallic mineral associated with the ore, appears in three generations. An earlier, pre-ore pyrite is associated with organic materials, particularly coalified wood (Pl. 2, figs. 1, 2; Pl. 3, fig. 2). The pyrite core of nodules, about which clay minerals and urano-organic materials have

accumulated (Fig. 18), may also be of pre-ore age but later than that associated with the wood. The second generation of pyrite is that deposited during uranium mineralization and forms in zoned pods and pisolites containing ore and as crystals disseminated in the ore (Fig. 18; Pl. 1, fig. 2; Pl. 3, fig. 6). A third generation of post-ore pyrite is represented by a few streaks cutting ore masses.

Small amounts of marcasite may be present throughout the mining district, but the most noticeable occurrences are near or within the collapse. Bands of marcasite up to half an inch thick are present in fractures in cores from the collapse (Pl. 1, fig. 6). These are not associated with the ore. Marcasite is mixed with pyrite in ore-bearing nodules from the collapse (Fig. 18, D). Away from the collapse, it forms small radial clusters within pyrite-replaced coalified wood.

X-ray-diffraction measurements of some pyrite and marcasite from Temple Mountain are shown in Table 13. Pyrite associated with the ore contains arsenic in quantities ranging between .x and x. per cent. The lattice constant a_0 determined on the basis of hkl (421) averages 5.413 Å and ranges from 5.408 Å to 5.417 Å for four pyrites. The lattice constants for two pyrites listed on the ASTM Index Cards are 5.4046 Å and 5.407 Å. Kerr, Holmes, and Knox (1945) give the lattice constant a_0 for pyrite from Leadville as 5.40667 ± .00007 Å. The pyrite from Temple Mountain has slightly larger cell dimensions. This may result from the presence of arsenic in the lattice. According to a summary of the occurrence of minor elements in some sulfide minerals (Fleischer, 1955), the average arsenic content of sedimentary pyrites is 600-900 ppm and of hydrothermal pyrites 400-700 ppm. There is more arsenic in low-temperature vein pyrite than in higher-temperature vein pyrite. Neuhaus (*in* Fleischer, 1955) reported 5 per cent arsenic in pyrite with a unit cell of 5.442 Å. The general belief is that the arsenic is present in true solid solution and causes the increase in cell dimension.

Both marcasite and pyrite are found in many sedimentary deposits. From a study of the effect of temperature and acidity on the formation of marcasite and wurtzite, Allen, Crenshaw, and Merwin (1914, p. 430-431) concluded that the unstable forms, marcasite and wurtzite, formed from acid solutions. However, they were usually mixed with the corresponding stable forms, pyrite and sphalerite. The higher the maximum temperature

of the experiment, if other conditions remain unchanged, the greater the quantity of the stable forms. The higher the acidity, if other conditions remain unchanged, the greater the quantity of the unstable forms. Acid concentration necessary to give rise to pure marcasite

of galena, however, may be indicated in the calyx area on the basis of X-ray diffraction of some turbid urano-organic material (Table 14). Galena occurs in small crystals and nodular-

TABLE 14.—X-RAY DIFFRACTION MEASUREMENTS OF TWO VARIETIES OF URANO-ORGANIC MATERIAL

From small amounts picked from a polished surface. Angles of reflection of galena followed by their intensities are from Swanson and Fuyat (1953).

| Clear gray | Turbid gray | | Possibilities |
|------------|-------------|------|-----------------------|
| | d(Å) | I | |
| 5.25 | 6 | | Unknown |
| | | 3.44 | Galena (3.429-84) |
| 3.34 | 1 | | Unknown (?quartz) |
| 3.13 | 1 | 3.13 | Uraninite, sphalerite |
| | | 2.99 | Galena (2.969-100) |
| 2.73 | 1 | 2.72 | Uraninite |
| | | 2.11 | Galena (2.099-57) |
| 1.92 | 1 | 1.92 | Uraninite, sphalerite |
| | | 1.80 | Galena (1.790-35) |
| 1.65 | 1 | 1.64 | Uraninite, sphalerite |

falls with the temperature and is close to neutrality at ordinary temperatures. Marcasite, therefore, may be expected to be deposited from acid solutions, or conversely, "... it becomes evident that the alkaline nature of the water, irrespective of the temperature, its sufficient to condition the formation of pyrite" (Allen, Crenshaw, and Merwin, p. 428). The temperature of formation of a specimen of natural marcasite from Obira, Japan, has been recorded as 279° C. on the basis of liquid inclusions (Ingerson, 1955).

The alternation of bands of pyrite and marcasite in a nodule from the collapse may indicate local changes in pH. Bernauer (1935) noted that marcasite altering with pyrite resulted from volcanic exhalations. If the temperature of the ore solutions was slightly elevated, the pH of the solutions at the time of deposition was neutral to slightly acidic, rather than alkaline. This interpretation would agree with the solution of carbonate below the Moss Back.

Lead Minerals

Lead has not been determined by X-ray spectrographic analyses of the ore. The pres-

TABLE 15.—X-RAY-DIFFRACTION MEASUREMENTS OF MONTROSEITE

| Montroseite Temple Mountain* | | Montroseite Weeks <i>et al.</i> (1953) | |
|------------------------------|-----|--|----|
| d(Å) | I | d(Å) | I |
| 4.29q | 4 | 4.75 | VF |
| 3.37q | 10b | 4.31 | S |
| 2.95u | 2 | 3.38 | M |
| 2.63 | 9 | 2.644 | S |
| 2.47 | 4 | 2.495 | M |
| 2.41 | 1 | 2.423 | W |
| 2.20 | 3 | 2.217 | M |
| 2.15 | 2 | 2.151 | F |
| 1.96 | 1 | 1.965 | W |
| 1.93 | 1 | 1.918 | W |
| | | 1.841 | Fb |
| | | 1.731 | W |
| | | 1.689 | W |
| 1.62 | 1 | 1.605 | W |
| 1.50 | 1 | 1.512 | M |
| 1.47 | 1 | 1.467 | W |
| 1.41 | 1 | 1.391 | W |
| | | 1.302 | F |
| | | 1.282 | F |

* X-ray diffractometer, Cu/Ni. q = quartz contamination, u = unknown, b = broad line. Separated from ore. Black grains, opaque with submetallic luster and black streak. X-ray spectrograph yields xx. per cent V and x. per cent Fe.

like clusters of crystals found in drill cores from the upper Coconino and possibly Kaibab in the collapse. However, ore has not been found in association with these occurrences.

Uranium Minerals

Uraninite (var. pitchblende) is present in small amounts throughout most of the ore at Temple Mountain. It generally occurs as small crystals and irregular grains scattered at random throughout masses of ore (Fig. 18, E). These small particles furnish radioactive centers for autoradiographic reactions on polished surfaces. Radiation emanates from small light-gray hard grains. If nuclear-track plates are used, black reactions indicate particles of uraninite; elsewhere the tracks are irregularly scattered and in a few places ir-

regularly concentrated throughout the urano-organic material. Large masses of this mineral have not been noted. Only rarely have grains been identified on the order of 1 or 2 mm in diameter.

Although uraninite is well known as a replacement of fossil wood elsewhere, all urani-

TABLE 16.—X-RAY-DIFFRACTION MEASUREMENTS OF SPHALERITE

| Sphalerite Temple Mountain* | | Sphalerite A.S.T.M. index card 5-0566 | |
|-----------------------------|----|---------------------------------------|-----|
| d(Å) | I | d(Å) | I |
| 3.343q | 2 | | |
| 3.124p | 10 | 3.123 | 100 |
| 2.708p | 3 | 2.705 | 10 |
| 2.415p | 1 | | |
| 2.209p | 1 | | |
| 1.911 | 8 | 1.912 | 51 |
| 1.629p | 5 | 1.633 | 30 |
| 1.559 | 1 | 1.561 | 2 |
| 1.443p | ½ | | |
| 1.348 | ½ | 1.351 | 6 |
| 1.241 | 1 | 1.240 | 9 |
| | | 1.209 | 2 |
| 1.1040 | 1 | 1.1034 | 9 |
| 1.0412 | 1 | 1.0403 | 5 |
| 0.9567 | ½ | 0.9557 | 3 |
| 0.9139 | ½ | 0.9138 | 3 |

* X-ray powder film, Cu/Ni. Contaminants are q = quartz, p = pyrite.

nite identified from specimens examined is restricted to the urano-organic ore that shows no cell structure and has a texture indicative of a fluid or semifluid state at the time of deposition.

Vanadium Minerals

The source of secondary vanadium minerals appears to be in part from montroseite, which has been identified by Weeks, Cisney, and Sherwood (1953) from the Rex No. 2 mine and from Calyx Hole mine No. 8 (Table 15). At the latter locality, it occurs mixed with the urano-organic ore. Separation of the heavy-mineral fraction and subsequent purification with the Frantz Isodynamic Separator yields material satisfactory for identification. Examination of the heavy minerals separated from the ore at other Calyx-South Workings localities may reveal that montroseite is more common than is here noted.

“Montroseite is the least oxidized vanadium mineral thus far found in the Colorado Plateau uranium-vanadium ores, and it is thought to be a primary mineral” (Weeks, Cisney, and Sherwood, 1953, p. 1241). Garrels (1953) considers V_2O_5 (or its hydrate) the lowest-valent vanadium oxide expected. It should occur under reducing conditions common in nature and oxidize to the next-higher-valent vanadium oxide at about the same potential necessary to convert sulfide ion to sulfate. It would be represented in the “... original montroseite-pyrite-pitchblende type of ore” (Garrels, 1953, p. 1265).

Zinc Minerals

Kerr and Lapham (1954) found sphalerite in an arsenic-bearing nodule, disseminated in quartz and pyrite (Fig. 18). It forms small crystals and irregularly shaped particles scattered through the ore. Ore containing relatively abundant sphalerite particles contains Zn in concentration on the order of x. per cent. Rarely, stringers of sphalerite cut pyrite that has replaced rims of silicified logs. In a few cases, sufficient material can be isolated from these occurrences for X-ray diffraction (Table 16). Optical, etch (Short, 1940), and microhardness properties are similar to disseminated particles of sphalerite found in the ore (Pl. 3, fig. 6). Zinc is concentrated on the order of xx. per cent. Determinations of the lattice constants are approximate because of quartz and pyrite lines in the patterns. However, on the basis of one X-ray pattern, the (hkl) spacing (531) gives a_0 5.407 Å.

Attempts at separation and purification of the small quantities of sphalerite were abandoned because of the fine size, sporadic distribution, and, in many samples, mixture with fine particles of quartz and pyrite. Sufficient material was not found for flotation and froth separations. Thus sphalerite has not been used as a geological thermometer (Kullerud, 1953). The FeS content on the basis of the lattice constant given above would be on the order of 25 per cent. This would yield an anomalous temperature.

Sphalerite reported in the presence of excess iron sulfide (pyrite) at the Happy Jack mine in White Canyon, Utah, and the Hidden Splendor mine (Delta mine) in the San Rafael Swell results in temperature determinations of less than 138° C. (Coleman, 1957).

Recently, some doubt has been expressed concerning the accuracy of the Kullerud

method, and the question of the effect of water and other components on the FeS-ZnS system is discussed in the literature (Fryklund and Fletcher, 1956; Kullerud, 1956). Even if purification of the Temple Mountain sphalerite at depth. It does not appear to be influenced in deposition by organic material.

Galena from the upper part of the Coconino has been obtained in drill cores in the collapse. It may be present locally in minor amounts

TABLE 17.—HEAVY METALLIC MINERALS SEPARATED FROM SELECTED ORE ZONES

Particle size was between 60–120 mesh. Separation was by tetrabromethane settling and Frantz Isodynamic Separator. Identification was by X-ray diffraction.

| Locality | Metallic minerals | Metallic-element concentration of separations (average)* | | |
|--|---|--|-------|-----------------------|
| | | xx. | x. | .x |
| Collapse (DDH V-5; 777 feet) | Arsenic†, marcasite†, pyrite†, unknown | Fe | As | Cu, Mn, Sr, Zn |
| Collapse border (Camp Bird Mine No. 7) | Arsenic†, (realgar)†, pyrite†, sphalerite-uraninite, unknowns | As, Fe | Zn, V | Cr, Mn, Ni, U |
| Calyx Mine area (Calyx Mine No. 8) | Montroseite†, pyrite†, sphalerite-uraninite | V, Fe | | As, Cu, Mn, Ni, U, Zn |
| Flat Top Mesa (north end) | Arsenic, pyrite, sphalerite-uraninite, unknowns | Fe | As | Cu, Mn, Ni, U, V, Zn |

* Metallic-element concentration was by X-ray spectrograph.

† Most abundant.

is possible, it is doubtful that the resulting determination of FeS content and temperature would be reliable. Pyrite is the only mineral on which the presumption may be made that FeS saturation existed during deposition of the sphalerite. Whether pyrite is as reliable an indicator as pyrhotite has not been established, although it is being used on the Colorado Plateau (Coleman, 1957). The pyrite at Temple Mountain occurs in several generations and probably cannot be used.

* Distribution of Metallic Minerals

Arsenic, uraninite, sphalerite, and montroseite occur in and near urano-organic ore masses. Arsenic occurs in cores at depth as indicated by arsenic sulfides assumed to represent oxidation of the native metal. A common origin is indicated for As, Zn, V, and U, and an affinity for the organic material in representative metallic minerals is found.

Pyrite and marcasite may occur independently or associated with the ore. Various methods of deposition explain pyrite distribution. Most marcasite not associated with ore occurs near or within the collapse, particularly

in the ore horizon. Deposition probably occurred accompanying the introduction of the other metallic elements.

ZONING: Ores with a relatively high concentration of metallic elements generally exhibit metal-bearing minerals. Lateral zoning by metallic elements is reflected in the mineral content of the ore (Table 17). Vanadium, which increases in the ore away from the collapse, yields occurrences of montroseite in the Calyx area. Uraninite and sphalerite are widely distributed in the ore, both near and away from the collapse. The increase in uranium and zinc in the ore away from the collapse reflects the concentration of the urano-organic material in the calyx area (Fig. 6). Arsenic, which increases in concentration in the ore toward the collapse, appears as native arsenic. No primary minerals of cobalt and selenium have been identified.

Data are inadequate to establish vertical zoning. Galena is found at depth in the collapse, whereas native arsenic, marcasite, and pyrite occur with mineralized organic material from the Kaibab or equivalent depth. The three are also present in the ore horizon.

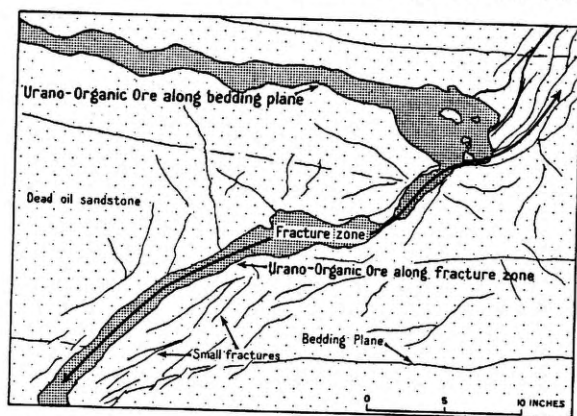


FIGURE 14.—URANO-ORGANIC ORE ALONG BEDDING AND FRACTURE

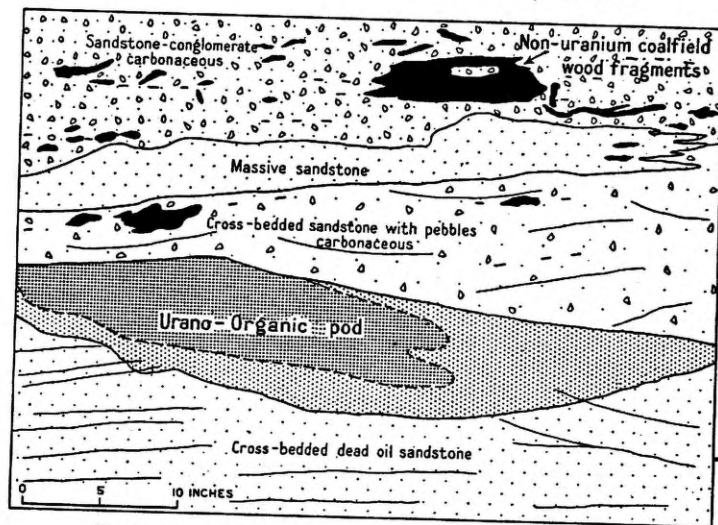


FIGURE 15.—URANO-ORGANIC ORE POD ALONG LITHOLOGIC CONTACT

ORE AGGREGATES

General Statement

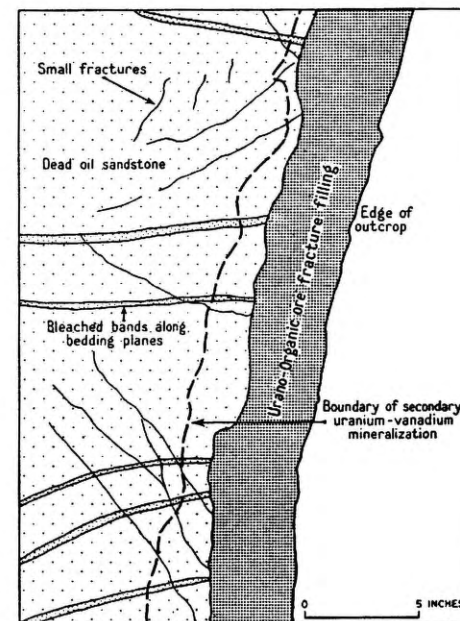
The urano-organic materials occur as interstitial disseminations, pisolites, masses, streaks, and bands. Distribution occurs along bedding planes, lithologic contacts, in porous beds, on fractures, and along faults (Figs. 14-16). The

greatest concentrations occur in permeable horizons and along lithologic contacts.

Two common ore forms occur in about equal abundance. The first consists of irregularly shaped masses which range from disseminated particles 0.2 mm thick to replacement masses several feet across. Ore also occurs in pisolites that are elliptical to spherical and range from minute spherules a millimeter in diameter to pods more than a foot across.

Pisolitic forms identical to those of the San Rafael Swell are found at Elk Ridge, Utah, in urano-organic materials (Kelley, D. R., Oertel, E., and Wichtner, J., 1953, unpub. U.S.A.E.C. Project Rept.), and Erickson,

pellets and interstitial streaks coalesce to form pellet groups or larger single pellets and larger streaks or irregular patches of up to 2 cm in diameter. The outlines of the forms of the first stage are generally preserved (Fig. 17, D).

FIGURE 16.—URANO-ORGANIC ORE ALONG FRACTURE
Lower Wingate, South Temple Mountain

Myers, and Horr (1954) mention solid "asphaltite pellets", containing as much as 1.6 per cent uranium, found by the U. S. Geological Survey in well cuttings from the Panhandle gas field near Amarillo, Texas. The writers recognize the following sequence in the development of large ore masses.

- (1) Initial replacement occurs at the expense of the interstitial clay cement and extends to detrital grains. The mineralization develops principally parallel to bedding along more permeable zones, or secondarily along fracture or fault trends. It forms with relatively sharp as well as irregular external boundaries. In the initial replacement, either small pellets less than a few millimeters in diameter form with sharp boundaries (Fig. 17, A) or irregular interstitial streaks and disseminations form irregular boundaries (Fig. 17, B).
- (2) Further replacement occurs at the expense of the detrital grains. During this stage, the smaller

- (3) A final stage is represented by large pellets, pods, patches, and streaks of more than a few centimeters in diameter, in which the detrital grains consist of a few scattered, corroded remnants. The outline of the smaller forms may be preserved by stringers of carbonate or clay that fill contraction fractures developed around the relict boundaries (Fig. 17, E). However, a massive body of urano-organic material generally results (Fig. 17, F).

Concentric development of pisolites is common. Massive and crystalline pyrite and, to a lesser extent, clay may form the nucleus of a nodule (Fig. 18, B, E). Subsequent alteration during the last stages of hydrothermal activity may convert the sulfide to the sulfate, jarosite (Fig. 18, F). The clay and pyrite cores are slowly replaced as the organic material accumulates. Nodules may be composed of one type of organic material (Fig. 18, A),

or they may show concentric bands of slightly different organic materials, in part translucent, in part opaque (Fig. 18, B). Concentric banding is seen in some larger disseminated ore masses.

Nodules composed of metallic minerals in which the ore is either absent or constitutes a minor portion are much less common. Pyrite nodules in which organic material and other

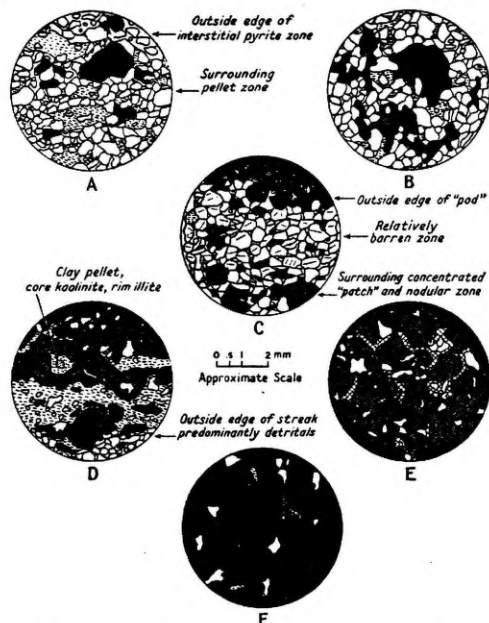


FIGURE 17.—DIAGRAMMATIC DEVELOPMENT OF MASSES OF URANO-ORGANIC MATERIAL
Moss Back Sandstone of Temple Mountain

A. Zone of scattered nodules of urano-organic material surrounding a large interstitial pyrite saturated body. Cement is dominantly intermixed kaolinite and illite.

B. Irregular interstitial patches of urano-organic material replacing clay cement

C. Border of large urano-organic pod showing narrow barren zone separating the edge of pod made up of coalescing nodules and the surrounding thin zone of patches and nodules of organic material

D. Coalescing of urano-organic patches and a few nodules to form streaks of ore along bedding planes. Ore associated with strong illitization.

E. Almost complete coalescing of patches and nodules to form masses of urano-organic material. Thin stringers of carbonate outline and in a few places penetrate small bodies of ore.

F. Massive ore with remnants of detrital grains and thin stringers of clay

No attempt was made to represent minute amounts of metallic minerals. Urano-organic material is dark stippling. Pyrite is lighter stippling. Clays are dashed (dominantly illite). Carbonates are cross-hatched. Detrital grains are outlined.

The ore mass may be surrounded by accretions of pisolitic or irregular forms, or a single zone of isolated pellets, or small interstitial streaks or patches. In some cases, a relatively barren zone of a few millimeters may separate the pod from the surrounding aggregate pellet zone (Fig. 17, C). In a few cases a partially spherical zone of scattered pellets and patches may be surrounded by a zone of interstitial pyrite (Fig. 17, A).

metallic minerals are absent are scattered throughout the district. Other metallic nodules in which the ore occurs as scattered inclusions and in a few places as rims are the least common and seem to be restricted to the collapse and immediate surroundings (Fig. 18, D, E, H, I). Cyclic deposition, as indicated by repetition of concentric mineral bands, is shown in the arsenic-bearing nodule described by Kerr and Lapham (1954) (Fig. 18, G), in which two

generations of pyrite-sphalerite occur, and by the alteration of pyrite and marcasite in nodule 4 (Fig. 18). The concentric banding and cyclic deposition reflect local changes in the intensity,

any theory of detrital origin. In general, the presence of pyrite, clay, or silica core, particularly in the larger forms, and the spherical shape suggest the necessity of a nucleus for the

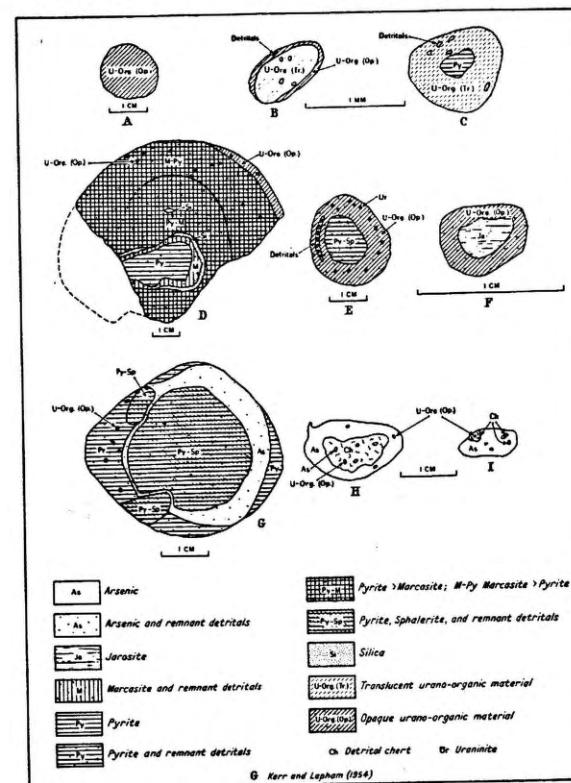


FIGURE 18.—SOME ORE-BEARING NODULES
Temple Mountain, Utah

composition, and quantity of the hydrothermal solutions. Urano-organic materials, and rarely uraninite, as disseminated inclusions and rims, appear to be restricted to the outer portion of nodules containing iron- and zinc sulfide (Fig. 18, D, E, G), but in a few cases are found as inclusions throughout nearly pure arsenic nodules (Fig. 18, H, I).

The pisolitic forms at Temple Mountain contain remnant sedimentary quartz grains, which are indicative of replacement. This texture, together with the mechanism of development of large masses of ore, eliminates

precipitation and localization of some of the ore and associated metallic minerals.

Refluxing Temple Mountain semifluid tar in water shows that the tar may be circulated in solution as irregular spherical masses. These flocculate to form larger spherical masses, which in turn redispense to smaller bodies during agitation of the solution. The margins of semifluid petroleum-impregnated sandstones contain irregular spherical bodies of viscous oil (Pl. 1, fig. 1). Similarly, the margins of massive ore patches contain pisolitic forms (Pl. 1, fig. 2). Upon emplacement or flocculation

of the emulsoid, the greater surface tension of the more viscous substance results in spherical forms similar to those produced from colloidal suspensions (Bastin, 1950). The contraction cracks developed during the shrinkage of

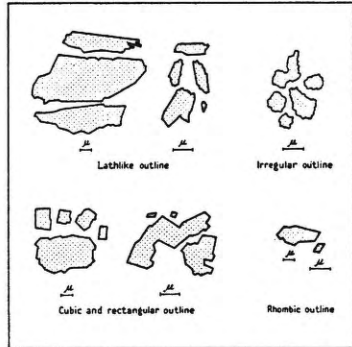


FIGURE 19.—COMPOSITE ELECTRON MICROGRAPHS OF URANO-ORGANIC ORE
Lower Wingate, South Temple Mountain

colloidal material after deposition are similar to those produced during syneresis from the loss, or reorganization, of organic components upon induration and polymerization of a petroliferous material. Thus the texture of the urano-organic ore is indicative of semifluid or fluid material and reflects the probable petroliferous origin of the ore.

The spherical forms of the metallic nodules, however, are indicative of replacement and

deposition about a nucleus rather than deposition of a colloid. No contraction fractures have been observed in these nodules.

Included Metallic Minerals

Pods of irregularly disseminated pyrite are found up to 10 inches in diameter. However, electron photomicrographs show submicroscopic particles ranging in size from less than a micron to more than 10 microns in diameter. Most of these particles are irregularly shaped (Fig. 19; Pl. 4) and represent organic material, aggregate crystallites of pitchblende (Sciaccia, 1954), or other mineral inclusions. Lathlike, cubic, rectangular, or rhombic outlines indicate fine crystals. Some correspond in shape to synthetic pitchblende, others to pyrite, clay, and carbonates.

With the exception of pyrite and the metallic nodules, the metallic minerals are generally submicroscopic or microscopic. Where microscopically visible, they range from minute irregular particles to crystals and are scattered at random, clustered, or occur as irregular concentrations in a matrix of urano-organic material (Pl. 3, fig. 5). Radioactivity intensity, as revealed by autoradiographs of polished surfaces, is irregularly distributed throughout the ore. However, in many cases the radioactivity is not correlative with microscopically visible particles.

Where two types of urano-organic material can be distinguished on a polished surface, a preferential orientation is noted in a few cases for the contaminant inclusions. The clear light-gray ore contains no microscopically

PLATE 3.—PHOTOMICROGRAPHS: SOME MINERALS ASSOCIATED WITH THE ORGANIC MATERIALS

FIGURE 1. Asphalt filling fracture in goethite vein penetrating lower Wingate Sandstone. Massive secondary goethite (g) lies along the fracture wall; massive asphalt (a) fills the center of the fracture. Magnetite and minor calcite (m) fill shrinkage cracks in and around the asphalt. Thin section, using both transmitted and reflected light. Adjacent to collapse area.

FIGURE 2. Partially spherical mass of pyrite in vitrain. Pyrite (black) crystallizing in fragment of vitrain causes distortion of the woody texture. From the Moss Back Sandstone of the calyx area. Thin section.

FIGURE 3. Arsenic and orpiment in turbid urano-organic ore. Small crystals of native arsenic (As) are grouped near the edge of urano-organic ore mass (Uo). Secondary massive orpiment (Or) is interstitial to the corroded detrital quartz fragments (shown as variable gray). From the Moss Back Sandstone bordering the collapse area. Polished surface.

FIGURE 4. Arsenic and orpiment in turbid urano-organic ore. Euhedral and subhedral native arsenic crystals (As) being oxidized to orpiment (Or) in massive urano-organic ore (Uo). From the Moss Back Sandstone bordering the collapse area. Polished surface.

FIGURE 5. Turbid urano-organic ore under high magnification. Minute contaminant mineral particles scattered in massive urano-organic ore cause the turbidity. From the Moss Back Sandstone of the calyx area. Polished surface.

FIGURE 6. Pyrite and sphalerite in the urano-organic ore. Small subhedral particles of pyrite (Py) and sphalerite (Sp) with remnant corroded quartz fragments (dark gray) in massive urano-organic ore (Uo). From the Moss Back Sandstone of the calyx area. Polished surface.

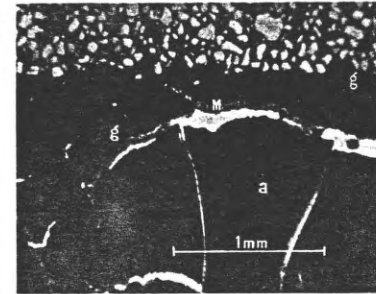


FIGURE 1

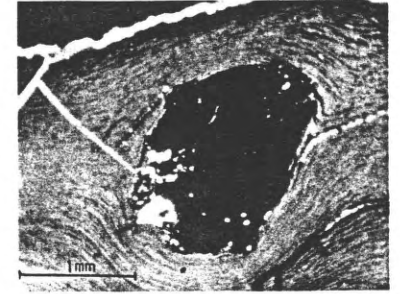


FIGURE 2



FIGURE 3



FIGURE 4

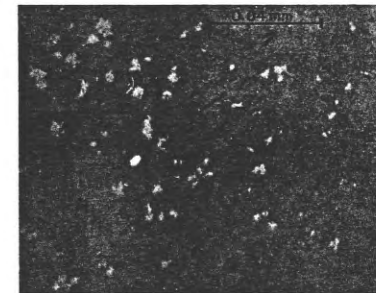


FIGURE 5

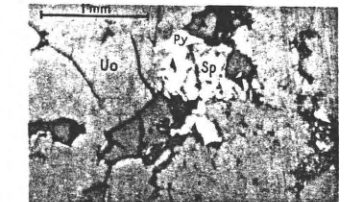


FIGURE 6

PHOTOMICROGRAPHS: SOME MINERALS ASSOCIATED WITH THE ORGANIC MATERIALS

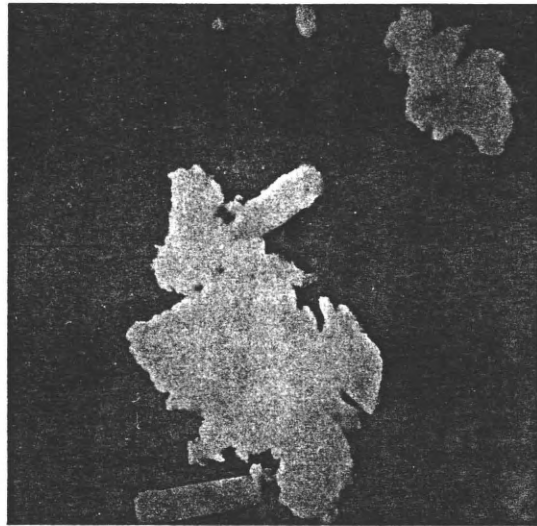


FIGURE 1

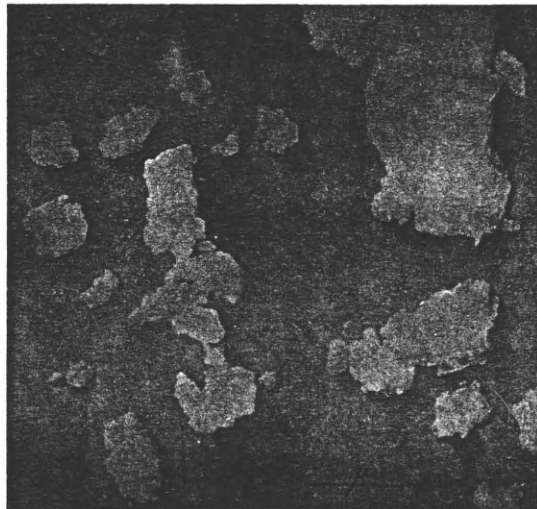


FIGURE 2

ELECTRON PHOTOMICROGRAPHS OF URANO-ORGANIC ORE
(PALLADIUM SHADOWED AT AN ANGLE OF 30°)

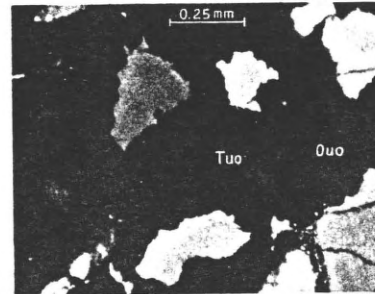


FIGURE 1

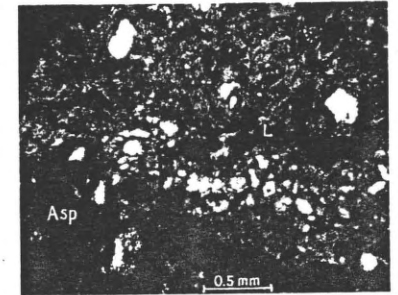


FIGURE 2

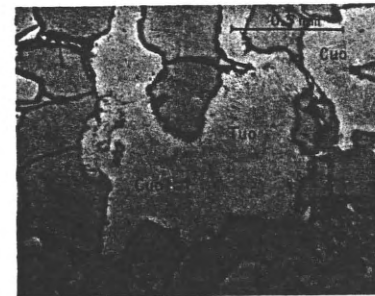


FIGURE 3

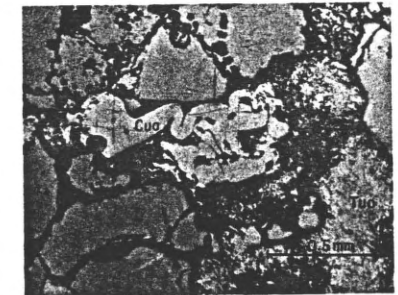


FIGURE 4

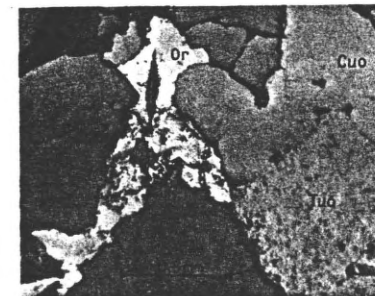


FIGURE 5

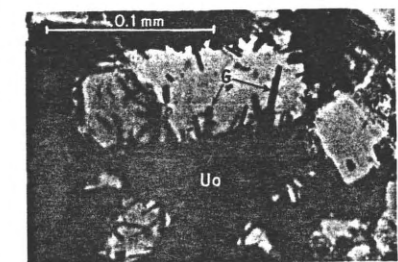


FIGURE 6

PHOTOMICROGRAPHS: URANO-ORGANIC ORE

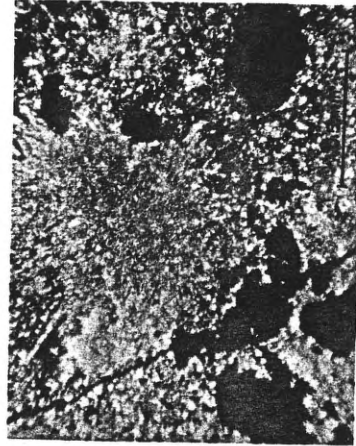


FIGURE 1

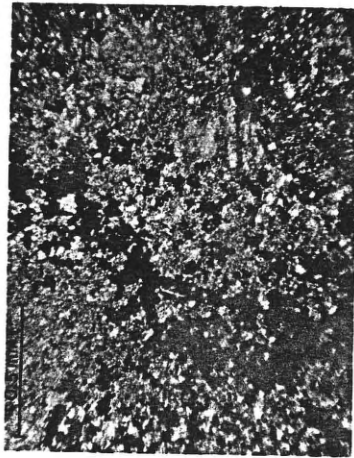


FIGURE 2

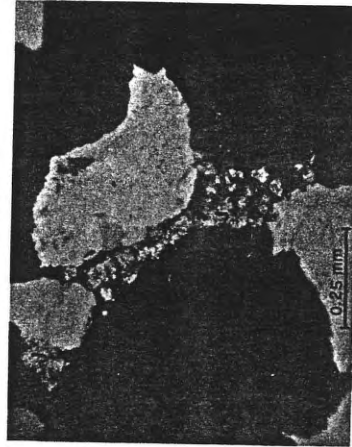


FIGURE 3

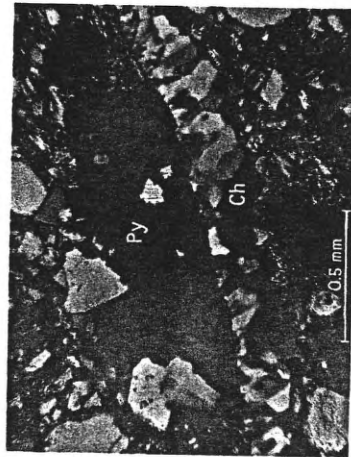


FIGURE 4

PHOTOMICROGRAPHS: SILICIFICATION AND JAROSITE

visible contaminants and in many cases is located interstitial to patches of remnant detrital grains (Pl. 5, figs. 3, 4, 5). The turbidity of the darker-gray ore, which generally makes up the mass of urano-organic material, is caused by minute contaminants (Pl. 3, fig. 5).

The irregular distribution would be unlikely to result before the emplacement of the organic material while it was fluid; otherwise, an alignment of particles should be noticed. Therefore, the crystallite particles apparently formed during or after emplacement.

On polished surfaces, in some cases particles of pyrite and carbonate are arranged in cubic and rhombic patterns. These relict outlines, plus the presence of corroded quartz fragments, plus inclusions of other sedimentary minerals as well as alteration minerals, indicate replacement of these contaminants during emplacement of the organic material.

Some minute particles of arsenic, sphalerite, and uraninite, which are essentially restricted in occurrence to masses of ore, show crystal form, which suggests direct crystallization. The distribution through the ore, rather than along the periphery, suggests two possibilities: (1) that the particles formed from the organic material during emplacement or induration, or (2) they were precipitated from the ore

solutions by the organic material during emplacement but before induration.

The occurrence of small amounts of sphalerite and uraninite throughout most of the ore indicates that the Zn and U content of the ores is not wholly represented by metallo-organic complexes. Considering that the contaminant particles are submicroscopic as well as microscopic, possibly little of either Zn or U may be present as a metallo-organic compound. Fine grinding of the ore "... indicates that most of the uranium is not now chemically associated with the organic matter" (Bregger and Deul, 1955). Whether the elements As, Co, Se, and V are tied up as discrete mineral particles or metallo-organic complexes is less certain. The metallic minerals of these elements are not universally found through the ore.

Other Ore Textures

There is a strong corrosion of the sedimentary and alteration minerals by the organic ore—considerably more corrosion than occurs with either pyrite or the carbonates. The non-uranium-bearing organic materials of either petroliferous or carbonaceous origin show no corrosive effect on the sediments. The corrosive properties of the ore are, therefore,

PLATE 5.—PHOTOMICROGRAPHS: URANO-ORGANIC ORE

FIGURE 1. Translucent and opaque urano-organic ore. Patches of variably translucent ore (Tuo) and opaque ore (Ouo) are not sharply outlined. From the Moss Back Sandstone of the calyx area. Thin section. The translucency is caused by intimate mixture of the ore with particles of other minerals.

FIGURE 2. Diffusion band of low-grade urano-organic ore. A diffusion band (L) of low-grade urano-organic material in mineralized asphaltic (Asp) impregnated Moss Back Siltstone from the calyx area. Thin section.

FIGURE 3. Interstitial turbid urano-organic ore (Tuo) and clear urano-organic ore (Cuo) in the Moss Back Sandstone from the calyx area. Polished surface.

FIGURE 4. Vermicular patch of clear urano-organic ore (Cuo) in interstitial mass of turbid urano-organic ore (Tuo) in the Moss Back Sandstone of the calyx area. Polished surface.

FIGURE 5. Orpiment associated with clear and turbid ore. Interstitial patch of orpiment (Or) along the edge of mass of clear (Cuo) and turbid (Tuo) urano-organic ore. Knoop microhardness indentation can be noticed in the orpiment. From the Moss Back Sandstone bordering the collapse. Polished surface.

FIGURE 6. Goethite associated with urano-organic ore. Minute needles of goethite (G) are shown penetrating corroded quartz grains from interstitial masses of urano-organic ore (Uo). From the Moss Back Sandstone of the calyx area. Thin section.

PLATE 6.—PHOTOMICROGRAPHS: SILICIFICATION AND JAROSITE

FIGURE 1. Chalcedony along the basal Moss Back contact. An aggregate of chalcedony contains disseminated particles and streaks of urano-organic ore (black). From the calyx area. Thin section, crossed nicols.

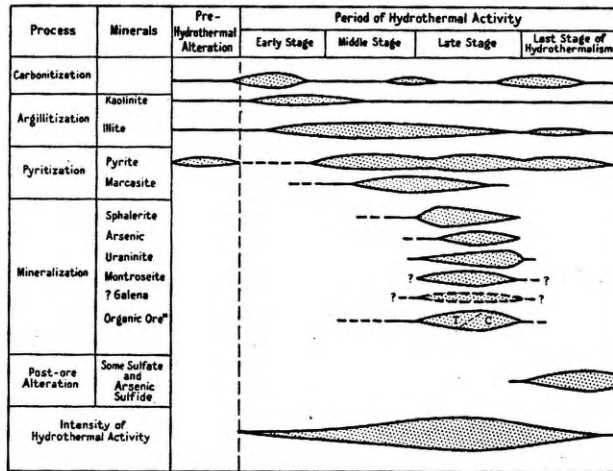
FIGURE 2. Chalcedony spherule. A chalcedony spherule (Cs) in aggregate chalcedony along the basal Moss Back contact. Irregular masses of ore (black) are scattered through the silicified zone. From the calyx area. Thin section, crossed nicols.

FIGURE 3. Chalcedony from the collapse area. A chalcedony band (Ch) associated with pyrite (Py) has developed in the argillized breccia zone in the collapse. From a core fragment. Thin section, crossed nicols.

FIGURE 4. An aggregate of jarosite. Jarosite (J) is peripheral to interstitial urano-organic ore masses (black) in the Moss Back Sandstone bordering the collapse. Thin section, crossed nicols.

attributed to the metallic components of the ore, or, more likely, their associated solutions. Consequently, emplacement of the ore must have occurred during the time the organic

are slight. Galena present at depth is included as a product of hydrothermal mineralization. The individual replacement sequences represent surges rather than a clean-cut progression



* T—Turbid urano-organic ore; C—Clear urano-organic ore.

FIGURE 20.—PARAGENESIS OF ALTERATION AND MINERALIZATION OF THE MOSS BACK SANDSTONE

material was in association with the metallic components or with the ore solution.

There is evidence that local distribution of the ore was influenced by tectonic preparation of the sediments. Detrital grains are minutely fractured in many specimens (Fig. 17, C). These fractures may be aligned, and a few are filled with alteration clay minerals. Such fractures do not extend into patches of ore or correspond to syneresis fractures. Many of the masses of urano-organic material are irregularly elongated parallel to these fractures.

Thin rings of low-grade urano-organic material, similar in form to Liesegang rings, indicate some diffusion of aqueous-organic solutions and further illustrate the original fluid nature of the organic ore (Pl. 5, fig. 2).

Mineral Sequence

Figure 20 is a diagrammatic representation of the paragenesis of the various minerals deposited during hydrothermal alteration and mineralization of the Moss Back ore horizon at the Temple Mountain uranium mining district. The time relationships between the metallic minerals are tentative, and differences

of minerals ending in the emplacement of the ore. Repetition of certain minerals occurs with maximum periods of emplacement at particular times. The emplacement of uranium apparently culminated in a single epoch of mineralization. An early stage was dominated by argillitization and minor carbonitization, a middle stage by pyritization, and a final stage by the emplacement of the urano-organic materials and associated metallic elements. The earlier stages were not completed when the emplacement of the ore occurred.

ALTERATION ASSOCIATED WITH MINERALIZATION

Hypogene Alteration

Although more detailed study of the alteration is in progress (Bodine, 1956) a summary of alteration features is included here to complete the discussion of mineralization.

Three major alteration effects have been recognized at Temple Mountain (Kerr, Bodine, Kelley, and Keys, 1956; Bodine, 1956):

- (1) The early argillitization of upper Moenkopi and lower Chinle near the collapse and of lower

Chinle near ore deposits removed from the collapse

- (2) A later carbonate stage involving emplacement of dolomite with some calcite at the expense of detrital silicates of upper Chinle and Wingate near the collapse
- (3) The final stage of siderite and hematite formation in upper Chinle and Wingate near the collapse

The distribution of the three alteration effects may be outlined as in Figure 21.

The writers believe that removal of carbonate and iron from Kaibab and Moenkopi sediments at depth occurred as a result of ascending mineralizing solutions acidic in nature. Concentration of the carbonate ion increased as the solutions moved upward through carbonate-

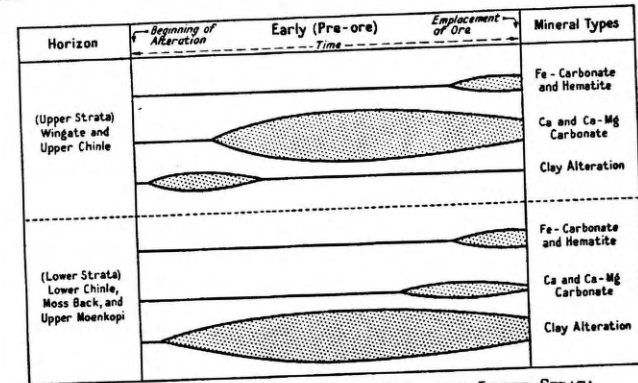


FIGURE 21.—PRE-ORE ALTERATION IN UPPER AND LOWER STRATA

In general, this sequence applies to individual stratigraphic units, yet the three stages occurred essentially contemporaneously, because of significant changes in the ascending hydrothermal solutions and original differences of lithic composition of the various strata. This is shown by the following:

- (1) Field examination of the Moss Back Sandstone indicates that clay alteration continued up to the time of maximum ore emplacement.
- (2) Most of the clay-forming elements were derived from the sediments being altered.
- (3) Where clay minerals formed, carbonitization is negligible.
- (4) Carbonitization occurs in upper Chinle and Wingate, where argillitization is a minor feature.
- (5) Adequate feldspars and sedimentary clay minerals occur in the lower Chinle, Moss Back, and upper Moenkopi and yield alteration clays.
- (6) Clay-forming elements are less concentrated in the massive sandstones of the Wingate and upper Chinle.
- (7) Argillitization was facilitated in the lower horizons and hindered in the upper horizons (5 and 6) by the presence or absence of clay-forming elements.
- (8) Solution of carbonates in lower horizons and deposition of carbonates in upper horizons reflect a vertical change in the character of the solutions.

bearing Moenkopi. As a result, acidity decreased. Neutralization was possibly aided by reaction with the alkali elements in dominantly argillaceous strata. Deposition and reconstitution of clays occurred through upper Moenkopi and lower Chinle; the solutions became essentially neutral in the lower Chinle. The pH continued to rise with further removal of carbonate and reaction with alkalis in the Chinle sediments. Concurrently, deposition of masses of Ca, Ca-Mg, and Fe carbonate occurred at the expense of upper Chinle and Wingate sediments. The silica of the sediments, removed by this replacement, remained in solution and was carried away, except for minor amounts resulting from replacement of the Moss Back Sandstone, which was precipitated near the base.

ALTERATION OF THE MOSS BACK ORE HORIZON: Argillic alteration occurs in the interstices between grains in the Moss Back Sandstone (Kelley and Kerr, 1957). Near collapse features and close to ore zones, kaolinite and mica clay (illite) become more abundant. Mixtures of 1M and 2M₁ mica polymorphs are typical. The 2M₁ mica polymorph becomes a more abundant constituent of the mixtures, and aggregate birefringence and particle size appear to increase. Near collapse areas, micro-

TABLE 18.—METALLIC-ELEMENT DISTRIBUTION IN ARGILLIC ALTERATION ASSOCIATED WITH URANO-ORGANIC MATERIALS

(In per cent on basis of X-ray spectrographic data)
A. Moss Back Sandstone east side of Temple Mountain collapse

| | Wall rock Sandstone | Fault Silty mudstone | Fault Urano-organic ore |
|-------------------------------|---------------------|----------------------|-------------------------|
| U ₃ O ₈ | — | — | 1.8 |
| Co | — | — | .x |
| Ni | — | — | x. |
| Mn | — | —x | —x |
| Se | — | — | x. |
| As | — | .x | x. |
| V | —x | .x | —x |
| Cr | .x | —x | .x |
| Zn | —x | — | — |
| Fe | .x | x. | .x |

B. Lopez Incline, South Workings, Calyx Mine area

| | Fault Altered sandstone | Fault Urano-organic ore | Wall rock* Altered sandstone | Wall rock Urano-organic ore |
|-------------------------------|-------------------------|-------------------------|------------------------------|-----------------------------|
| U ₃ O ₈ | 0.37 | 4.19 | — | 2.48 |
| Co | — | — | — | .x |
| Ni | — | — | — | —x |
| Mn | — | — | — | —x |
| Se | — | — | — | — |
| As | — | —x | —x | — |
| V | .x | — | — | — |
| Cr | .x | .x | .x | .x |
| Zn | — | — | — | .x |
| Fe | .x | .x | .x | .x |

* Contains chromium mica clay

vermicular aggregate growths of kaolinite become common. In unaltered and nonore-bearing sediments, the 2M₁ mica-clay polymorph has not been observed, and 2M₁ detrital muscovite flakes found along bedding appear to be breaking down to a 1M structure. The mica clay at Temple Mountain, which contains the 2M₁ polymorph, is believed to have been deposited by hydrothermal solutions accompanying urano-organic ore deposition, on the basis of the hydrothermal synthesis of mica polymorphs by Yoder and Eugster (1955). The transition of 1M to 2M₁ mica polymorphs appears to occur between 200° C. and 350° C.

at 15,000 p.s.i. water pressure. The source of the clay-forming elements is probably not only the original interstitial material but also includes detrital feldspar replaced during the development of ore masses.

Increased crystallinity of clays in nonore-bearing lower Chinle toward the collapse areas appears to be associated with an increase in iron, as shown by the X-ray spectrograph. Argillic alteration associated with ore in the Moss Back Sandstone may show a concentration of metallic elements locally characteristic of urano-organic ore (Table 18). The concentration may be attributed to either of two processes:

- (1) Leaching of the ore and metallic elements subsequent to deposition of both the ore and clays.
- (2) "Absorption" of the metallic elements by the clays and precipitation accompanying the deposition during hydrothermal mineralization.

Both leaching and absorption with precipitation may have been active in the Temple Mountain mining district. In some localities, the presence of sulfates intermixed with the clays, sulfate replacement of pyrite, and physical characteristics of the ore indicate that leaching was responsible for the concentration of ore elements in the clays (Table 18, A). However, in other localities there is no direct evidence of significant leaching of the ore and associated metallic elements (Table 18, B).

SILICATE REPLACEMENT: Silicification of logs is a common feature in the Chinle of the Colorado Plateau. However, this silicification occurred before the alteration accompanying mineralization of the Moss Back Sandstone. Silicification of the Moss Back Sandstone along the contact with the underlying Monitor Butte Member of the Chinle and within this member also occurs at a number of localities on the San Rafael Swell.

At Temple Mountain, silicification along the lower contact of the Moss Back has been observed at the Vanadium King claims, Calyx Hole Mine No. 3, and near North Mesa No. 9. It probably occurs in other places not noted. The silica occurs as chalcidony and forms veinlets and nodular masses associated with concentration of urano-organic materials. Urano-organic materials are found as irregular disseminations, nodular patches, and concentrations in poorly defined and noncontinuous bands in the chalcidony (Pl. 6, figs. 1, 2). Most of the ore is later than the chalcidony, but it may be in part contemporaneous. The

TABLE 19.—MINERALS OF THE TEMPLE MOUNTAIN URANIUM AREA
Unless otherwise indicated the minerals have been identified in this study.

HYPOGENE MINERALIZATION

| Metallic mineralization | | Alteration | |
|-------------------------|--|--------------------------|---|
| Urano-organic material | Uranium hydrocarbon | Kaolinite | Al ₂ O ₃ ·2SiO ₂ ·2H ₂ O |
| Uraninite | UO ₂ | Illite | |
| Pyrite | FeS ₂ | Chrome-bearing mica clay | |
| Marcasite | FeS ₂ | Calcite | CaCO ₃ |
| Sphalerite | ZnS | Dolomite | CaMg(CO ₃) ₂ |
| Native arsenic | As | Siderite | FeCO ₃ |
| (?) Arsenopyrite | FeAsS | Hematite | Fe ₂ O ₃ |
| (?) Loellingite | FeAs ₂ | Jarosite | K ₂ Fe ₄ (OH) ₁₂ (SO ₄) ₄ |
| Montroselite | V ₂ O ₅ ·H ₂ O | Adularia | KAlSi ₃ O ₈ |
| Galena | PbS | Alunite | K ₂ Al ₄ (OH) ₁₂ (SO ₄) ₄ |
| (?) Chalcopyrite | CuFeS ₂ | Opal | SiO ₂ ·nH ₂ O |
| (?) Covellite | CuS (Gruner and Gardiner, 1952) | Chalcidony | SiO ₂ |
| (?) Bornite | Cu ₅ FeS ₄ (Gruner and Gardiner, 1952) | | |

SUPERGENE MINERALIZATION

| | | |
|--------------------|--|-------------------------------|
| Metatorbernite | Cu(UO ₂) ₂ (PO ₄) ₂ ·6-8H ₂ O | Gruner and Gardiner, 1952 |
| Zeunerite | Cu(UO ₂) ₂ (AsO ₄) ₂ ·8-10H ₂ O | Gruner and Gardiner, 1952 |
| Carnotite | K ₂ O·2UO ₃ ·V ₂ O ₅ ·3H ₂ O | Gruner and Gardiner, 1952 |
| Tyuyamunite | CaO·2UO ₃ ·V ₂ O ₅ ·3H ₂ O | Gruner and Gardiner, 1952 |
| Abernathyite | K ₂ (UO ₂) ₂ (AsO ₄) ₂ ·10-12H ₂ O | Thompson <i>et al.</i> , 1956 |
| Uvanite | 2UO ₃ ·3V ₂ O ₅ ·15H ₂ O | Weeks and Thompson, 1954 |
| Rauvite | CaO·2UO ₃ ·5V ₂ O ₅ ·16H ₂ O | Gruner, 1952 |
| (?) Uranospinitite | Ca(UO ₂) ₂ (AsO ₄) ₂ ·8-10H ₂ O | |
| Corvusite | V ₂ O ₅ ·6V ₂ O ₅ ·nH ₂ O | Gruner and Gardiner, 1952 |
| Metahewettite | CaO·3V ₂ O ₅ ·11H ₂ O | Gruner and Gardiner, 1952 |
| Pascoite | 2CaO·3V ₂ O ₅ ·11H ₂ O | Hess, 1922 |
| Pintadoite | 2CaO·V ₂ O ₅ ·9H ₂ O | Hess, 1922 |
| Erythrite | Co ₃ (AsO ₄) ₂ ·8H ₂ O | Gruner and Gardiner, 1952 |
| Realgar | As ₂ S ₂ | |
| Orpiment | As ₂ S ₂ | |
| Gypsum | CaSO ₄ ·2H ₂ O | |
| Jarosite | K ₂ Fe ₄ (OH) ₁₂ (SO ₄) ₄ | |
| Alunite | K ₂ Al ₄ (OH) ₁₂ (SO ₄) ₄ | |
| Copiapite | Fe ₄ (OH) ₁₂ (SO ₄) ₄ | Hess, 1922 |
| Halotrichite | FeSO ₄ ·(Al ₂ SO ₄) ₃ ·24H ₂ O | Hess, 1922 |
| Celadonite | Fe, Mg, K silicate | Hess, 1922 |
| Brochantite | CuSO ₄ ·3Cu(OH) ₂ | Gruner and Gardiner, 1952 |
| Kaolinite | Al ₂ O ₃ ·2SiO ₂ ·2H ₂ O | |
| Illite | | |
| Calcite | CaCO ₃ | |
| Magnesite | MgCO ₃ | |
| Goethite | FeO(OH) | |
| Limonite | Fe(O, OH)·2H ₂ O | |
| Sulfur | S | Hess, 1922 |

chalcedony replaces early interstitial alteration clays. The silica is believed to have been derived from detrital quartz replaced by urano-organic materials and alteration clays.

Supergene Alteration

Oxidation of the ore and associated metallic minerals produced a large suite of secondary

TABLE 20.—X-RAY DIFFRACTION OF JAROSITE FROM THE CAMP BIRD MINES (Cu/Ni)

| Associated with alteration about carbonaceous trash (diffractometer) | | Associated with alteration about ore pod (microcamera*) | | Jarosite U.S.N.M.-R6299 Warsaw (1956) | |
|--|------|---|----|---------------------------------------|----|
| d(Å) | I† | d(Å) | I† | d(Å) | I |
| 5.90 | 4 | 5.88 | 7 | 5.94 | 3 |
| 5.71 | 6 | | | | |
| 5.06 | 10 | | | | |
| 4.247 | 5** | 5.08 | 8 | 5.74 | 2 |
| 3.646 | 1 | 4.41 | ½ | 5.09 | 4 |
| 3.34 | 13** | 3.62 | ½ | 3.65 | 1 |
| 3.103 | 12 | | | | |
| 3.07 | 16 | 3.06 | 10 | 3.11 | 6 |
| 2.96 | 3 | 2.84 | 1 | 3.08 | 10 |
| 2.864 | 5 | | | 2.97 | 1 |
| 2.546 | 3 | 2.54 | 3 | 2.87 | 2 |
| 2.453 | 1** | 2.302 | 4 | 2.547 | 3 |
| 2.287 | 5** | | | 2.292 | 5 |
| 2.246 | 2** | 1.97 | 4 | 1.978 | 5 |
| 1.975 | 6** | | | 1.941 | 2 |
| | | | | 1.913 | 1 |
| | | | | 1.823 | 5 |
| 1.825 | 5** | 1.86 | 3 | 1.823 | 5 |
| 1.688 | 2** | | | | |
| 1.535 | 3** | | | 1.539 | 3 |
| 1.509 | 2 | | | 1.512 | 3 |
| 1.482 | 1 | | | 1.484 | 1 |
| 1.373 | 2** | | | | |

* Separation of interstitial material gave strong ferric iron and sulfate tests chemically

† Intensities relative

** Quartz

Small, irregular, nodularlike masses of opal and bands of chalcedony (Pl. 6, fig. 3) are found in a few places in interstitial material in the collapse. Similarly, a concentric band of silica from replaced quartz is present in ore-bearing nodules (Fig. 18, D). Silicification along fractures in the collapse may extend several inches into the bordering sediments (Pl. 1, fig. 5).

Small aggregate patches of carbonate are locally scattered through and mixed with the clay minerals in the Moss Back. Carbonate alteration is essentially insignificant in the ore horizon.

minerals (Table 19). These minerals reflect the metallic composition of the ores and, in part, the distribution of metallic components.

Hydrous oxides of uranium and vanadium are present throughout the mining district. Carnotite and tyuyamunite are the most abundant. The others are present only in minor amounts locally. Concentrations of the secondary vanadium minerals in the ore horizon are more noticeable away from the collapse in the calyx mining area, particularly the South Workings. Above the ore horizon, the hydrous vanadium oxides are associated with ore in

TABLE 21.—X-RAY DIFFRACTION OF JAROSITE, TEMPLE MOUNTAIN (Diffractometer Cu/Ni)

| Temple Mountain | | Jarosite U.S.N.M. R6299 | Karphosiderite U.S.N.M. R6266† |
|-----------------|----|-------------------------|--------------------------------|
| d(Å) | I | d(Å) | I |
| 5.92 | 2 | 5.94 | 3 |
| 5.676 | 2b | 5.74 | 2 |
| 5.562 | 1 | 5.56 | 3 |
| 5.063 | 5 | 5.09 | 4 |
| 4.247x | 2b | 3.66 | 1 |
| 3.660 | 1b | 3.65 | 1 |
| 3.424 | 1 | 3.48 | 1 |
| 3.333x | 10 | 3.11 | 6 |
| 3.104 | 8 | 3.08 | 10 |
| 3.067 | 10 | 2.97 | 1 |
| 2.958 | 2b | 2.870 | 2 |
| 2.837 | 2 | 2.870 | 2 |
| 2.540 | 3 | 2.547 | 3 |
| 2.456x | 2b | 2.292 | 5 |
| 2.327 | 1b | 2.125x | 1b |
| 2.277x | 3b | 1.977 | 4b |
| 2.125x | 1b | 1.931 | 1 |
| 1.977 | 4b | 1.921 | 1 |
| 1.931 | 1 | 1.893 | 1b |
| 1.921 | 1 | 1.826 | 4 |
| 1.893 | 1b | 1.819x | 2 |
| 1.826 | 4 | 1.744 | 1 |
| 1.819x | 2 | 1.717 | 1 |
| 1.744 | 1 | 1.703 | 1 |
| 1.717 | 1 | 1.648 | 1 |
| 1.703 | 1 | 1.539x | 2 |
| 1.648 | 1 | 1.535 | 2 |
| 1.539x | 2 | 1.539 | 3 |
| 1.535 | 2 | 1.529 | 1 |

Not Continued

* Jarosite, Meadow Valley Mine, Pioche, Nevada. $KFe_2(SO_4)_2(OH)_2$ (Warsaw, 1956)

† Karphosiderite, Greenland. $Fe_2(SO_4)_2(OH)_2 \cdot (H_2O)$ (Warsaw, 1956)

x—Quartz

b—Broad

the Wingate Sandstone. Uranium arsenates appear to be more abundant near or adjacent to the collapse area. Abernathyite, a new mineral, has been identified from the tongue of the collapse (Thompson *et al.*, 1956). The writers tentatively identified uranospinite, a hydrous calcium uranium arsenate, near the

collapse at the Camp Bird mines on the basis of optical properties and X-ray diffraction.

Occurrences of erythrite, realgar, and orpiment are scattered but seem to occur in greatest concentration near or within the collapse and faults. Considerable amounts of realgar and orpiment can be found at the Camp Bird mines.

POSSIBLE LATE HYDROTHERMAL ALTERATION: Although paragenetic relations indicate that alunitization and jarositization occurred later than the ore, the distribution, particularly of jarosite, suggests deposition before other typical supergene minerals.

Jarosite may be found in intimate mixture with the interstitial alteration clays bordering or within the collapse features and faults, or as nearly pure masses and veinlets associated with carbonized wood fragments and urano-organic materials near or within the collapse (Pl. 6, fig. 4). The occurrence with clays is similar to that noted for jarosite in California Tertiary argillites and sandstones (Briggs, 1951) and for jarosite in Pennsylvania underclays (Warsaw, 1956), where the extreme small size and mixture with other materials make mechanical separation and optical identification unreliable. However, X-ray-diffractometer patterns of the clays at Temple Mountain in a few cases show spacings representative of jarosite, and qualitative chemical tests of these clays yield strong ferric iron and sulfate. X-ray microcamera patterns confirm the identification of jarosite (Table 20).

X-ray-diffractometer patterns of the purer material (Table 21) associated with organic substances indicate that the sulfate consists of a mixture of jarosite ("high" potassium-iron sulfate) and either karphosiderite ("low" potassium-iron sulfate) or natrojarosite, the sodic analogue of jarosite (Warsaw, 1956). X-ray-diffractometer patterns of natrojarosite are similar to karphosiderite. The agreement of some spacings with karphosiderite and the presence of abundant iron qualitatively suggest karphosiderite rather than natrojarosite, particularly where the associated clays are high in potassium, not sodium.

At the Camp Bird mines, slightly altered interstitial clays surrounding pyritized wood fragments contain few, if any, sulfates, whereas the extensively altered clays surrounding nonpyritized wood contain abundant mixed sulfate. In many cases pyrite constitutes the core of urano-organic nodules. Within the Moss Back collapse, where considerable al-

TABLE 22.—X-RAY-DIFFRACTION MEASUREMENTS OF FAINTLY TRANSLUCENT MATERIAL ASSOCIATED WITH ORGANIC MATERIALS (Cu/Ni)

| Ore pod* Powder camera | Ore pod† Micro- camera | Organic material in alteration about ore pod** (nonore) Micro- camera | | Mineral possi- bilities |
|------------------------------|------------------------------|---|----|-------------------------------|
| | | d(Å) | I | |
| | | 10.4 | 1 | Mica |
| | | 7.36 | 1 | Kaolinite |
| | | 7.1 | 1 | Jarosite |
| | | 6.1 | 5 | Jarosite |
| 5.38 | 7 | 5.0 | 2 | Jarosite |
| 4.82 | 8 | 4.81 | 10 | Orpiment |
| | | 4.45 | 2 | Kaolinite |
| | | 4.33 | 1 | Mica |
| 4.25 | 6 | 3.97 | 5 | Quartz |
| 3.98 | 1 | 3.63 | 5 | Orpiment |
| | | 3.63 | 1 | Jarosite, kaolinite, hematite |
| 3.40 | 10 | | | Quartz |
| | | 3.35 | 6 | Jarosite |
| 3.15 | 5 | 3.16 | 2 | Orpiment |
| 3.04 | 1 | 3.04 | 1 | Jarosite, orpiment |
| 2.94 | 2 | 2.97 | 1 | Arsenic |
| | | 2.842 | 5 | Orpiment |
| 2.746 | 3 | 2.779 | 6 | Arsenic |
| 2.690 | 3 | 2.695 | 7 | Orpiment, hematite |
| 2.570 | 1 | 2.555 | 1 | Jarosite, orpiment, hematite |
| 2.441 | 2 | 2.435 | 7 | Quartz, orpiment |
| | | 2.350 | 1 | Unknown |
| | | 2.300 | 1 | Orpiment |
| 2.269 | 2 | 2.202 | 1 | Quartz |
| | | 2.118 | 1 | Jarosite, hematite |
| 2.120 | 1 | 2.073 | 2 | Orpiment |
| | | 2.012 | 1 | Orpiment, hematite |
| 1.968 | 1 | 1.910 | 2 | Orpiment, quartz |
| 1.811 | 1 | | | Orpiment |
| 1.674 | 1 | | | Quartz |
| 1.537 | 1 | | | Quartz |
| 1.371 | 2 | | | Quartz |

teration is evident, nearly pure jarosite makes up the core of nodules. Petrographic study indicates that the iron and sulfate were derived from the pyrite associated with the organic materials in these cases. Near or within the collapse, the concentration of mixed jarosite increases where there is an increase in concentration of alteration clays toward the ore zones.

The mechanism for the production of jarosite at Temple Mountain is similar to that proposed for the jarosite in the underclays of Pennsylvania (Warsaw, 1956). Oxidation of pyrite associated with organic materials under acidic conditions took place locally near collapse features and faults. The solutions were most acid near the sulfide concentrations (Merwin and Posnjak, 1937). Away from the oxidizing pyrite, the acidity was lowered by dilution and reaction of the acid solutions with alkalies, particularly illite. Deposition of the basic ferric sulfate occurred within the clay masses. Development of the gossan zone (Kerr, Bodine, Kelley, and Keys, 1957) in upper Chinle and lower Wingate at the collapse may represent the final stage in the oxidation of pyrite concentrations. Under alkaline conditions, final deposition of iron in the form of limonitic goethite occurred.

Jarosite is present in only minor amounts outside of the collapse, and these occurrences are generally near or within faults. However, pyrite is nearly as abundant outside of the collapse as within it. The abundance of jarosite bordering and within the collapse suggests that the mineral formed during the last stages of hydrothermal alteration after deposition of ore and associated metallic elements. Hutton and Bowen (1950, p. 560-561), for example, consider that the jarosite in pneumatolytically altered volcanic rocks in California "... may represent the very latest or hydrothermal phase of the long and varied sequence of crystallization and metasomatism. . ."

Goethite replacement of the lower Wingate is common near the collapse. Tentatively identified goethite, intimately associated with the Moss Back ore near or within the collapse, may have formed during the period of development of jarosite from oxidation of iron in the urano-organic material (Pl. 5, fig. 6).

* Ore pod: Mostly orpiment and quartz, minor jarosite or alunite and arsenic.

† Ore pod: Mostly orpiment with minor jarosite, kaolinite, mica, arsenic, and possibly hematite.

** Nonradioactive mobile organic material: Mostly jarosite and kaolinite.

INTIMATE MINERAL MIXTURES ASSOCIATED WITH THE ORE: Many small, poorly defined patches along the edges of masses of organic material are composed of intimate mixtures of secondary minerals. These mixtures are most prevalent near the collapse area. In thin section, these areas are irregularly and faintly translucent. On polished surfaces, they may be distinguished from the opaque gray organic ore by irregular faint anisotropism and in a few cases by slight yellowish to reddish-brown internal reflections. X-ray-diffraction patterns of patches associated with the ore at the Camp Bird mines contain fine mixtures of orpiment with minor amounts of jarosite, kaolinite, mica, arsenic, and possibly hematite (Table 22, footnote 2). Patches associated with nonuranium-bearing petroliferous materials lack the arsenic compounds and are composed of fine mixtures of jarosite and kaolinite (Table 22, footnote 3).

The abundance of these mixtures near the collapse and their association with considerable jarositization in the vicinity of the collapse area suggest that they represent post-mineralization hydrothermal activity.

In summary, most of the jarosite and some of the secondary arsenic sulfides, alunite, and clays may represent a late hydrothermal phase after deposition of the ore. Late weathering and downward percolating ground water, however, yielded the large suite of supergene minerals; the source of the metallic elements was the urano-organic ore and associated metallic minerals.

CONCLUSION

The writers believe that evidence favors the emplacement of uranium ore at Temple Mountain by hydrothermal solutions:

- (1) A rough zonal relation in the Moss Back involves metallic trace elements in the ore, metallic minerals, and alteration. Arsenic, cobalt, and selenium are present near or within the collapse (or certain faults), whereas uranium, zinc, and vanadium appear to increase away from the collapse.
- (2) The greatest known vertical spread of mineralization occurs at the collapse area.
- (3) The sediments are most highly altered around the collapse.
- (4) The solution of carbonate at depth and redeposition in large masses of dolomite above, coupled with the increase in marcasite at depth near and within the collapse, indicate a change in the rising solutions. Neutral to slightly acidic condi-

tions prevailed from the lower Chinle downward, and neutral to slightly alkaline conditions prevailed from upper Chinle upward.

In addition to the migration pattern of the mineralizing solutions, the mineralogy of the ores suggests temperatures in the vicinity of 200°C. Considering a geothermal gradient of about 5°C. per 1000 feet of sediments under an approximate load of 10,000 to 12,000 feet, an estimated minimum of 50°C. above normal surface temperatures should have existed. An upper limit would probably be established by the argillic alteration of about 350°C. to 400°C. In determining a likely temperature within this range, several features indicate temperatures above those normally attributed to circulating ground waters:

- (1) Native arsenic apparently would be deposited at elevated temperatures about 300° C. Recorded occurrences and the probable conditions of deposition in the presence of iron and sulfur confirm this conclusion.
- (2) The abundance of the 2M₁ mica polymorph in alteration mica clays toward the collapse and deposits of ore in the Moss Back (Kelley and Kerr, 1957) suggest temperatures in the vicinity of 200° C., on the basis of synthetic mica experiments (Yoder and Eugster, 1955).
- (3) The deposition of large replacement masses of replacement dolomite near the collapse would probably result from solutions having elevated temperatures (Bodine, 1956).
- (4) The writers believe that induration of the organic material occurred under the influence of heat and the action of solutions rather than by radioactive polymerization.

Field observation and laboratory data suggest a progressive development of ore masses. Initially weak mineralizing solutions infiltrated permeable sediments. The interstices between sand grains were filled and the cement was replaced. This was accompanied by extraction of uranium from solution and coagulation of the immiscible hydrocarbon present as an interstitial film. The hydrocarbon formed either as small stringers and interstitial disseminations or as nodules. As the strength of the mineralization increased, more uranium was extracted, and coagulation increased; the hydrocarbons coalesced to form larger nodules and patches, which in turn eventually formed large patches of massive ore. Replacement of the sedimentary grains and previous interstitial alteration products occurred. Pyrite present was slowly replaced. Some concentric banding of the hydrocarbons and

associated metallic elements developed as the intensity, composition, and quantity of the mineralizing solutions varied through time. Coagulation of colloidal dispersed minor amounts of precipitating pitchblende and other metallic minerals accounts for their irregular distribution in the uranium hydrocarbon. Finally, induration of the hydrocarbon occurred, accompanied by some volume loss compensated by contraction fissures which were later filled by alteration products.

Miller's study of the chemical environment of pitchblende (1955b) suggests that sulfur, in the form of sulfide or sulfate, may be important as a precipitant of pitchblende. The association of pre-ore pyrite with the ore at Temple Mountain suggests that sulfur may have facilitated the extraction of uranium from mineralizing solutions and perhaps determined in part the distribution of the immiscible coagulating hydrocarbon. Possibly some of the contemporaneous and post-ore sulfide (pyrite) represents reduction of sulfate solutions and attendant oxidation of the hydrocarbons, as postulated by Ginter (1934). It is reasonable to infer that warm, slightly acid sulfate solutions carrying uranyl-ion decarbonized the Chible and lower sediments; when it came in contact with hydrocarbons and sulfides, the uranium was extracted from the solution, the sulfate oxidized the hydrocarbons in part to carbonate and in turn was reduced to sulfide. The reduction that attended oxidation of the hydrocarbons resulted in the formation of the native arsenic, montroseite, sphalerite, and uraninite associated with the ore. The induration of the hydrocarbons was accomplished by polymerization and oxidation of the hydrocarbon by heated solutions.

Heat and oxidation conditions must have persisted after completion of the alteration and mineralization cycle to cause induration of the initial post-ore hydrocarbons, to form the asphalt of Temple Mountain, and to produce abundant jarosite and some minor arsenic sulfides near the collapse area.

The lack of variety and scarcity of the metallic elements in the ores at Temple Mountain is a feature of the relatively barren uppermost (hot-spring) portion of hydrothermal vein systems in general. The pattern of alteration surrounding the collapse corresponds to that proposed by Schmitt (1950a; 1950b) for epithermal mineral deposits based on hot-spring areas. It consists of a basal CO₂ leaching phase, medial potassic and sodic phases, and an upper sulfide-sulfate phase. In view of the

location of argillic alteration with respect to the main ore at Temple Mountain, Schmitt's (1950b, p. 199) statement is significant: "It may be found that 'epithermal' ore deposition is usually just above (or to one side of) the hypogene clay zone and presumably associated with a sericitic-quartz or potassic phase." The peculiar collapse and the form of this structure are similar to the conelike or wedge-like upward flares of channel structures in hot-spring areas.

Most of the metallic elements associated with the ore at Temple Mountain have been found in minor amounts locally in hot-spring areas. Arsenic and jarosite deposits associated with hot springs have recently been summarized by White (1955). In general, the Temple Mountain collapse is suggestive of a fossil hot-spring region. The considerable amount of silica dissolved during the carbonate replacement of Wingate must have made siliceous deposits above the Wingate of extent comparable to those at hot springs. A warm-spring area bordering the San Rafael River in the northeast portion of the swell has been reported to have above normal concentrations of uranium in solution, which is not only depositing siliceous sinter and sulfates but appears to be carrying hydrocarbons.

At the Little Joe Claims along the west side of the swell, urano-organic ore is localized along a large fault zone which has an associated collapse structure and a radioactive warm spring. Near the small urano-organic ore deposits at Calf Mesa at the north end of the swell is a nonuranium-bearing fossil hot-spring deposit in the Moss Back Sandstone, containing sulfide pipes. Small crystals of sulfur are scattered in hydrocarbon-sulfate saturated sandstones above the pipes. In the ore at Calf Mesa, somewhat similar sulfide pipes are locally present and contain urano-organic material. The considerable amount of sulfides associated with the ore have formed, upon leaching, an unusual occurrence of secondary iron minerals.

In speaking of epithermal quicksilver deposits associated with many hot springs, Lindgren (1933, 464) states:

"A scant association of ore minerals characterizes these deposits. Besides cinnabar and a few secondary minerals, they contain almost invariably pyrite or marcasite. . . Among gangue minerals we have predominantly opal, chalcedony, and quartz, also calcite and dolomite. . . Replacements of adjoining country rock by dolomitic carbonates or by opal are common. . . Hydrocarbons are frequent."

In conclusion, the urano-organic ore at Temple Mountain is considered to have resulted from epithermal mineralization of hot-spring type. Solutions were introduced into the ore horizon at the collapse, and to a lesser extent, along faults or fractures. Away from these channels, evidence of hydrothermal activity diminishes. The principles of carbonate alteration (Bodine, 1956) and the features of argillization (Kelley and Kerr, 1957), together with the occurrence of sulfates and zonal elemental distribution, may be widely applicable to the determination of centers of uranium mineralization elsewhere on the Colorado Plateau. It is significant that uranium mineralization is relatively sparse at these centers but may be more abundant near by.

REFERENCES CITED

- Abraham, H., 1920, Asphalts and allied substances: N. Y., D. Van Nostrand Co., 608 p.
- Allen, E. T., Crenshaw, J. L., and Merwin H. E., 1914, Effect of temperature and acidity in the formation of marcasite (FeS) and wurtzite (ZnS): Am. Jour. Sci., 4th ser., v. 38, p. 393-431
- Baker, A. A., 1946, Geology of the Green River Desert-Cataract Canyon region, Emery, Wayne, and Garfield counties, Utah: U.S. Geol. Survey Bull. 951, 122 p.
- Barthauer, G. L., Rulfs, C. L., and Pearce, D. W., 1953, Investigations of thucholite: Am. Mineralogist, v. 38, p. 802-814
- Bastin, E. S., 1950, Interpretation of ore textures: Geol. Soc. America Mem. 45, 100 p.
- Bass, N. W., 1944, Correlations of basal Permian and older rocks in southwestern Colorado, northwestern New Mexico, northeastern Arizona, and southeastern Utah, 1944: U.S. Geol. Survey Oil and Gas Invs. Prelim. Chart no. 7, accompanied by paper on Paleozoic stratigraphy as revealed by deep wells in parts of southwestern Colorado, northwestern New Mexico, northeastern Arizona, and southeastern Utah, 20 p.
- Bernauer, F., 1935, Rezent Erzbildung auf der Insel Vulcana, Teil I: Neues Jahrb. für Min. Geol. und Paläontologie Abh., Beil. 64, Abt. A., p. 60-92
- Bowie, S. H. U., 1955, Thucholite and hisingerite-pitchblende complexes from Nicholson Mine, Saskatchewan, Canada: Geol. Survey Gt. Britain Bull. 10, p. 45-57
- Breger, I. A., and Deul, M., 1955, The association of uranium with carbonaceous materials on the Colorado Plateau: U.S. Atomic Energy Comm., TEIR-539, p. 1-35
- Breger, I. A., Deul, M., and Meyrowitz, R., 1955, Geochemistry and mineralogy of a uraniferous subbituminous coal: Econ. Geology, v. 50, p. 610-624
- Breger, I. A., Deul, M., and Rubinstein, S., 1955, Geochemistry and mineralogy of a uraniferous lignite: Econ. Geology, v. 50, p. 206-226
- Briggs, L. I., 1951, Jarosite from the California Tertiary: Am. Mineralogist, v. 36, p. 902-906
- Coleman, R. G., 1957, Mineralogical evidence on the temperature of formation of the Colorado Plateau uranium deposits: Econ. Geology, v. 52, p. 1-4
- Crawford, A. L., 1949, Gilsonite and related hydrocarbons of the Uinta Basin, Utah, p. 235-260 in Hansen, G. H., and Bell, M. M., The oil and gas possibilities of Utah: Utah Geol. Mineralog. Survey, 341 p.
- Croft, W. J., 1954, An X-ray line study of uraninite: U.S. Atomic Energy Comm., Ann. Rept. (pt. 11), RME-3096, p. 7-71
- Davidson, C. F., and Bowie, S. H. U., 1951, Related hydro-carbon-uraninite complexes: Geol. Survey Gt. Britain Bull. 3, p. 1-19
- Dietrich, R. V., 1956, Is anthraxolite related genetically to coal or to oil?: Econ. Geology, v. 51, p. 649-664
- Ellsworth, R. V., 1928, Thucholite from the vicinity of Parry Sound, Ontario: Am. Mineralogist, v. 13, p. 419-442
- Erickson, R. L., Myers, A. T., and Horr, C. A., 1954, Association of uranium and other metals with crude oil, asphalt, and petroliferous rock: Am. Assoc. Petroleum Geologists Bull., v. 38, p. 2200-2218
- Evans, N. N., 1903, Native arsenic from Montreal: Am. Jour. Sci., 4th ser., v. 15, p. 92-93
- Fleischer, M., 1955, Minor elements in some sulfide minerals: Econ. Geology, 50th Anniversary Volume, p. 970-1024
- Fryklund, V. C., and Fletcher, J. D., 1956, Geochemistry of sphalerite from the Star mine, Coeur d'Alene District, Idaho: Econ. Geology, v. 51, p. 223-247
- Garrels, R. M., 1953, Some thermodynamic relations among the vanadium oxides, and their relations to the oxidation state of the uranium ores of the Colorado Plateau: Am. Mineralogist, v. 38, p. 1251-1265
- Gilluly, J., 1929, Geology and oil and gas prospects of part of the San Rafael Swell, Utah: U.S. Geol. Survey Bull. 806, p. 69-130
- Ginter, R. L., 1934, Sulphate reduction in deep subsurface waters: Am. Assoc. Petroleum Geologists, Problems of Petroleum Geology (Sidney Powers Memorial Volume), p. 907-925
- Glass, H. D., 1954, Investigation of rank in coal by differential thermal analyses: Econ. Geology, v. 49, p. 294-309
- Gott, G. B., Wyant, D. G., and Beroni, E. P., 1952, Uranium in black shales, lignites, and limestones in the United States: U.S. Geol. Survey Circ. 220, p. 31-35
- Gruner, J. W., and Gardiner, L., 1952, Mineral associations in the uranium deposits of the Colorado Plateau and adjacent region with special emphasis on those in the Shinarump formation: U.S. Atomic Energy Comm., Ann. Rept., July 1, 1951, to June 30, 1952 (pt. III), p. 1-41
- Hacquebard, P. H., 1950, The nomenclature and classification of coal petrography: Nova Scotia Dept. Mines, Conf. on Origin and Constitution of Coal, p. 8-48
- Hess, F. L., 1922, Uranium-bearing asphaltite sediments of Utah: Eng. and Min. Jour., v. 114, p. 272-276

- Hunt, J. M., Stewart, F., and Dickey, P. A., 1954, Origin of Hydrocarbons of Uinta Basin, Utah: *Am. Assoc. Petroleum Geologists Bull.* v. 38 (pt. 2), p. 1671-1698
- Hutton, C. O., and Bowen, O. E., 1950, An occurrence of jarosite in altered volcanic rocks of Stoddard Mountain, San Bernardino County, California: *Am. Mineralogist*, v. 35, p. 556-561
- Ingerson, E., 1955, Methods and problems of geologic thermometry: *Econ. Geology*, 50th Anniversary Volume, p. 341-410
- Joubin, F. R., 1954, Uranium deposits of the Algoma district, Ontario: *Can. Inst. Min. Met. Trans.*, v. 58, p. 431-437
- Kelley, D. R., and Kerr, P. F., 1956, Emplacement of uraniumiferous hydrocarbons at Temple Mountain, Utah: *U.S. Atomic Energy Comm., Ann. Rept. for June 30, 1955, to April 1, 1956*, p. 1-79
- 1957, Clay alteration and ore, Temple Mountain, Utah: *Geol. Soc. America Bull.*, v. 68, p. 1101-1116
- Kerr, P. F., and Hamilton, P. K., 1958, Chrome mica-clay, Temple Mountain, Utah: *Am. Mineralogist*, v. 43, p. 34-47
- Kerr, P. F., and Kelley, D. R., 1956, Urano-organic ores of the San Rafael Swell, Utah: *Econ. Geology*, v. 51, p. 386-391
- Kerr, P. F., and Kulp, J. L., 1948, Multiple differential thermal analysis: *Am. Mineralogist*, v. 33, p. 387-419
- Kerr, P. F., and Lapham, D. M., 1954, Report on a nodule from Temple Mountain, Utah: *U.S. Atomic Energy Comm., RME-3096* (pt. 1), p. 7-15
- Kerr, P. F., Holmes, R. J., and Knox, M. S., 1945, Lattice constants in the pyrite group: *Am. Mineralogist*, v. 30, p. 498-504
- Kerr, P. F., Rasor, C. A., and Hamilton, P. K., 1951, Uranium in Black King Prospect, Placer-ville, Colorado: *U.S. Atomic Energy Comm., Ann. Rept.*, RMO-797, p. 25-43
- Kerr, P. F., Bodine, M. W., Kelley, D. R., and Keys, W. S., 1957, Collapse features, Temple Mountain uranium area, Utah: *Geol. Soc. America Bull.*, v. 68, p. 933-982
- Kerr, P. F., Kelley, D. R., Bodine, M. W., and Keys, W. S., 1955, Collapse features, Temple Mountain uranium area, Utah: *U.S. Atomic Energy Comm., RME-3110* (pt. 3), p. 1-138
- Keys, W. S., 1955, Deep drilling in the Temple Mountain Collapse, San Rafael Swell, Utah: *United Nations, Geneva Conf. on Peaceful Uses of Atomic Energy, Proc.*, v. 6, p. 371-378
- Keys, W. S., and White, R. L., 1956, Investigation at the Temple Mountain collapse and associated features, San Rafael Swell, Emery County, Utah: *U.S. Geol. Survey Prof. Paper* 300, p. 285-298
- Kullerud, G., 1953, The FeS-ZnS system a geological thermometer: *Saertrykk av Norsk Geologisk Tidsskrift*, b. 32, h. 2-4, p. 61-147
- 1956, Geochemistry of sphalerite from the Star Mine, Coeur d'Alene District, Idaho: *Econ. Geology*, v. 51, p. 828-830
- Larsen, E. S., 1921, The microscopic determination of nonopaque minerals: *U.S. Geol. Survey Bull.* 697, p. 1-294
- Lindgren, W., 1933, Mineral deposits: N. Y., McGraw Hill Book Co., 930 p.
- Marshall, C. E., 1955, Coal petrology: *Econ. Geology*, 50th Anniversary Volume, p. 757-834
- Merwin, H. E., and Posnjak, E., 1937, Sulphate incrustations in the Copper Queen Mine, Bisbee, Arizona: *Am. Mineralogist*, v. 22, p. 567-571
- Miller, L. J., 1955a, Uranium ore controls of the Happy Jack Deposit, White Canyon, San Juan County, Utah: *Econ. Geology*, v. 50, no. 2, p. 156-169
- 1955b, The chemical environment of pitchblende: *U.S. Atomic Energy Comm., RME-3110* (pt. 1), p. 1-49
- Moore, G. W., 1954, Extraction of uranium from aqueous solution by coal and some other materials: *Econ. Geology*, v. 49, p. 652-658
- Murray, A. N., 1950, The gilsonite deposits of the Uinta Basin, Utah, p. 115-118 in Eardley, A. J., *Editor*, Petroleum geology of the Uinta Basin: *Guidebook to the Geology of Utah*, no. 5, 152 p.
- O'Brien, T. C., 1953, Uranium occurrence in asphaltites: *U.S. Atomic Energy Comm., RME-3040*, p. 1-6
- Onishi, H., and Sandell, E. B., 1955, Geochemistry of arsenic: *Geochim. et Cosmochim. Acta*, v. 7, p. 1-33
- Palache, C., Berman, H., and Frondel, C., 1944, Dana's system of mineralogy: v. 1, 7th Ed., N. Y., John Wiley & Sons, 834 p.
- Prommel, H. W. C., and Crum, H. E., 1927, Salt domes of Permian and Pennsylvanian age in southeastern Utah and their influence on oil accumulation: *Am. Assoc. Petroleum Geologists Bull.*, v. 11, p. 373-393
- Ridgway, R., 1912, Color standards and color nomenclature: Published by author, Washington, D. C., 43 p., 53 pls.
- Ries, H., 1949, Economic geology: 7th Ed., N. Y., John Wiley & Sons, Inc., 720 p.
- Robinson, S. C., 1950, Mineralogy of the Goldfields District, Saskatchewan (Interim Account): *Geol. Survey Canada Paper* 50-16, 38 p.
- Schmitt, H., 1950a, The fumarolic-hot spring and "epithermal" mineral deposit environment, in *Applied Geology*, a symposium: *Colo. School Mines Quart.* v. 45, no. 1B, p. 209-229
- 1950b, Origin of the epithermal mineral deposits: *Econ. Geology*, v. 45, p. 191-197
- Schopt, J. M., 1956, A definition of coal: *Econ. Geology*, v. 51, p. 521-527
- Sciaccia, T. P., 1954, Electron micrographs of synthetic pitchblende precipitates: *U.S. Atomic Energy Comm., RME-3096* (pt. 2), p. 93-99
- Short, M. N., 1940, Microscopic determination of the ore minerals: *U. S. Geol. Survey Bull.* 914, p. 1-314
- Siever, R., 1952, X-ray diffraction study of rank increase in coal: *Nova Scotia Dept. Mines, 2nd Conf. on Origin and Constitution of Coal*, p. 341-362
- Spence, H. S., 1930, A remarkable occurrence of thucholite and oil in a pegmatite dyke, Parry Sound, Ontario: *Am. Mineralogist*, v. 15, no. 11, p. 499-520
- Stevenson, J. S., 1954, Determination of columbium in ores by X-ray fluorescence: *Am. Mineralogist*, v. 39, no. 5-6, p. 436-443
- Stieff, L. R., Stern, J. W., and Milkey, R. G., 1953, A preliminary determination of the age of some uranium ores of the Colorado Plateau by the lead-uranium method: *U. S. Geol. Survey Circ.* 271, 19 p.
- Swanson, H. E., and Fuyat, R. K., 1953, Standard x-ray diffraction powder patterns: *N.B.S. Circ.* 539, v. II, p. 19
- Thompson, M. E., Ingram, B., and Gross, E. B., 1956, Abernathyite, a new uranium mineral of the metatorbernite group: *Am. Mineralogist*, v. 41, no. 1-2, p. 82-90
- Vine, J. D., 1955, Uranium bearing coal in the United States: *United Nations Conf. Paper* 55, v. 6, p. 452-457
- Warren, C. H., 1903, Native arsenic from Arizona: *Am. Jour. Sci.*, 4th Ser., v. 16, p. 337-339
- Warshaw, C. M., 1956, The occurrence of jarosite in underclays: *Am. Mineralogist*, v. 41, no. 3-4, p. 288-296
- Weeks, A. D., Thompson, M. E., 1954, Identification and occurrence of uranium and vanadium minerals from the Colorado Plateaus: *U. S. Geol. Survey Bull.* 1009-B, 62 p.
- Weeks, A. D., Cisney, E. A., and Sherwood, A. M., 1953, Montroseite, a new vanadium oxide from the Colorado Plateaus: *Am. Mineralogist*, v. 38, p. 1235-1241
- Wengard, S. A., and Strickland, J. W., 1954, Pennsylvanian stratigraphy of the Paradox Salt Basin, Four Corners region, Colorado and Utah: *Am. Assoc. Petroleum Geologists Bull.*, v. 38, p. 2157-2199
- White, D. E., 1955, Thermal springs and epithermal ore deposits: *Econ. Geology*, 50th Anniversary Volume, p. 99-154
- Yoder, H. S., and Eugster, H. P., 1955, Synthetic and natural muscovites: *Geochim. et Cosmochim. Acta*, v. 8, no. 5/6, p. 225-280
- Young, R. S., 1954, Preliminary X-ray investigation of solid hydrocarbons: *Am. Assoc. Petroleum Geologists Bull.*, v. 38, no. 9, p. 2017-2020

DEPARTMENT OF GEOLOGY, COLUMBIA UNIVERSITY,
NEW YORK 27, N. Y.
MANUSCRIPT RECEIVED BY THE SECRETARY OF THE
SOCIETY, MAY 14, 1957

- Copper Electrowinning. 96-154
- Bernard, G.M.: *Andacollo Gold Production in Sight Ahead of Schedule and Under Budget*. 96-25
- Bishop, M.D., Gray, L.A., Young, T.L., Greene, M.G.: *Technical Developments Leading to Modern Solvent Extraction Diluents*. 96-49
- Cacanour III, J.B., Harbuck, D.D.: *On-Line Analysis and Process Control in the Copper Industry Using Line-Scan Video Photometry*. 96-101
- Celik, M.S., Akin, Y., Hancer, M.: *Decompression of Electrical Doublelayer with Monovalent Cations*. 96-91
- Cho, C., Vance, R., Mardi, N., Qian, Z., Prisbey, K.: *Neural Network Based Nonlinear Model Predictive Control vs. Linear Quadratic Gaussian Control*. 96-17
- Cho, E.H., Yanief, G., Yang, D.C., Peng, F.F.: *Carrier Flotation for the Removal of Radionuclides from Contaminated Soils*. 96-14
- Cole, J.A., Stoiber, C.: *The Implementation of Caro's Acid as a Cyanide Tailings Treatment Method at Lone Tree Mine*. 96-153
- Coleman, R., Veloo, C.: *P.T. Freeport Indonesia Concentrator Expansion*. 96-161
- Dasgupta, R., Guan, Y.C., Han, K.N.: *The Dissolution Behavior of Gold in Ammoniacal Solutions at 75 Degrees C*. 96-70
- Eddy, T.W., Nesbitt, C.C.: *Mercury Removal from Sulfidic Concentrates Using Low Temperature Thermal Applications*. 96-109
- Fahey, M.P., Moudgil, B.M.: *Mechanisms of Silica Recovery During Anionic Phosphate Flotation*. 96-18
- Forsberg, E., Wang, Y.: *Comminution of Carbonate Minerals in a High-Pressure Roller Mill*. 96-143
- Foster, T., Moffatt, S.A., Sinha, V.T.: *Selecting the Optimum Addition Points for Flocculants in Decanter Feedwells*. 96-140
- Freeman, M.B., Mahar, R.C., Robertson, S.T.: *Polymeric Dispersants for Mineral Processing*. 96-76
- Freer, R.: *PTFE Membrane Filter Media for Solid-Liquid Separation*. 96-12
- Groppo, J.G., Parekh, B.K.: *Pilot Scale Testing of Hyperbaric Filtration for Fine Coal Dewatering*. 96-26
- Groppo, J.G., Robl, T.L., Graham, U.M., McCormick, C.J.: *A Selective Beneficiation Process for High LOI Fly Ash*. 96-57
- Guan, Y.C., Han, K.N.: *The Electrochemical Study on the Dissolution Behavior of Gold in Ammoniacal Solutions at Temperatures above 100 Degrees C*. 96-66
- Gula, M.J., Dreisinger, D.B.: *The Ion Exchange Control of Iron in Copper Electrolyte Streams Using Eichrom's Diphonix Resin*. 96-39
- Hales, L., Colby, R., Ynchausti, R.: *Adaptive Control of Mineral Processing Applications*. 96-147
- Hales, L.B., Colby, R., Walker, C.: *Using Neural Networks to Model Column Flotation*. 96-148
- Hall, S., Reed, M.: *Cross Contamination of ODC Solvent Extraction Circuits*. 96-162
- Harris, L., Conway, T., Santa Cruz, C., Schwalb, F., Diaz, M., Arguelles, L., Cotts, N., Villanueva, M., Meza, F., Guerra, F., Orams, P., Chang, J.: *Minera Yanacocha, Three Years Later*. 96-61
- Hodouin, D., Bazin, C., Makni, S.: *Dynamic Material Balance Algorithms: Application to Industrial Flotation Circuits*. 96-158
- Hunter, C.J., Nicholson, H.M., Mensa-Abrampah, D.: *Refractory Gold Ore Processing at the Ashanti Goldfields Company Ltd, Sansu Treatment Plant Using Biox Technology*. 96-88
- Jiang, C.L., Parekh, B.K., Leonard, J.W., Wang, X.H.: *The Role of Colloid and Solution Chemistry of Iron Ions in the Pyrite Flotation with Xanthate*. 96-38
- 96-35
- Laplante, A.R., Doucet, R.: *A Laboratory Procedure to Determine the Amount of Gravity Recoverable Gold*. 96-174
- LaPoint, D.J.: *Mineralogical and Geochemical Guides for Exploring for New SX-EW Sandstone Copper Deposits*. 96-4
- Lin, H.K., Zheng, X.P.: *Process Mineralogy of Scandium and Europium-Containing Iron-Making Slag*. 96-93
- Maltesh, C., Somasundaran, P., Gruber, G.A.: *Fundamentals of Oleic Acid Adsorption or Phosphate Flotation Feed During Anionic Conditioning*. 96-28
- Manrique, M., Vidal, E.E., Accorsi-Lamb, I., Taylor, P.R.: *Pyrometallurgical Treatment of Ilmenite and Zircon Concentrates to Obtain Ceramic Materials*. 96-59
- McLaughlin, R.J., Danzberger, A.H., McLaughlin, R.E.: *A Comparison of Selected Acid Mine Drainage Treatment Processes*. 96-145
- Mehta, R.K., Chatterjee, I., Misra, M., Nelson, M., Raichur, A.M.: *Simultaneous Grinding and Triboelectrification of Coal Followed by Separation in an Electrocentrifugal Field*. 96-155
- Meloy, T.P., Bilgesu, I., Williams, M.C.: *Stopped Cracks and Changes in Fragment Shape and Slope*. 96-142
- Meng, X., Han, K.N.: *The Dissolution Kinetics of Gold in Moderate Aqueous Potassium Iodide Solutions with Oxygen under Pressure*. 96-72
- Mensah-Biney, R., Reid, K.J., Hepworth, M.T.: *Kinetics of Gold-Bromide Loading onto Activated Carbon*. 96-73
- Miller, J.D., Veeramani, S., Azevedo, M.A.D., Yalamanchili, M.R.: *Particle Interactions in High Ionic Strength Solutions*. 96-50
- Misra, M., Mehta, R.K., Chen, S., Kimbrell, J.: *Selective Flotation of Ultra Fine Radionuclides from Johnston Atoll Coral Sand*. 96-137
- Misra, M., Mehta, R., Chen, S., Kimbrell, J.: *Physico-Chemical Characterization and Flotation of Thorium Contaminated Soil from Kirtland AFB*. 96-150
- Murray, J.A., Nees, M.R., Krag, P.W.: *Acid Mist Containment in Electrowinning using Bechtel's Electrode Cap*. 96-173
- Patzelt, N., Knecht, J.: *The Implementation of HPGR Mills in Existing Grinding Circuits*. 96-110
- Pazhianur, R., Richardson, P.E., Adel, G.T., Yoon, R.H.: *Cathodic Protection to Minimize Corrosive Wear in Ball Mills*. 96-165
- Perkins, W., Ynchausti, R., Procter, R., Crawford, W.: *On-Line Analysis for Advanced Process Control at J.R. Simplot's Smoky Canyon Phosphate Mine*. 96-146
- Pirzada, S.A., Manrique, M., Taylor, P.R.: *High Temperature, In-flight Conversion of Alumina to Sodium Aluminate*. 96-58
- Cyprus Sierrita. 96-13
- Torma, S.C., Reddy, R.G., Torma, A.E.: *Process Technologies for Remediation of Lead Contaminated Soils*. 96-47
- Torres, V.M., Viana Jr., A.: *Copper Recovery by Bacterial Leaching for Arapiraca Ore*. 96-95
- Torres, V.M., Horta, R.M.: *Empirical Correlations to Determine Laboratory Mill Grinding Time*. 96-96
- Uhrie, J.L., Nesbitt, C.C., Marsh, K.S.: *Reclamation of Metal Contaminated Soils and Sediments Using Sulfidization and Froth Flotation*. 96-108
- Van Weert, G., van Soelen, P.C.D., Derksen, J.J.: *Oxygen Transfer from Air to Sand Slurries in Stirred Tanks - Rushton Turbine vs. the A315 Impeller*. 96-16
- Veeramunsei, S., Yalamanchili, M.R., Miller, J.D.: *The Influence of Oxygen Defect States on the Surface Charge of Alkali Halides*. 96-138
- Yang, K., Mehta, R., Misra, M.: *Inexpensive and Non-Regenerable Sorbents for the Removal of CO2 and SO2 Present in Coal Flue Gases*. 96-24
- Young, C.A., Cashin, S.P., Jordan, T.S.: *Remediation Technologies for the Separation and Destruction of Aqueous Cyanide Species*. 96-149
- Zheng, J., Harris, C.C., Somasundaran, P.: *The Effect of Additives on Stirred Media Milling of Limestone*. 96-151

GEOLOGY

- Berentsen, E.J., Nanna, R.F., Hazlitt, J.S., Estes, L.D.: *Discovery and Geology of Gold Mineralization at the Turquoise Ridge Project Humboldt County*. 96-2
- Kawulak, M., Niec, M., Salamon, E.: *Environmental Limitations to Exploration and Mining of Mineral Deposits in Poland*. 96-131
- Niec, M.: *The Role of the State of the Art Geology in Discoveries in Poland*. 96-130
- Rempe, N.T.: *Waste Disposal in Underground Mines - A Technology Partnership to Protect the Environment*. 96-43
- Riyazulla, M.S., Ahmed, S.A., Pathan, A.M.: *Geothermobarometric Studies of the Metabasalt of the Hutti Area of Hutti Greenstone Belt, India*. 96-92

MINERAL RESOURCE MANAGEMENT

- Campbell, G.A.: *International Trends and Market Relationships of the Rare Earths*. 96-71
- Davis, G.A.: *The Effect of NAFTA on the Economics of Mineral Production*. 96-44
- Edmonson, N.: *The Impact of High-Cost Canadian Sulfur Production on Sulfur Trade*. 96-82
- Marjanemi, D.K., Dupree, J.A., Sawyer, M.B.: *Major Mines, Mineral Processing Operations, and Mineral Resources in the U.S./Mexico Borderlands*. 96-15
- Pierson, G.: *Commodity Prices from a Monetary Perspective*. 96-8

SEND PREPRINT ORDERS TO:

SME, Inc.
 Publications Sales
 PO Box 625002
 Littleton, CO 80162-5002

Preprint Order Must Be Prepaid - U.S. Dollars Only.
 Colorado Residents Add Applicable Sales Tax.